1 3

OF/DE

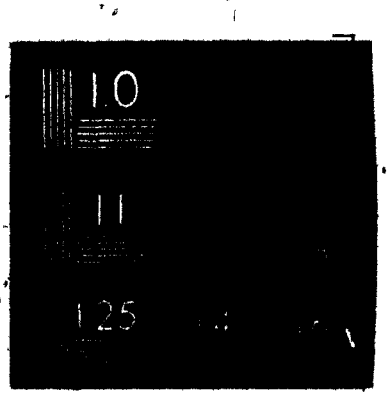

18702

NATIONAL LIBRARY
OTTAWA

CANADA

BIBLIOTHÈQUE NATIONALE
OTTAWA

NAME OF AUTHOR.....Rameshwar Singh Sidhu.....

TITLE OF THESIS..The Purification and Kinetic Studies of...
...Human Liver Aldehyde Dehydrogenase.....
.....

UNIVERSITY.....Dalhousie University.....

DEGREE FOR WHICH THESIS WAS PRESENTED..Ph.D.....

YEAR THIS DEGREE GRANTED...September, 1973.....

Permission is hereby granted to THE NATIONAL LIBRARY OF CANADA to microfilm this thesis and to lend or sell copies of the film.

The author reserves other publication rights, and neither the thesis nor extensive extracts from it may be printed or otherwise reproduced without the author's written permission.

(Signed) [redacted]

PERMANENT ADDRESS:

V.& P.O. Thandewala.....

Teh. Muktsar.....

Distt. Faridkot (Punjab) INDIA

DATED..September 14.....1973

NL-91 (10-68)

THE PURIFICATION AND KINETIC STUDIES OF HUMAN LIVER ALDEHYDE DEHYDROGENASE

by

Rameshwar Singh Sidhu

SUBMITTED TO THE FACULTY OF GRADUATE STUDIES IN PARTIAL FULFILMENT OF THE REQUIREMENTS FOR THE DEGREE OF DOCTOR OF PHILOSOPHY IN BIOCHEMISTRY

DALHOUSIE UNIVERSITY AUGUST, 1973

Dalhousie University

Faculty of Graduate Studies

The undersigned hereby certify that they have read and recommend to the Faculty of Graduate Studies for acceptance a thesis entitled "The Purification and Kinetic Studies of Human Liver Aldehyde Dehydrogenase" submitted by Rameshwar Singh Sidhu in partial fulfillment of requirement for the degree of Doctor of Philosophy.

14 September 1973

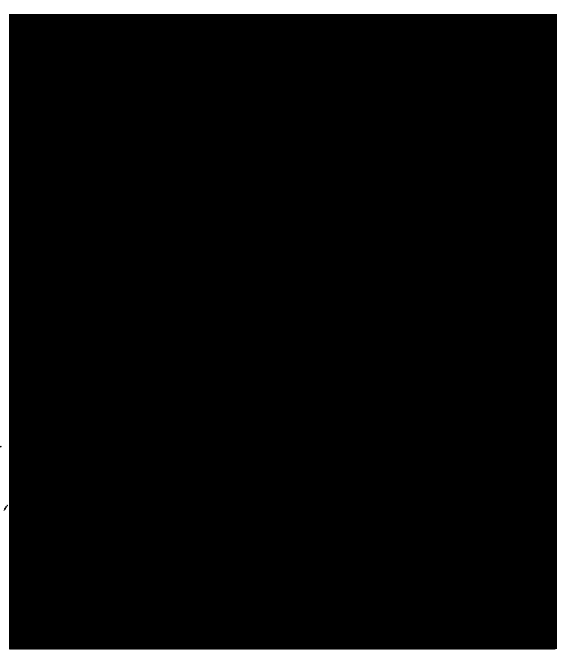

DALHOUSIE UNIVERSITY

Date September 14, 1973

Author Rameshwar Singh Sidhu

Title The Purification and Kinetic Studies of Human Liver Aldehyde Dehydrogenase

Department or School Department of Biochemistry

Degree PhD Convocation Fall Year 1973

Permission is herewith granted to Dalhousie University to circulate and to have copied for non-commercial purposes, at its discretion, the above title upon the request of individuals or institutions.

[redacted]

Signature of Author

TABLE OF CONTENTS

ABSTRACT

The purification of human liver aldehyde dehydrogenase by both conventional procedures (i.e., ion-exchange chromatography and gel-filtration) and recently developed techniques (e.g. isoelectric focusing) was carried out in an attempt to obtain an homogeneous preparation. Although, this goal was not achieved, certain improvements were made in the existing purification procedure. The addition of glutathione and EDTA during DEAE-cellulose column chromatography improved recovery of enzyme activity from the column. The inclusion of a PAB-cellulose treatment before the DEAE-cellulose chromatography gave some additional increase in specific activity. Fractionation by calcium phosphate gel after the DEAE-cellulose chromatography step resulted in a further 2.5-fold purification. Gel filtration studies have confirmed a molecular weight of 200,000 reported by this laboratory which was twice that reported by other workers.

Kinetic studies of aldehyde dehydrogenase were carried out in order to define the mode of interaction of substrates and coenzymes with the human enzyme. The examination of a number of NAD^+-analogues demonstrated that NAD^+ is the best coenzyme for this enzyme. Initial velocity studies on the dehydrogenase reaction showed convergent linear double reciprocal plots, indicating a sequential mechanism in which both substrates must bind to enzyme before any product is released. Certain NAD^+-analogues were dead-end inhibitors:

competitive with respect to NAD^+ and noncompetitive with respect to aldehyde. Conversely, aldehyde analogue gave competitive inhibition with respect to aldehyde and noncompetitive inhibition with respect to NAD^+. This dead-end inhibition data is consistent with a mechanism in which the order of binding of substrates is not obligatory.

Human liver aldehyde dehydrogenase was also found to be capable of hydrolyzing p-nitrophenyl acetate. The superimposed elution pattern of both dehydrogenase and esterase activities from a DEAE-sephadex column demonstrated that one enzyme was responsible for both activities. Initial rates of hydrolysis did not obey Michaelis-Menten kinetics, but rather, exhibited substrate activation at high ester concentrations. Evidence for the existence of a second site responsible for this behavior was obtained. Competitive inhibition of esterase activity by aldehyde and the analogue chloral hydrate indicated that p-nitrophenyl acetate was hydrolyzed at the aldehyde binding site. Assuming that a common acyl-enzyme intermediate is formed in the dehydrogenase and esterase reactions, the rate limiting step in the dehydrogenase reaction appeared to be prior to the deacylation step. Analysis of kinetic data obtained for the NAD^+ activation of esterase reaction has demonstrated that NAD^+ and ester bind randomly to the human enzyme. Also, kinetic constants calculated from esterase data have supported a steady state random Bi Bi mechanism rather than a rapid equilibrium random Bi Bi mechanism for the dehydrogenase

reaction.

Metal chelating agents such as 1,10-phenanthroline, 2,9-dimethyl-1,10-phenanthroline and α,α′-dipyridyl were found to be inhibitors of the human enzyme. The results obtained for these chelators have shown that the inhibition is not due to the chelation of any metal atom present in the enzyme but rather it is due to the competition between NAD^+ and chelating agents for the NAD^+-binding site.

Evidence was also obtained for the effect of protein-protein interactions between different proteins on enzyme activity. Among various proteins tested (including serum albumins) it was observed that bovine serum albumin has a specific activating effect. Furthermore, the effect was more pronounced in the physiological pH range than at the pH optimum for this enzyme. This finding highlights the potential importance of such protein-protein interactions in vivo.

ABBREVIATIONS

NAD^+	Nicotinamide adenine dinucleotide, oxidized form
NADH	Nicotinamide adenine dinucleotide, reduced form
$NADP^+$	Nicotinamide adenine dinucleotide phosphate, oxidized form
$NAD(P)^+$	NAD^+ or $NADP^+$
3-Acetylpyridine-AD^+	3-acetylpyridine adenine dinucleotide, oxidized form
3-Acetylpyridine-HD^+	3-Acetylpyridine hypoxanthine dinucleotide, oxidized form
Pyridine-3-aldehyde-AD^+	Pyridine-3-aldehyde adenine dinucleotide, oxidized form
Pyridine-3-aldehyde-HD^+	Pyridine-3-aldehyde hypoxanthine dinucleotide oxidized form
Deamino-NAD^+	Nicotinamide hypoxanthine dinucleotide, oxidized form
Thionicotinamide-AD^+	Thionicotinamide adenine dinucleotide, oxidized form
ADP-ribose	Adenosine diphosphoribose
GSH	Glutathione
EDTA	Ethylenediaminetetraacetate
p-CMB	p-Chloromercuribenzoate
BSA	Bovine serum albumin
K_m	Michaelis constant
V_{max}	Maximum velocity
v	Initial velocity
K_i	Inhibition constant

K_{is}	Inhibition constant (slope)
K_{ii}	Inhibition constant (intercept)
p-NTPA	p-Nitrophenyl acetate
p-NTPP	p-Nitrophenyl propionate
p-NTPB	p-Nitrophenyl butyrate
p-NP	p-Nitrophenol
Ald	Aldehyde
I	Inhibitor
nm	Nanometer
NN	Nicotinamide nucleotide
glyc.	Glyceraldehyde

ACKNOWLEDGEMENT

The author wishes to express his sincere gratitude to his supervisor, Dr. A. H. Blair, for his patience, guidance and criticisms throughout the course of this work.

Thanks are due to Dr. W. W. Cleland, University of Wisconsin, for providing computer programs. The author is indebted to Mr. Randolph Barkhouse, University Computer Center, without whose help computer analysis of enzyme kinetic data would not have been possible.

The author would also like to thank Mrs. Helen Varga for her skilful technical assistance in performing the kinetic experiments, the Audio Visual Department for the preparation of graphs, Miss A. Comeau for the careful typing of this thesis, and the Medical Research Council of Canada for financial support.

LIST OF EQUATIONS

INTRODUCTION

A. THE FATE OF ALCOHOL

Alcohol is a food, as well as a drug. It exerts two kinds of effects on the human body: pharmacological and metabolic. These effects are very different at high and low levels of ethanol consumption. When consumed in moderate quantities, alcohol seems to act mainly as a nutrient. However, when consumed in large quantities it becomes a drug that can produce many serious metabolic effects (1).

It is generally accepted that alcohol is metabolized by a pathway which involves initial oxidation to acetaldehyde and further oxidation of acetaldehyde to acetyl CoA, via the intermediate formation of acetic acid. Alcohol dehydrogenase (EC 1.1.1.1), which catalyzes the oxidation of ethanol to acetaldehyde, is mainly present in liver although traces of this enzyme have been noted in other tissues (2,3,4). The enzyme is found in the supernatant fraction of the liver cell.

However, more recent studies indicate that in addition to alcohol dehydrogenase, liver microsomes are capable of oxidizing ethanol. Normally, two-thirds to three-quarters of the ethanol is metabolized via alcohol dehydrogenase and one-fourth to one-third via an alternate pathway, possibly, the microsomal ethanol oxidizing system (5,6,7,8).

B. ACETALDEHYDE METABOLISM

Oxidation of ethanol, the first step in the main pathway of its metabolism, produces a more toxic metabolite: acetaldehyde. The main source of acetaldehyde in the body is the ingestion of alcohol; however, there is evidence which indicates that endogeneous production of acetaldehyde does occur (9,10). Acetaldehyde is toxic in the sense that it exerts pronounced pharmacological effects at low concentration (11). Clinical symptoms of acetaldehyde administration include nausea, vomiting, and sweating; moreover, it stimulates the release of catecholamines and the depression of oxidative phosphorylation (12,13,14,15,16,17). The fact that there is a mechanism which rapidly removes acetaldehyde as it is formed, prevents accumulation of highly toxic levels during ethanol ingestion. The first biochemical characterization of the system responsible for the elimination of acetaldehyde was provided by Racker with the isolation of an NAD^+-dependent aldehyde dehydrogenase (EC 1.2.1.3) from bovine liver (18). This enzyme catalyzes the oxidation of acetaldehyde to acetic acid. It is responsible for the oxidation of 80% of acetaldehyde in the body (19).

The oxidation of acetaldehyde to acetic acid and its further conversion to acetyl CoA is believed to be the major route of acetaldehyde metabolism. The direct conversion of acetaldehyde to acetyl CoA takes place in micro-organisms (20,21) but the existence of this pathway in mammalian systems has not been confirmed. In addition, there are alternate

pathways for acetaldehyde metabolism but the contribution of these pathways to overall acetaldehyde metabolism is quite small compared to the major route. Alternate enzyme systems can be divided into two groups, i.e., oxidases and lyases.

Oxidases:

The oxidases include xanthine oxidase (EC 1.2.3.2) and aldehyde oxidase (EC 1.2.3.1). Both these enzymes have a wide range of substrate specificity (22,23). Acetaldehyde and other aldehydes are oxidized to the corresponding acids by both enzymes. Unbranched short chain aliphatic aldehydes are metabolized by xanthine oxidase at about the same rate as the natural substrates, xanthine and hypoxanthine. Xanthine oxidase and aldehyde oxidase are flavoproteins and contain stoichiometric amounts of iron, molybdenum, and coenzyme Q (24,25,26,27).

Lyases:

This group includes those enzymes which have the capacity to condense acetaldehyde with a second reactant. The following are the known systems:

(a) Deoxyriboaldolase (EC 4.1.2.4) condenses acetaldehyde with glyceraldehyde-3-phosphate to form 2-deoxyribose-5-phosphate, a reaction intermediate that links ethanol metabolism. This enzyme is present mainly in liver and thymus (28).

(b) Two distinct aldolases, threonine aldolase (EC 4.1.2.5) and allothreonine aldolase (EC 4.1.2.6), catalyze the synthesis of threonine or allothreonine from acetaldehyde

and glycine (29). Both enzymes are present in liver (29). Since both reactions are reversible, it represents one of the plausible sources of endogeneous acetaldehyde. The conversion of acetaldehyde formed in this way to ethanol by alcohol dehydrogenase action can explain endogeneous formation of ethanol.

(c) Pyruvate dehydrogenase system

This system synthesizes small amounts of acetoin from pyruvic acid in the presence of thiamine pyrophosphate and magnesium ions. Pyruvic acid is first decarboxylated to acetaldehyde which is then condensed with a second molecule of pyruvic acid to form acetoin (9,30,31,32,33,34). The pyruvate dehydrogenase system is widely distributed in animal tissues (30,31,33).

(d) An enzyme which catalyzes the condensation of acetaldehyde with 2-ketoglutaric acid to yield 5-hydroxy-4-ketohexanoic acid has been found in homogenates of most rat tissues (35). The activity is present in both mitochondria and microsomes. The significance of this product in alcohol metabolism or in usual metabolic pathways has not yet been determined.

C. ALDEHYDE DEHYDROGENASES

Broad specificity aldehyde dehydrogenases using NAD^+ as the electron acceptor (EC 1.2.1.3) are primarily involved in the major route of oxidation of acetaldehyde. The present review will primarily deal with this class of general aldehyde

dehydrogenases. Such enzymes have been isolated from many sources among animals, plants and micro-organisms. Recently, horse liver (36) Pseudomonas aeruginosa (37), and yeast aldehyde dehydrogenases (38) have been purified to homogeneity.

Jakoby has classified all aldehyde dehydrogenases into three classes on the basis of the type of the reaction catalyzed (39). In general, the reaction can simply be represented by the following equation:

$$RCHO + NAD(P)^+ + HA = RCOA + NAD(P)H + H^+ \quad (1)$$

Class I includes enzyme systems in which A represents OH. When A represents phosphate, arsenate or a mercaptan, the enzyme is placed into Class II. Enzymes belonging to Class III combine another function with those listed above, e.g., malonic semialdehyde oxidative decarboxylase catalyzes the oxidation and decarboxylation of malonic semialdehyde to acetyl CoA. Aldehyde dehydrogenases which have been discussed by Jakoby as well as those isolated more recently are listed in Table I. The properties of Class I enzymes only will be discussed here.

Substrate specificity:

Aldehyde dehydrogenases of Class I can be divided into two sub-groups on the basis of their substrate specificity. The first group, including aldehyde dehydrogenases from human (44,62), beef (18), horse (36) and rabbit liver (40), yeast (47) and Pseudomonas aeruginosa (37), oxidizes a wide variety

TABLE I

ALDEHYDE DEHYDROGENASES

Dehydrogenase	Source	Substrate	NN	Cosubstrate or Cofactor	Ref
Aldehyde	Bovine liver	Wide variety	NAD^+	-	18
Aldehyde	Rabbit liver	Wide variety	NAD^+	steroid	40
Aldehyde	Rabbit liver	Aromatic	NAD^+	-	41
Aldehyde	Mouse liver	Wide variety	NAD^+	-	42
Aldehyde	Rat kidney	Wide variety	NAD^+	-	43
Aldehyde	Human liver	Wide variety	NAD^+	-	44
Aldehyde	Bovine brain	Aliphatic	NAD^+	-	45
Aldehyde	Pig brain	Wide variety	NAD^+	-	46
Aldehyde	Horse liver	Wide variety	NAD^+	-	36
Aldehyde	Yeast	Wide variety	NAD^+ >$NADP^+$	K^+, Rb^+	47
Aldehyde	Yeast	Aliphatic	$NADP^+$	Mg^{++}	48
Aldehyde	Acetobacter	Aliphatic	$NADP^+$ >NAD^+	-	49
Aldehyde	Pseudomonas	Wide Wide variety	NAD^+ >$NADP^+$	phosphate	50
Aldehyde	Pseudomonas	Wide variety	NAD^+ >$NADP^+$	K^+, NH_4^+	37
Aldehyde	Germinating seed	Wide variety	NAD^+	phosphate	51

TABLE I (Cont.)

ALDEHYDE DEHYDROGENASES

Dehydrogenase	Source	Substrate	NN	Cosubstrate or Cofactor	Ref
Succinic semialdehyde	Pseudomonas	Specific	$NADP^+$ >NAD^+	-	52
Succinic semialdehyde	Monkey brain	Specific	NAD^+	-	53
Succinic semialdehyde	rat brain	Specific	NAD^+	-	54
Aminobutyr-aldehyde	Pseudomonas	Specific	NAD^+	-	55
Benzaldehyde	Pseudomonas	Specific	$NADP^+$	K^+,Rb^+,NH_4^+	56
Glutamic semialdehyde	Ox liver	Specific	NAD^+ >$NADP^+$	-	57
α-keto-aldehyde	Sheep liver	α-keto aldehyde	$NADP^+$ >NAD^+	-	58
Aldehyde	Clostridium	Aliphatic	NAD^+	CoA	20
Aldehyde	E. coli	Aliphatic	NAD^+	CoA	21
Formaldehyde	Bovine liver	Specific	NAD^+	GSH	59
Formaldehyde	Yeast	Specific	NAD^+	GSH	60
Aspartic semialdehyde	Yeast	Specific	NAD^+	phosphate	61

of simple aliphatic as well as aromatic aldehydes. Aldehyde dehydrogenases present in the liver, kidney, and small intestine of rabbit (63) as well as in bovine liver have also been shown to oxidize vitamin A aldehyde. An aldehyde dehydrogenase in rabbit liver is specific for aromatic aldehydes (41). Aldehyde dehydrogenase from bovine and monkey brain has been reported to oxidize aldehydes derived from biogenic amines as well as aliphatic aldehydes ranging from formaldehyde to palmitaldehyde (64). At least two aldehyde dehydrogenases exist in the supernatant fraction of rat liver, one of which exhibits broad substrate specificity whereas the other is more restrictive (65).

The second group uses only one specific aldehyde. Formaldehyde dehydrogenase (EC 1.2.1.1) present in bovine liver and yeast (59,60), glutamic semialdehyde dehydrogenase present in ox liver (57) and succinic semialdehyde dehydrogenase (EC 1.2.1.16) from monkey and rat brain and Pseudomonas (53,54) belong to this second category.

Substrate form:

In aqueous solution most aldehydes exist partly as the corresponding gem-diol, with widely different degrees of hydration depending on substituent groups in the molecule. Thus, it is possible that either the free carbonyl form or the hydrated form of the aldehyde is the actual substrate for aldehyde dehydrogenases. Xanthine oxidase from milk and chicken liver uses the free carbonyl form of acetaldehyde (66,67). Aldehyde dehydrogenase from yeast uses the free carbonyl form

of acetaldehyde and butyraldehyde (67). Human liver aldehyde dehydrogenase, which oxidizes several aldehydes differing in the extent of hydration in aqueous solution, has also been shown to utilize the free carbonyl form of acetaldehyde and formaldehyde (68). There is no instance in the literature where aldehyde dehydrogenase has been shown to use the hydrated form of aldehyde.

Sub-cellular distribution:

Walkenstein and Weinhouse observed that mitochondria of rat and pigeon liver and rat kidney could oxidize a variety of long and short chain aldehydes to the corresponding acids (69). NAD^+-dependent aldehyde oxidizing capacity was also observed by Deitrich in the supernatant, mitochondrial and microsomal fractions of liver from pigeon, beef and rat (70). The partial purification of supernatant and mitochondrial fractions from rat liver by gel chromatography led Deitrich to suggest that the aldehyde dehydrogenase activities in each fraction were catalyzed by distinct proteins (70). More recently, Marjenen has also analyzed sub-cellular fractions of rat liver for aldehyde dehydrogenase activity. The results indicate that 80% of the total activity is localized in the mitochondrial fraction and the remaining 20% in the cytoplasm, under his particular experimental conditions (71). Neither the microsomal fraction nor the nuclear fraction possessed aldehyde oxidizing capacity. Evidence presented by Smith and Packer suggests that the NAD^+-dependent aldehyde dehydrogenase is localized on the outer membrane of rat liver

mitochondria (72).

The presence of more than one aldehyde dehydrogenase in an organism, tissue or sub-cellular fraction has also been observed. Three aldehyde dehydrogenases are present in the rabbit liver. Two of these have similar, broad specificities (40). They are distinguished by the fact that only one is sensitive to steroid hormones (40,73). The third enzyme is specific for aromatic aldehydes (41). Similarly, yeast contains two aldehyde dehydrogenases differing in their ion requirements. One is activated by potassium and the other by magnesium (47,48). The magnesium activated enzyme (EC 1.2.1.4) is specific for $NADP^+$ whereas the potassium activated enzyme (EC 1.2.1.5) utilizes both NAD^+ and $NADP^+$ (47,48). Evidence for the presence of more than one aldehyde dehydrogenase in the rat brain and liver has also been presented by Deitrich (64,70). Studies of Deitrich et al. have also indicated that there are two NAD^+-dependent aldehyde dehydrogenases in the supernatant fraction of rat liver. The enzymes differ with respect to their substrate specificity, response to induction by phenobarbital, disulfiram inhibition and heat stability (74). Shum and Blair have also recently provided evidence that two aldehyde dehydrogenases, separable by DEAE-cellulose chromatography, exist in the supernatant fraction of rat liver (65).

Sub-unit structure:

Most of the aldehyde dehydrogenases are relatively high molecular weight proteins. Therefore, it is quite likely

that they are composed of subunits. The homogeneous preparation of potassium activated aldehyde dehydrogenase from baker's yeast consists of four subunits each with a molecular weight of 56,000 daltons (75). Feldman and Weiner have also reported a subunit structure for horse liver aldehyde dehydrogenase. The enzyme is a tetramer composed of subunits of molecular weight 57,000 (36).

The existence of association and dissociation phenomenon in aldehyde dehydrogenases has been shown by the finding that yeast aldehyde dehydrogenase, denatured in 6M guanidine hydrochloride, (dissociation into subunits) could be reassociated to yield a functional enzyme of higher molecular weight (47, 75).

Irreversible reaction:

Oxidations catalyzed by Class I enzymes (described on Page 5) have not been experimentally reversed. The free energy change for the reaction at 25° and pH 7.0 (R represents CH_3 and $NAD(P)^+$ represents NAD^+ in equation 1) has been determined to be -12.5 Kcal (76,77). A change of free energy of -4.2 Kcal, calculated from equilibrium data by Burton and Stadtman (78), has been reported for the reversible reaction in which CoA represents HA in equation 1.

Michaelis constants for aldehydes:

Many aldehyde dehydrogenases exhibit very low K_m values for aldehydes. The K_m values for simple aliphatic aldehydes with the dehydrogenases isolated from bovine brain (64) and human (44), beef (18) and horse liver (36) are in the range

of 10^{-6} — 10^{-7} M. The NAD^+-dependent aldehyde oxidizing enzyme from rat liver is an exception. The K_m values reported by Deitrich for this enzyme ranged between 1 x 10^{-3}M and 4.5 x 10^{-3} M (70). Shum and Blair have also obtained apparent K_m values in the range of 10^{-3} M for simple aliphatic aldehydes with two partially purified aldehyde dehydrogenases from the supernatant fraction of rat liver (65).

Metal content:

Stoppani et al. reported that yeast and bovine liver aldehyde dehydrogenases resembled several well-documented zinc metallo-dehydrogenases with respect to their behavior towards zinc chelating agents (79). Zinc complexing agents inhibited both enzymes. The order of decreasing effectiveness with both yeast and bovine liver aldehyde dehydrogenase was 8-hydroxyquinoline > 1,10-phenanthroline > α',α'-dipyridyl > thiourea (79). Inhibition was instantaneously reversible. The effectiveness of the chelators in the order given above was in agreement with the stability constants of their respective zinc complexes. Jakoby et al. (38,47), however, did not report the presence of zinc in their homogeneous preparation of yeast aldehyde dehydrogenase. This suggests that zinc-complexing agents may act through a mechanism other than zinc chelation.

Characterization of sulfhydryl and disulfide groups:

Aldehyde dehydrogenases can be inhibited to different degrees by a variety of sulfhydryl reagents, e.g., p-CMB, iodoacetamide, iodoacetate (39). p-CMB has proved to be the

strongest inhibitor among these sulfhydryl reagents. The finding that some of the aldehyde dehydrogenases are activated by exogeneous mercaptans, while others have an absolute requirement for them provides additional evidence for the participation of sulfhydryl groups in the catalytic activity (37,47,80). These findings have encouraged several investigators to speculate that aldehyde dehydrogenases bear sulfhydryl groups at the active site and that the blockage of these groups by oxidation, alkylation or mercaptide formation leads to a loss of enzyme activity (18,81,82). Sulfhydryl groups have frequently been thought to react with the pyridine nitrogen of the coenzyme (83,84,85,86). However, there is no concrete evidence for the direct participation of sulfhydryl groups in the catalytic reaction. Enzyme inhibition by sulfhydryl reagents might also be the result of changes in enzyme conformation.

Evidence for the presence of sulfhydryl groups in the active center region has come from substrate protection studies. Inhibition of aldehyde dehydrogenase by sulfhydryl reagents can be protected against by prior incubation of the enzyme with substrates or coenzymes, provided of course that the substrate chosen binds sufficiently strongly at the active site compared to the inhibitor. NAD^+-specific bovine liver aldehyde dehydrogenase is protected against inactivation by p-chloromercuribenzoate, o-iodosobenzoate, 3-amino-4-hydroxyphenylarsenoxide by NAD^+ but not by $NADP^+$ (82,87). Similarly, the $NADP^+$-specific yeast enzyme is protected by $NADP^+$, but

not by NAD^+, against inactivation by N-ethylmaleimide, o-iodosobenzoate, iodoacetate and p-chloromercuribenzoate (82,87). The $NAD(P)^+$-specific yeast aldehyde dehydrogenase is protected against inactivation by 3-amino-4-hydroxyphenylarsenoxide, N-ethylmaleimide, iodoacetate and o-iodosobenzoate by both NAD^+ and $NADP^+$ (82,87). NAD^+ protection against inhibition by phenylmercuric acetate and arsenosophenylbutyrate was reported by Deitrich for the bovine enzyme (88).

In comparison to the results with coenzymes, the data on aldehyde protection against inhibition by various sulfhydryl reagents is relatively inconclusive. Studies with the bovine liver enzyme have indicated that acetaldehyde afforded protection against inhibition by mapharside, iodosobenzoate, N-ethylmaleimide but not against that caused by p-chloromercuribenzoate (87). The $NAD(P)^+$-specific yeast aldehyde dehydrogenase but not the $NADP^+$-specific enzyme is protected by acetaldehyde against inhibition by N-ethylmaleimide, iodosobenzoate and p-chloromercuribenzoate (87).

The functional importance of disulfide groups is implied by the fact that aldehyde dehydrogenases are characteristically inhibited by arsenite and this inhibition is greatly increased in the presence of exogeneous mercaptan (89). The inhibition is reversed only by dimercaptans and not by monomercaptans. The mechanism postulated for this interaction is that exonegeous mercaptan is required to first reduce a disulfide linkage, thereby generating adjacent sulfhydryl groups for the arsenite attack (90).

Using an uncharged trivalent arsenical (arsenosophenyl butyrate) Deitrich found that inhibition of bovine liver aldehyde dehydrogenase did not require exogeneous mercaptan. Moreover, inhibition was greater than that obtained using arsenite and thiol together (88). These results cast doubt on the validity of the mechanism generally believed to account for arsenite inhibition and also on the existence of closely situated sulfhydryl groups in the active center of aldehyde dehydrogenases.

Disulfiram Interaction:

It was found a number of years ago that disulfiram (Antabuse) interferes with the normal metabolism of ethanol and thereby causes the accumulation of a toxic metabolite which induces an aversion response to alcohol (91,92,93,94). According to Hald's original theory, disulfiram causes an accumulation of acetaldehyde by inhibiting aldehyde dehydrogenase, the enzyme responsible for its elimination (92,93). Bovine liver aldehyde dehydrogenase was shown to be inhibited by disulfiram in vitro (95,96,97). On the other hand, this drug had very little effect in vitro on human liver aldehyde dehydrogenase (44). More recent work by Deitrich and Erwin has indicated that administration of disulfiram to rats irreversibly inhibits aldehyde dehydrogenase activity and return of activity is dependent on protein synthesis (98).

NAD$^+$ conformation:

By labelling the coenzyme at its reduced site with deuterium Vennesland and Westheimer (99) were able to show the non-identical nature of two C_4 pyridine hydrogens in the reduced nicotinamide coenzyme. Two forms of both nicotinamide nucleotides (NAD$^+$ and NADP$^+$) may be specified on the basis of these observations. These two forms, referred to as the A and B forms, are distinguished by their relative geometries with respect to the plane of the reduced nicotinamide ring. Enzymes specific for the two different C_4 hydrogens are specified as A and B dehydrogenases, respectively.

Kaplan and Sarma have recently applied high frequency proton nuclear magnetic resonance to the study of the conformation of nicotinamide coenzymes in the solution. They have postulated three structures: an open form and two folded forms. The folded forms, distinguishable by the relative positions of the pyridine and purine rings, are referred to as the right (P) and left (M) helices. According to their hypothesis (P) and (M) helices are in equilibrium with each other and their interconversion proceeds through an open form (100). Furthermore, they propose that the difference in specificities of A and B dehydrogenase may be related to their ability to recognize the (M) and (P) helices. Attempts are being made in Kaplan's laboratory to determine the differences in the binding of the two helices to the various nicotinamide nucleotide linked dehydrogenases (100).

NAD$^+$-analogues:

The study of the mechanisms of nicotinamide coenzyme dependent enzyme reactions has been greatly aided by the present availability of structural analogues of nicotinamide nucleotides. A list of important NAD$^+$-analogues with modifications in the pyridine and/or adenine rings is given in Table II. The pioneer work in the preparation of NAD$^+$-analogues and in their use as coenzymes in the dehydrogenase systems was done by Kaplan (101,102,103,104). Kaplan et al. tested various dehydrogenases for their affinities towards different NAD$^+$-analogues with a view to demonstrating differences between dehydrogenases from different tissues or species (105). They pointed out that it is possible to classify animals not only by their physiological and morphological characteristics but also by the affinities of their dehydrogenases for the coenzymes or their analogues (105).

Lactic dehydrogenases from lobster heart and thorax muscle reduce 3-acetylpyridine-AD$^+$ faster than NAD$^+$ whereas beef heart and rabbit skeletal muscle lactic dehydrogenase reduce this analogue at a lower rate than NAD$^+$. 3-acetylpyridine-AD$^+$ is reduced more rapidly by horse liver alcohol dehydrogenase and beef liver glutamic dehydrogenase. In contrast, yeast alcohol dehydrogenase and glyceraldehyde-3-phosphate dehydrogenase reduce the analogue more slowly than NAD$^+$ (103,105). Overall, NAD$^+$-analogues are more readily reduced by horse liver alcohol dehydrogenase system than by the yeast system (106).

TABLE II

SOME NAD^+-ANALOGUES SUBSTITUTED IN THE NICOTINAMIDE AND/OR ADENINE RINGS

Analogue	Substituents	
	Pyridine Ring (C_3)	Purine Ring (C_6)
Deamino-NAD	—	—OH
3-Acetylpyridine-AD	$-C(=O)-CH_3$	—
3-Acetylpyridine-HD	$-C(=O)-CH_3$	—OH
Pyridine-3-aldehyde-AD	$-C(=O)-H$	—
Pyridine-3-aldehyde-HD	$-C(=O)-H$	—OH
Thionicotinamide-AD	$-C(=S)-NH_2$	—

NAD^+-analogues have recently been used in the study of kinetic reaction mechanisms of yeast and bovine liver aldehyde dehydrogenase. The results indicate that both aldehyde dehydrogenases are distinct in their behavior towards different NAD^+-analogues (107,108). Neither the yeast enzyme nor the bovine enzyme reduces NAD^+-analogues at a greater maximal rate than NAD^+. The NAD^+-analogues are less reactive with yeast aldehyde dehydrogenase than with the bovine liver enzyme.

NAD^+-analogues have not only helped in the understanding of the reaction mechanism of various dehydrogenases but also they have been found useful in obtaining information on the conformation of nicotinamide coenzymes (107,108,109,110,111, 112,113).

Kinetic reaction mechanism:

According to Cleland all enzyme catalyzed reactions can be classifed according to two major kinetic mechanisms: (1) sequential mechanism (2) Ping pong mechanism (114). A sequential mechanism requires the addition of all the substrates to the enzyme before any product is released. On the other hand, in ping pong mechanisms, one or more products are released before all the substrates have bound to the enzyme. Sequential mechanisms are further divided into two sub-groups: (1) ordered (2) random. An ordered sequential mechanism is one in which the order of addition of substrates and release of products is obligatory. The mechanism is random when the order of addition of substrates and dissociation of products is not obligatory. Several sequential and

ping pong mechanisms for enzymes with two substrates and two products (Bi Bi) are diagrammed below:

Sequential Mechanisms:

Ordered Bi Bi

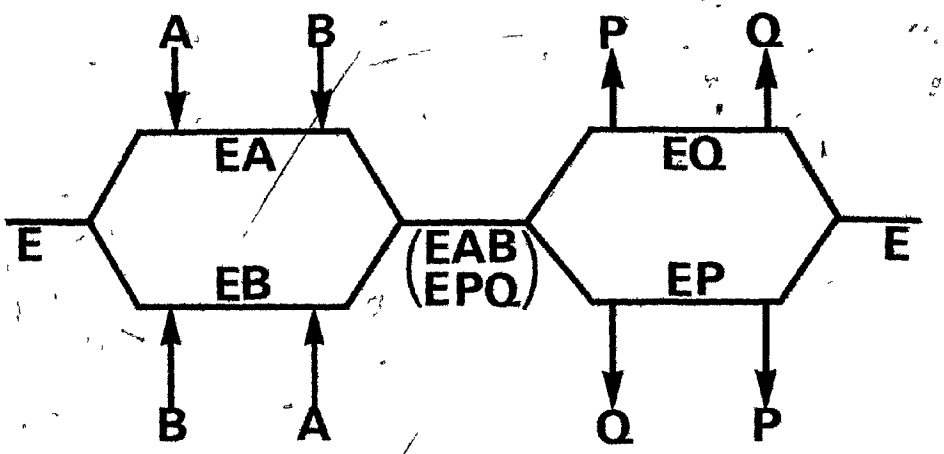

Random Bi Bi

Ping Pong Bi Bi Mechanism:

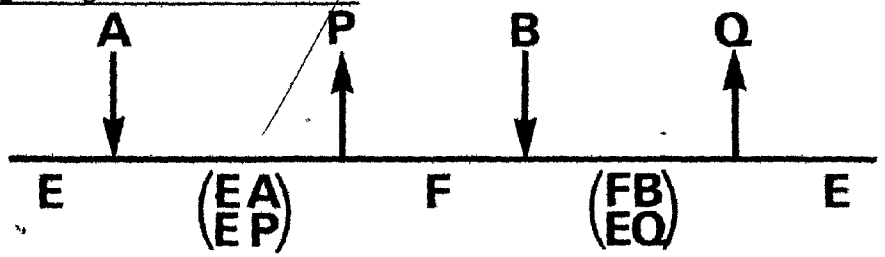

Two general rate equations in kinetic constant form and with the product concentrations set equal to zero are presented as examples:

1. Sequential Bi Bi mechanism (ordered or rapid equilibrium random)

$$v = \frac{VAB}{K_{ia}K_b + K_aB + K_bA + AB} \qquad (2)$$

2. Ping Pong Bi Bi mechanism

$$v = \frac{VAB}{K_aB + K_bA + AB} \qquad (3)$$

Where v = initial velocity in the absence of products

A and B = substrates

K_{ia} = inhibition constant for A

K_b = Michaelis constant for B

K_a = Michaelis constant for A

V = maximum velocity

It is particularly interesting to note that the rate equation for the ping pong mechanism does not contain a constant term. Initial velocity studies can easily distinguish sequential from ping pong mechanisms. In double reciprocal plots of initial velocity versus substrate concentration,

an intersecting initial velocity pattern is characteristic of a sequential mechanism, a parallel pattern of a ping pong mechanism.

All aldehyde dehydrogenases which have been investigated follow a sequential mechanism. A compulsory order mechanism with NAD^+ binding prior to aldehyde has generally been assumed to apply. Pig brain and horse liver aldehyde dehydrogenases have been reported to follow a compulsory order mechanism in which NAD^+ binds before aldehyde (115,116). Kinetic studies with yeast and bovine liver aldehyde dehydrogenase have indicated a similar mechanism (107,108). In this case a series of coenzymes and substrate analogues were used to get information on the order of binding of NAD^+ and aldehyde.

Bradbury and Jakoby have shown that the yeast enzyme follows a mechanism in which aldehyde binds first (117). This conclusion was reached on the basis of the results obtained with NADH inhibition and equilibrium binding experiments. NADH inhibition was competitive with respect to NAD^+ and uncompetitive with respect to aldehyde. Their equilibrium binding data indicated that NAD^+ does not bind to the yeast enzyme in the absence of aldehyde.

Esterolytic activity:

Glyceraldehyde-3-phosphate dehydrogenase (118) was the first non-hydrolytic enzyme reported to catalyze hydrolysis of p-nitrophenyl acetate, a commonly used substrate of esterases. The sequence analysis around the site of p-nitrophenyl acetate acylation of glyceraldehyde-3-phosphate de-

hydrogenase (EC 1.2.1.12) revealed the involvement of sulfhydryl (-SH) and amino ($-NH_2$) groups in the formation of an acyl-intermediate which was then considered as the common intermediate in both the dehydrogenase and the esterase reaction (119). Later on, carbonic anhydrase (EC 4.2.1.1) was also found to hydrolyze p-nitrophenyl acetate. Both the esterolytic and hydrolytic reactions took place at the same active center (120). More recently, α-glycerol phosphate dehydrogenase (EC 1.1.1.8) and horse liver aldehyde dehydrogenase (EC 1.2.1.3) have also been observed to possess the ability to catalyze hydrolysis of p-nitrophenyl acetate (121, 116). Feldman and Weiner proposed the formation of a common acyl-enzyme intermediate in both the dehydrogenase and esterase reactions on the basis of kinetic data for the esterase reaction.(116). The authors also suggested that acylation is the rate limiting step in both reactions.

The hydrolysis of p-nitrophenyl acetate by glyceraldehyde-3-phosphate dehydrogenase, carbonic anhydrase and horse liver aldehyde dehydrogenase was shown to follow normal Michaelis-Menten kinetics. However, it was observed by Serarez and Apitz-Castro that the esterolytic activity of α-glycerol phosphate dehydrogenase was activated allosterically by both dihydroxyacetone phosphate and glycerol phosphate, a product of the dehydrogenase reaction (122).

Bovine serum albumin was the first "non-enzymatic" protein found to hydrolyze p-nitrophenyl acetate (123). A detailed kinetic study of the reaction of bovine serum albumin

with p-nitrophenyl acetate showed that a biphasic curve was obtained when ester hydrolysis was plotted versus time. The biphasic nature of the curve was interpreted to mean that two separate sites, an acetylating site and a catalytic site, contributed to the observed esterase activity (124).

Enzyme Induction:

Investigations in the area of induction of liver aldehyde dehydrogenases are currently being pursued because these might provide answers to an unresolved aspect of alcoholism; namely, ethanol tolerance. Horton has reported an increase in aldehyde dehydrogenase activity in a mitochondrial fraction, but not in a microsomal fraction, isolated from liver of rats given ethanol orally. He has also postulated the presence of an aldehyde oxidizing system in peroxisomes or lysosomes (125). More recently, a possible biochemical basis for alcohol preference and tolerance has been suggested by the observation that mice from a strain which prefers to drink ethanol have an increased aldehyde oxidizing capacity in the liver compared with mice from a strain characterized by avoidance of alcohol. Aldehyde dehydrogenases from both strains are indistinguishable by electrophoresis and chromatography (126).

Redmond and Cohen (127) have recently observed a two-fold increase in aldehyde dehydrogenase activity in whole liver homogenates of mice after administration of phenobarbital for four days. A similar but much greater effect in rat liver has been demonstrated by Deitrich et al. (128). Their

results indicate that phenobarbital administration causes a ten-fold increase in aldehyde dehydrogenase activity present in the supernatant fraction. This effect is genetically controlled and is inherited as a dominant characteristic (128).

SCOPE

Human liver aldehyde dehydrogenase oxidizes a wide variety of differently substituted aldehydes, including biogenic amine and vitamin A metabolites, as well as acetaldehyde. Accordingly, this enzyme may affect the metabolic flux in diverse pathways. Also, inhibition of aldehyde dehydrogenase has been postulated to play a role in the physiological action of various drugs which produce an aversion reaction to alcohol. Thus, it was of interest to obtain a deeper understanding of the kinetic steps in the reaction path and of the manner in which different substrate and coenzyme analogues and inhibitors interact at the active center of the enzyme. Studies carried out to establish the pattern of addition of substrates and coenzymes to the enzyme form the major component of this thesis. In addition to oxidation of aldehydes, the human enzyme was found to catalyze ester hydrolysis. Study of esterolytic properties of this enzyme led to important insights into the kinetic mechanism and the relative rates of various catalytic steps in the esterase and dehydrogenase reactions. The esterase data has also provided experimental evidence for the existence of a second binding site responsible for substrate activation by p-nitrophenyl acetate.

Interactions between subunits of allosteric enzymes play an important role in the regulation of their activity. The importance of protein-protein interactions between different proteins has not been as extensively investigated. The

activation of human liver aldehyde dehydrogenase by bovine serum albumin observed in this study presented a situation where the contribution of such interactions to the catalytic power of this enzyme can be studied.

Inhibition of certain aldehyde dehydrogenases by metal complexing agents has led to reports that they are zinc metalloenzymes, but this hypothesis remains unproven. Human liver aldehyde dehydrogenase is also inhibited by such agents but analysis by atomic absorption spectrophotometry did not show the presence of stoichiometric amounts of zinc in the preparations examined (Blair, unpublished data). Studies directed toward investigating the nature of this inhibition seem to have provided an answer to this problem and are presented here.

MATERIALS AND METHODS

A. MATERIALS

1. Chemicals

All chemicals used for enzyme isolation were reagent grade unless otherwise specified. DEAE-cellulose (DE 32) was a product of Whatman Company. PAB-cellulose was purchased from Serva FeinBiochemica, GmbH & Co. DEAE-sephadex (A-50) and sephadex G-100 and G-200 were products of Pharmacia Fine Chemicals. BD-cellulose was obtained from Schwarz, BioResearch, Inc. Calcium phosphate gel was a product of CalBiochem, Inc.

β-NAD^+, β-NADH, p-nitrophenyl acetate, p-nitrophenyl propionate, p-nitrophenyl butyrate, benzoic acid, adenine hydrochloride, ovalbumin (crystallized), reduced glutathione, and N'-methylnicotinamide were purchased from Sigma Chemical Co. Adenine, adenosine, nicotinamide hypoxanthine dinucleotide, 3-acetylpyridine adenine dinucleotide, 3-acetylpyridine hypoxanthine dinucleotide, pyridine-3-aldehyde adenine dinucleotide, pyridine-3-aldehyde hypoxanthine dinucleotide, and thronicotinamide adenine dinucleotide were products of P.L. Biochemicals, Inc. 2,9-Dimethyl—1,10-phenanthroline, α,α'-dipyridyl, quinoline, hexadecyltrimethylammonium bromide, and chloral hydrate were obtained from Eastman Organic Chemicals, and γ,γ'-dipyridyl hydrochloride from K & K Laboratories, Inc. 1,10-Phenanthroline and gelatin were purchased from Fisher Scientific Company. Acetaldehyde was purchased

from Matheson Coleman and Bell, Inc. Glyceraldehyde was obtained either from Sigma Chemical Co. or Mann Research Laboratories. Ethylenediamine tetraacetic acid, disodium salt, was purchased from J.T. Baker Chemical Co. Bovine serum albumin (Pentex crystallized), bovine serum albumin (Fr V, Fatty acid free), human albumin (crystallized), human albumin (Fr V, Fatty acid free), rabbit albumin (crystallized), horse albumin (Fr V), sperm whale myoglobin (crystallized) and lysozyme (crystallized) were purchased from Miles Laboratories, Inc.

2. Solutions

Substrate and inhibitor solutions were prepared just prior to use. Acetaldehyde was distilled under nitrogen before use. Solutions of serum albumins and other proteins were freshly prepared in glass distilled water. p-Nitrophenyl esters were dissolved in acetone and diluted with water to a final concentration of 2.5 mM or less (final concentration of acetone 0.5% v/v). The resulting stock solutions remained transparent during the course of a series of esterase measurements.

B. EXPERIMENTAL PROCEDURES

1. Ion-exchange and Gel Chromatography

a. DEAE-cellulose

The ion-exchanger was suspended in 15 volumes (v/w) of 0.5N HCl and allowed to stand for at least 30 minutes. The supernatant liquor was then decanted and the DEAE-cellulose was washed with distilled water in a sintered glass funnel until the pH of the filtrate was near 4. The ion-exchanger was then stirred into 15 volumes of 0.5N NaOH. After 30 min the supernatant liquor was decanted. This NaOH treatment was repeated once. The DEAE-cellulose was freed of alkali by washing with distilled water in the funnel until the pH of the filtrate was close to neutrality. The washed ion-exchanger was then suspended in the equilibrating buffer (0.01M sodium phosphate, pH 6.2) and adjusted to pH 6.2 by adding the acid component of the buffer with stirring. After titration, the suspension was allowed to settle for 15-20 min after which the supernatant solution, containing fine particles, was decanted. The buffer treatment, along with removal of fine particles, was continued until the pH and conductivity of the supernatant layer were the same as that of the equilibrating buffer.

The column was packed by the pumped flow method. A slurry of DEAE-cellulose was prepared by adding equilibrating buffer to give a final volume equal to 150% of the wet settled volume of the exchanger. The stirred slurry was then poured into a column fitted with a extension tube half the

length of the column. After adding the slurry, the extension tube was connected immediately to the buffer reservoir via a peristaltic pump adjusted to provide continuous inflow of buffer under low pressure. The flow of buffer was continued until the exchanger bed reached a stable height. Then, the extension tube was removed and the outlet from the peristaltic pump was directly connected to the column. The packed column was washed with at least two further column volumes of buffer.

b. DEAE-sephadex

The sephadex ion-exchanger (A-50) was first allowed to swell in an excess of starting buffer (0.04M sodium phosphate, pH 6.8) for two days at room temperature. The swollen gel was washed several times with starting buffer until the supernatant layer had the same pH and conductivity as the equilibrating buffer. The fine particles were removed in conjunction with each buffer change by allowing the gel to settle for 15 min and then decanting the supernatant layer. The DEAE-sephadex column was prepared by the usual method as described in the Sephadex ion-exchanger Bulletin (Pharmacia Fine Chemicals).

c. PAB-cellulose

This ion-exchanger was first suspended in distilled water in order to remove fine particles. The suspension was allowed to settle for 15 min and then the supernatant liquid decanted. This procedure was repeated several times. The resulting relatively coarse PAB-cellulose frac-

tion was equilibrated with 0.01M sodium phosphate, pH 6.2, until the supernatant solution had the same pH and conductivity as the equilibrating buffer. The equilibrated PAB-cellulose was poured as a slurry into a column of chosen size.

d. BD-cellulose

BD-cellulose supplied by the manufacturer as a suspension in 2M sodium chloride, was equilibrated with starting buffer before pouring into a column. The packed column was washed with the buffer until the pH and conductivity of the eluate were similar to the buffer.

e. Calcium-phosphate Gel

Tricalcium phosphate gel was used without further treatment.

f. Sephadex-gels

Sephadex G-100 and G-200 were allowed to swell at room temperature in the filtration buffer for at least three days. The swollen gels were then equilibrated with the appropriate filtration buffer and cooled to 4°. The columns were packed at 4° according to the method described in the Sephadex Bulletin (Pharmacia Fine Chemicals). Upward flow of buffer with the recommended constant pressure head was used for all sephadex columns. The packed column was washed with two column volumes of filtration buffer prior to an experiment.

2. Isoelectric Focusing

An electrofocusing column of 110 ml volume (LKB8101) was prepared for use at 4° by following instructions given in the LKB 8100 Ampholine Instruction Manual. The ampholine carrier ampholytes for pH gradients 3-10, 5-8 and 3-6 were used in various runs. These ampholytes consist of a number of different aliphatic polyamino-polycarboxylic acids.

3. Protein Determination

Protein was determined by the method of Lowry et al. (129) using bovine serum albumin, fraction V (Nutritional Biochemicals Corp.), as the standard.

4. Conductivity Measurement

Conductivity was measured at 4° with a Radiometer conductivity meter, type CDM2d, using a type CDC114 electrode.

5. pH Determination

pH measurements were made with a Radiometer pH meter 26, using a type GK2302C glass electrode at 23°. The determination of the pH of fractions obtained from the isoelectric focusing column was carried out at 4°.

6. Assay of Enzyme Activity

a. Aldehyde dehydrogenase activity

Dehydrogenase activity at 22° was determined as described by Blair and Bodley (44) by measuring the NADH formation at 340 nm with a Cary 16K spectrophotometer equipped with a Honeywell Electronik 16 recorder and temperature controlled cell holder. Reaction mixtures for routine assay

contained 33 mM sodium pyrophosphate, pH 9.3, 8.3 mM acetaldehyde and 1.7 mM NAD^+. The final volume was 3.0 ml. The composition of reaction mixtures used in kinetic experiments is specified in the appropriate figure captions. The reaction was initiated by addition of enzyme. One unit of activity is defined as the amount of enzyme that catalyzed the formation of one μmole of NADH per min under the above conditions.

b. Esterase activity

Esterolytic activity at 22° was determined by measuring the formation of p-nitrophenolate ion at 400 nm. The composition of reaction mixtures is specified in the appropriate figure captions. The reaction was initiated by addition of enzyme. There was no significant increase in absorbance at 400 nm at low concentrations of p-nitrophenyl esters in the absence of enzyme. If any significant increase was observed at higher concentrations of esters it was subtracted from the corresponding absorbance change obtained in the presence of enzyme. NAD^+ or NADH alone did not catalyze any ester hydrolysis at pH 7.0 under the conditions used.

7. Enzyme preparation

Human liver samples were obtained at autopsy and stored frozen until used. The case history and pathological examination indicated the livers to be free of disease. The frozen liver samples (1000-1500 g) were thawed, cut into small pieces and passed through a cooled meat grinder. Subsequent steps were carried out at 0-4°. To the ground liver was

added: 0.5M sodium pyrophosphate, pH 7.0, (volume equal to 1.34 times the weight of ground liver), 1.05M sucrose (volume equal to 1.34 times the weight of ground liver), 0.1M $MgCl_2$ (volume equal to 0.032 times the weight of ground liver) and 0.1M EDTA (to give 1.0 mM in the final mixture). The resulting suspension was stirred for 15 min, after which 10% aqueous hexadecyltrimethylammonium bromide solution (volume equal to 0.146 times the weight of ground liver) was added dropwise during five min. After stirring for another 30 min, the suspension was centrifuged at 25,000 x g for 20 min and the sediment discarded. Solid ammonium sulphate equivalent to 40% saturation was added to the supernatant solution during a 30 min period. The suspension was stirred for one hour; then centrifuged at 25,000 x g for 20 min and the sediment discarded. Additional ammonium sulphate was added to the supernatant solution to bring the relative saturation to 55% and stirring was continued for another hour. The resulting suspension was centrifuged at 25,000 x g for 30 min and the precipitate was collected. The precipitate, containing enzyme activity, was dissolved in a minimum volume of 0.01M sodium phosphate, pH 6.2, and dialyzed against ten volumes of the same buffer for 17 hr. The dialyzing buffer was changed three times during the dialysis run. After dialysis, the enzyme solution was centrifuged at 25,000 x g for 30 min and the precipitated protein was discarded. The conductivity of the dialyzed solution was adjusted using distilled water to 1.0-1.5 times the conductivity of the equilibrating buffer

for the DEAE-cellulose column. The resultant enzyme solution was loaded onto a DEAE-cellulose column (4 x 40 cm), previously equilibrated with 0.01M sodium phosphate, pH 6.2, containing 1.0 mM GSH and 1.0 mM EDTA. After loading, the column was washed with two column volumes of starting buffer. Enzyme activity was then eluted by a linear salt gradient obtained with 4 litres of 0.01M sodium phosphate, pH 6.2, in the mixing bottle and 4 litres of 0.08M sodium phosphate, pH 6.2, in the reservoir. Both solutions contained 1.0 mM GSH and 1.0 mM EDTA. Fractions from the enzyme activity peak were combined and loaded onto a DEAE-sephadex column (2 x 35 cm), previously equilibrated with 0.04M sodium phosphate, pH 6.8, containing 1.0 mM GSH and 1.0 mM EDTA. Before loading, the conductivity of the combined fractions was adjusted to a value equal to the conductivity of the equilibrating buffer. After adsorption of the enzyme the column was washed with two column volumes of starting buffer. Enzyme activity was eluted by a linear salt gradient obtained with 600 ml of 0.04M sodium phosphate, pH 6.8, containing 1.0 mM GSH and 1.0 mM EDTA, in the receiver and 600 ml of 0.2M sodium phosphate, pH 6.8, containing 1.0 mM GSH and 1.0 mM EDTA, in the reservoir. Appropriate fractions from the single peak were pooled and concentrated by ammonium sulphate precipitation.

8. Kinetic Experiments

To get an accurate value of initial velocity, triplicate assays were performed for every point present on the velocity versus substrate concentration line in all the kinetic experiments described here. Wherever two out of three values were concordant or very close the third one was then discarded. In cases where triplicate assay values were not concordant then an average of three values was taken.

9. Data Processing

The kinetic data were processed by a CDC 6400 computer using FORTRAN programs as described by Cleland (130). The fits to appropriate equations were made using a least squares method and on the assumption of equal variances for experimental velocities. Preliminary reciprocal plots of initial velocity versus substrate concentrations were prepared in order to check the linearity of the lines. When the lines were linear, the experimental data were fitted to rate equation a by a program which provided the values for K_m/V, $\frac{1}{V}$, standard errors of their estimates and weighting factors. Secondary plots of slopes and intercepts (obtained from fits to equation a) were made against inhibitor concentration (inhibition studies) or reciprocal of changing fixed substrate concentration (initial velocity studies) to determine the type of inhibition or initial velocity pattern. The replots were also fitted to a straight line using weighting factors supplied by fits to equation a. The fits were then

made to an overall rate equation describing the observed type of inhibition or initial velocity pattern. Initial velocity data displaying intersecting lines were fitted to the sequential mechanism rate equation b, assuming either substrate A or B binds first to the enzyme. The inhibition data corresponding to linear competitive inhibition, linear noncompetitive inhibition and linear uncompetitive inhibition were fitted to equation c, d and e respectively. The substrate activation data (esterase reaction) were fitted to equation f.

$$v = \frac{VA}{K + A} \qquad (a)$$

$$v = \frac{VAB}{K_{ia}K_b + K_aB + K_bA + AB} \qquad (b)$$

$$v = \frac{VA}{K(1 + I/K_i) + A} \qquad (c)$$

$$v = \frac{VA}{K(1 + I/K_{is}) + A(1 + I/K_{ii})} \qquad (d)$$

$$v = \frac{VA}{K + A(1 + I/K_i)} \qquad (e)$$

$$v = \frac{V_2 + V_1K_2/(1 - V_1/V_2)S}{1 + K_2/(1 - V_1/V_2)S + K_1K_2/(1 - V_1/V_2)S^2} \qquad (f)$$

EXPERIMENTAL RESULTS

A. ENZYME PURIFICATION

1. DEAE-cellulose Chromatography

Human liver aldehyde dehydrogenase was purified as described by Blair and Bodley (44) with some modifications. The isolation and purification procedure is described under Methods. The first modification introduced was the inclusion of 1.0 mM GSH and 1.0 mM EDTA in the DEAE-cellulose column chromatography. These additions increased recovery from this column from 60% to 90%. The replacement of GSH with mercaptoethanol or cysteine also improved the recovery, though to a lesser extent than that obtained with GSH. In order to rule out the possibility of sulfhydryl compound activation, the direct effect of GSH on enzyme activity in the assay system was studied. 10^{-3} GSH in the assay system did not show any effect on the enzyme activity.

Some other commercially available ion-exchangers and gels were also tried in an attempt to increase the extent of purification.

2. PAB-cellulose Chromatography

The passage of a crude extract of this enzyme through a PAB-cellulose column previously equilibrated with 0.01M sodium pyrophosphate, pH 6.0, gave 1.5 fold purification. Similar treatment of the dialyzed 40 - 55% $(NH_4)_2SO_4$ precipitate resulted in two fold purification. The enzyme was

not adsorbed by PAB-cellulose under the conditions used; purification resulted from adsorption of impurities.

3. BD-cellulose Chromatography

The fraction obtained by $(NH_4)_2SO_4$ precipitation was dialyzed and loaded on a column which had been equilibrated with 0.01M sodium phosphate, pH 6.0. The enzyme was adsorbed so tightly that sodium phosphate buffers of increasing ionic strengths up to 0.08M did not elute it. The addition of NAD^+ or acetaldehyde to the eluting buffer (0.01M sodium phosphate, pH 6.0) was not found helpful. Attempts were also made to elute activity by increasing or decreasing the pH in association with increasing ionic strength but no success was achieved. At pH 8.0 only traces of activity were detected in the effluent. The addition to the eluting buffer (0.01M sodium phosphate, pH 6.0) of compounds having aromatic rings in their structure such as sodium benzoate, dimethylaminobenzaldehyde and sodium phthalate was also tried in an attempt to disrupt hydrophobic interactions between the enzyme and the benzene rings of BD-cellulose. However, this approach also failed to desorb the enzyme. The addition of GSH or EDTA or both in combination with some of the agents referred to above was also ineffective. No better results were obtained when sodium pyrophosphate buffer at different ionic strengths and pH values was used in place of sodium phosphate.

4. Calcium-phosphate Gel Chromatography

Small portions of calcium-phosphate gel (11% solids) were added with stirring at 4° to a DEAE-cellulose purified enzyme fraction, adjusted to an ionic strength equivalent to 0.01M sodium phosphate, pH 6.0, until no enzyme activity was detected in the supernatant solution.

The gel was removed by centrifugation and washed with an equal volume of 0.01M sodium phosphate, pH 6.0. After 5 min of stirring, the gel was again collected by centrifugation. The enzyme was eluted by stirring the gel with the same buffer containing 10% $(NH_4)_2SO_4$. This step was repeated. The first elution step gave 2.5-fold purification with 72% recovery of the starting enzyme activity. Seventeen percent of the initial activity was detected in the second fraction.

5. Sephadex-gel Filtration

Deitrich in his paper on the purification of human liver aldehyde dehydrogenase (62) reported a molecular weight of 100,000 daltons for this enzyme whereas the molecular weight reported by Blair and Bodley was 200,000 daltons (44). This discrepancy suggested that either the enzyme dissociated under certain conditions or error occurred in the determination of molecular weight in one of the laboratories. First of all, their findings were checked by running gel filtration experiments under the conditions they employed to isolate and chromatograph the enzyme. An

upward flow technique using 0.005M sodium phosphate, pH 7.0, as the filtration buffer was employed. It was found that enzyme, prepared either by Kraemer and Deitrich's procedure or Blair and Bodley's, emerged at the void volume of a sephadex G-100 column (2.5 x 30 cm). Proteins of molecular weights above the upper limit of fractionation range (4,000-150,000) are excluded from sephadex G-100. In order to see whether the enzyme behaved differently at different concentrations, two solutions, one at 60 mg protein/ml, the other at 4 mg protein/ml were run through sephadex G-100 (2.5 x 30 cm) and G-200 (2.5 x 90 cm) columns both in the presence and absence of EDTA. The elution volume was the same at both concentrations. Furthermore, a parallel experiment run in 0.01M sodium phosphate, pH 7.0, gave the same results. Finally, no change was observed in enzyme elution pattern as a function of flow rate.

6. Isoelectric Focusing

Further purification of DEAE-cellulose purified enzyme was attempted by the recently developed technique of isoelectric focusing. However, the enzyme precipitated during every run and lost its activity. The observation of virtually total loss of enzyme activity prompted the search for a solution to this problem. Incubation experiments were set up to examine the direct effect of ampholytes on enzyme activity. It was found that when enzyme was incubated in the presence of different concentrations of ampholyte in

0.005M sodium phosphate at pH 6.0 for 36 hrs, 50%, 72% and 75% of the original activity was lost at ampholyte concentrations of 2%, 4% and 6%, respectively. It was also observed that 93% of the enzyme activity could be recovered if glycerol at 20% concentration was present in the incubation medium. The replacement of glycerol by 1.0 mM EDTA did not protect the enzyme against inhibition by ampholytes. The ineffectiveness of EDTA indicated that enzyme inhibition by ampholytes was not due to the presence of heavy metals in commercial preparation of ampholine carrier ampholytes. Unfortunately, the use of a glycerol density gradient in place of sucrose in the electrofocusing column did not prevent precipitation and inactivation of the enzyme.

B. KINETIC STUDIES

1. Dehydrogenase Reaction

Initial velocity and inhibition studies were used in order to investigate the kinetic mechanism of human liver aldehyde dehydrogenase. Initial velocity studies were performed by varying one substrate at a fixed concentration of the other substrate (Bisubstrate mechanism). The very low K_m value for acetaldehyde makes it impossible to obtain accurate initial rates with this compound as variable substrate. To solve this problem, two approaches were attempted. First, certain NAD^+-analogues have been found to increase the concentration of acetaldehyde required for half-maximal velocity with alcohol dehydrogenase (109). It was hoped that this

might occur with human liver aldehyde dehydrogenase. Apart from this, comparison of the kinetic data obtained with various NAD^+-analogues could provide information on the essentiality of the functional groups of the NAD^+ molecule in the dehydrogenase reaction. Second, the use of other aldehyde substrates of higher K_m values should also overcome the problem of obtaining accurate initial rates.

a. Coenzyme activity of NAD^+-analogues and Michaelis constants for aldehyde substrates

Kinetic constants obtained using NAD^+-analogues as coenzymes (variable substrates) and acetaldehyde as the fixed saturating substrate are compared with corresponding values for NAD^+ in Table III. It is apparent that the highest V_{max} value for these analogues (obtained with 3-acetylpyridine-AD^+) is only 6% of the V_{max} value for NAD^+ while K_m values vary from 5.5×10^{-6}M, for thionicotinamide-AD^+, to 1.1×10^{-2}M, for deamino-NAD^+. In contrast, the highest V_{max} values for NAD^+-analogues with yeast aldehyde dehydrogenase and bovine liver aldehyde dehydrogenase were 53% (deamino-NAD^+) and 85% (3-acetylpyridine-AD^+), respectively, of the V_{max} value for NAD^+ (107,108).

When equal amounts (0.6 mM) of NAD^+ and NAD^+-analogues were used in the assay mixtures, thionicotinamide-AD^+ and pyridine-3-aldehyde-AD^+ inhibited the dehydrogenase activity whereas deamino-NAD^+, pyridine-3-aldehyde-HD^+, 3-acetylpyridine-AD^+ and 3-acetylpyridine-HD^+ had no effect. The kinetic data presented in Table IV were substituted into

TABLE III

MICHAELIS CONSTANTS AND MAXIMAL VELOCITIES FOR NAD^+-ANALOGUES TESTED AS COENZYMES FOR HUMAN LIVER ALDEHYDE DEHYDROGENASE

K_m and V_{max} values were calculated from data plotted in conventional double reciprocal form. Reaction mixtures contained: 33 mM sodium pyrophosphate, pH 9.3; 2 mM acetaldehyde; 0.07 unit of enzyme and the NAD^+-analogue varied over a ten-fold range in concentration. Total volume one ml.

Analogue	K_m	Relative V_{max}
	M	%
NAD^+	4.0×10^{-4}	100.0
Deamino-NAD^+	1.1×10^{-2}	4.1
3-Acetylpyridine-AD^+	3.4×10^{-4}	6.2
3-Acetylpyridine-HD^+	6.6×10^{-4}	2.5
Pyridine-3-aldehyde-AD^+	1.0×10^{-4}	3.5
Pyridine-3-aldehyde-HD^+	2.5×10^{-3}	1.4
Thionicotinamide-AD^+	5.5×10^{-6}	3.0

equation 4 for competing substrates to obtain a theoretical reaction rate value for each NAD^+-analogue.

$$v = \frac{V_{NAD}\left[NAD\right] + V_{analog}\,\frac{K_{NAD}}{K_{analog}}\left[analog\right]}{K_{NAD} + \left[NAD\right] + \frac{K_{NAD}}{K_{analog}}\left[analog\right]} \qquad (4)$$

As can be seen from Table IV, the experimental reaction rate values are in agreement with the theoretical reaction rate values in all cases except 3-acetylpyridine-AD^+ and 3-acetylpyridine-HD^+. Results of kinetic studies with NAD^+-analogues indicated that none of the analogues tested would be useful as a coenzyme in initial velocity studies with human liver aldehyde dehydrogenase.

The second approach involved testing various other aldehydes to determine their concentrations giving half-maximal velocity. It was found for hydroxyaldehydes (glycolaldehyde and glyceraldehyde) that the concentrations giving half-maximal velocity were far greater than those for simple aliphatic aldehydes (68). For example, the Michaelis constants for glyceraldehyde and acetaldehyde were found to be 4×10^{-4}M and $\sim 10^{-7}$M, respectively. Thus, it was decided to use glyceraldehyde as substrate and NAD^+ as coenzyme in the initial velocity studies.

TABLE IV

INHIBITORY EFFECT OF NAD^+-ANALOGUES ON HUMAN LIVER ALDEHYDE DEHYDROGENASE

Reaction mixtures contained: 33 mM sodium pyrophosphate, pH 9.3; 2 mM acetaldehyde; 0.03 unit of enzyme; 0.6 mM NAD^+ and 0.6 mM of the indicated analogue. Total volume one ml.

Analogue added	Calculated[a] v	Experimental v	Activity of mixture[b]
	ΔA_{340} min^{-1}	ΔA_{340} min^{-1}	%
None (NAD^+ alone)	—	0.035	100
Deamino-NAD^+	0.035	0.035	100
3-Acetylpyridine-AD^+	0.022	0.035	100
3-Acetylpyridine-HD^+	0.026	0.035	100
Pyridine-3-aldehyde-AD^+	0.012	0.016	48
Pyridine-3-aldehyde-HD^+	0.033	0.032	92
Thionicotinamide-AD^+	0.003	0.004	11

a Equation 4 was used to calculate these values

b Activity of mixture; expressed as % of activity with NAD^+ alone. Calculated from the values shown in the "Experimental" column.

b. Initial velocity studies

i. Initial velocity patterns

Initial velocity studies using glyceraldehyde as the variable substrate and NAD^+ as the changing fixed substrate were performed in order to determine the manner of addition of substrates to aldehyde dehydrogenase. The double reciprocal plot of initial velocity at pH 9.5 versus variable glyceraldehyde concentration, at different constant concentrations of NAD^+, showed convergent lines. This pattern indicates a sequential mechanism and rules out a ping pong mechanism (Figure 1). The secondary plots of slopes and intercepts from Figure 1 against non-varied substrate concentrations were linear (Figure 2). Therefore, the initial velocity data were fitted to rate equation 2 describing a sequential mechanism. However, this rate equation does not provide any distinction between random or ordered binding of the substrate. When the initial velocity data were plotted with NAD^+ as the variable substrate and glyceraldehyde as the fixed substrate, the lines still appeared to converge (Figure 3), if those lines for fixed glyceraldehyde concentrations giving substrate inhibition were not considered. The secondary plots of intercepts and slopes from Figure 3 versus reciprocal of glyceraldehyde concentration were linear and non-linear, respectively (Figure 4). The kinetic constants calculated from fits of initial velocity data to equation 2 assuming either NAD^+ binds first or glyceraldehyde binds first to the enzyme, are shown in Table V.

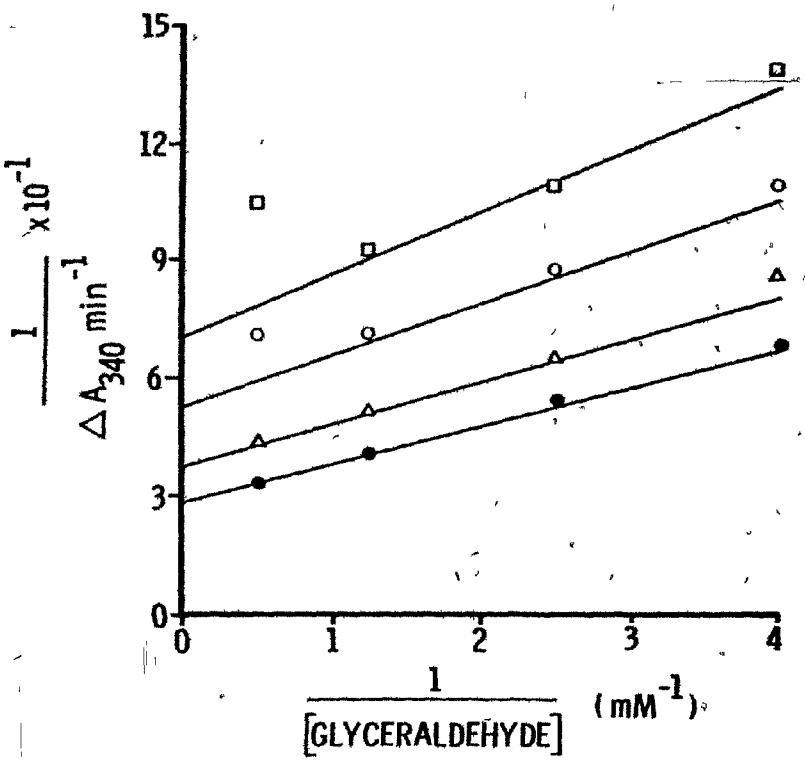

FIGURE 1

Double reciprocal plot with glyceraldehyde as the variable substrate and NAD^+ as the changing fixed substrate at pH 9.5. Reaction mixtures contained: 33 mM sodium pyrophosphate, pH 9.3; 0.018 unit of enzyme; glyceraldehyde as indicated and NAD^+: (□) 0.25 mM; (○) 0.4 mM; (△) 0.8 mM; (●) 2.0 mM. Total volume one ml. Solid lines were calculated from fits to equation (b).

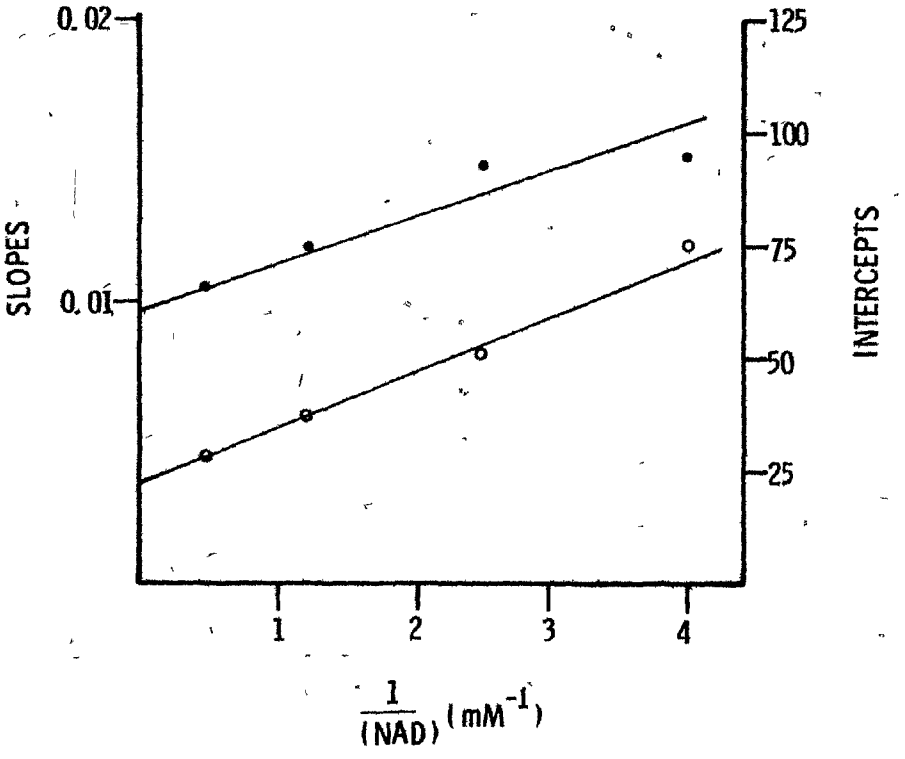

FIGURE 2

Secondary plot of slopes and intercepts versus reciprocal of NAD^+ concentration (•) slope; (o) intercept. Data taken from Figure 1.

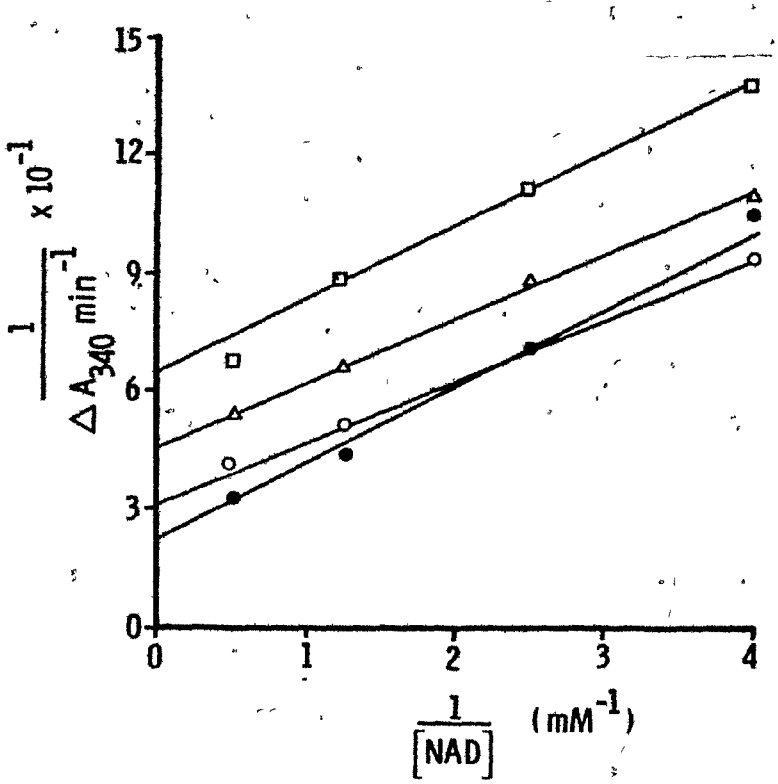

FIGURE 3

Double reciprocal plot with NAD^+ as the variable substrate and glyceraldehyde as the changing fixed substrate at pH 9.5. Reaction mixtures contained: 33 mM sodium pyrophosphate, pH 9.3; 0.018 unit of enzyme; NAD^+ as indicated and glyceraldehyde: (□) 0.25 mM; (Δ) 0.4 mM; (o) 0.8 mM; (●) 2.0 mM. Total volume one ml.

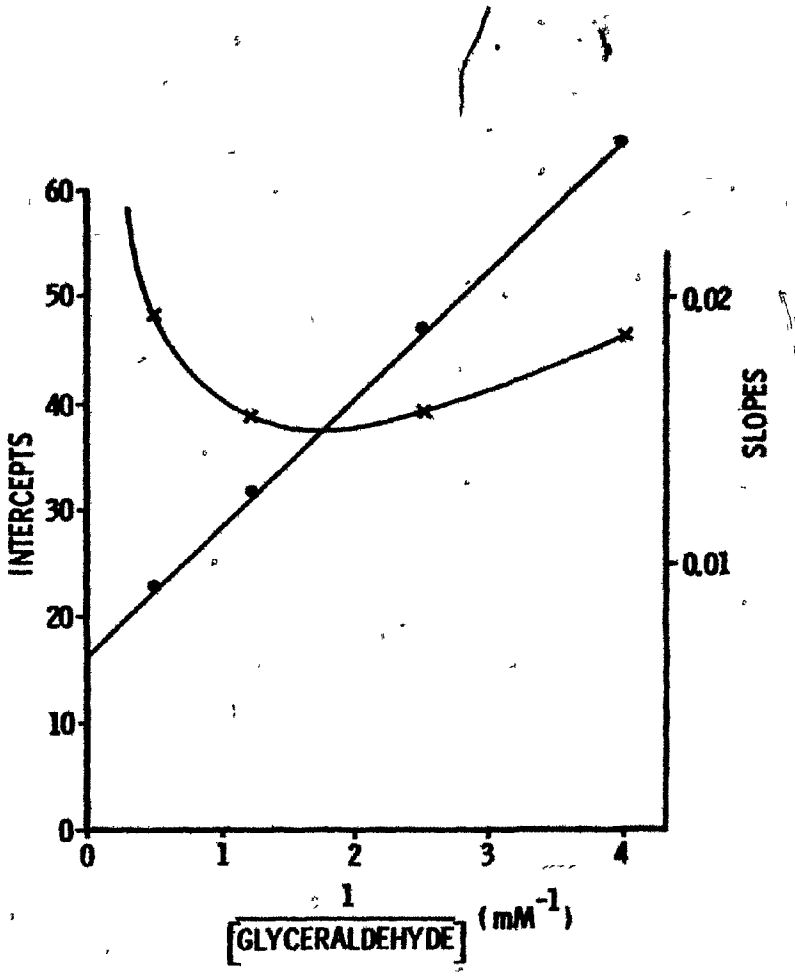

FIGURE 4

Secondary plot of slopes and intercepts versus reciprocal of glyceraldehyde concentration (×) slope; (●) intercept. Data taken from Figure 3.

TABLE V

KINETIC CONSTANTS FOR DEHYDROGENASE REACTION

CALCULATED FROM EQUATION 2

Nomenclature of Cleland (114)

Substrate	K_a	K_b	V	K_{ia}
	mM	mM	ΔA_{340} min^{-1}	mM
A = Glyceraldehyde B = NAD	0.43 ±0.07	0.54 ±0.109	0.045 ±0.003	0.15 ±0.09
A = NAD B = Glyceraldehyde	0.476±0.154	0.385±0.111	0.043±0.005	0.246±0.164

ii. Substrate inhibition

At pH 7.3, the double reciprocal plot of initial velocity data obtained using glyceraldehyde as the variable substrate and NAD^+ as the fixed substrate also gave intersecting lines, consistent with a sequential mechanism (Figure 5). Substrate inhibition (variable substrate glyceraldehyde) at low fixed concentrations of NAD^+ was much more pronounced at low pH, as evident in the upward curvature of the initial velocity patterns. The reciprocal plot of initial velocity against varying concentrations of NAD^+ at different fixed concentrations of glyceraldehyde showed that substrate inhibition by glyceraldehyde was competitive (Figure 6). In other words, only the slopes were affected. Saturating concentrations of NAD^+ overcame the inhibition caused by high concentrations of glyceraldehyde.

iii. Distinction between sequential and ping pong mechanisms

In Figures 1, and 3, the lines appear to be converging as required by a sequential mechanism. However, the lines are not very far from parallel which would be characteristic of a ping pong mechanism (Substrate inhibition introduces an additional complication in interpretation). This type of behavior can easily be misleading in the assignment of a particular mechanism to any enzyme under kinetic investigation. It can be seen that the sequential rate equation 2 has an extra term, $K_{ia}K_b$, when compared to the rate equation 3 for a ping pong mechanism. In cases

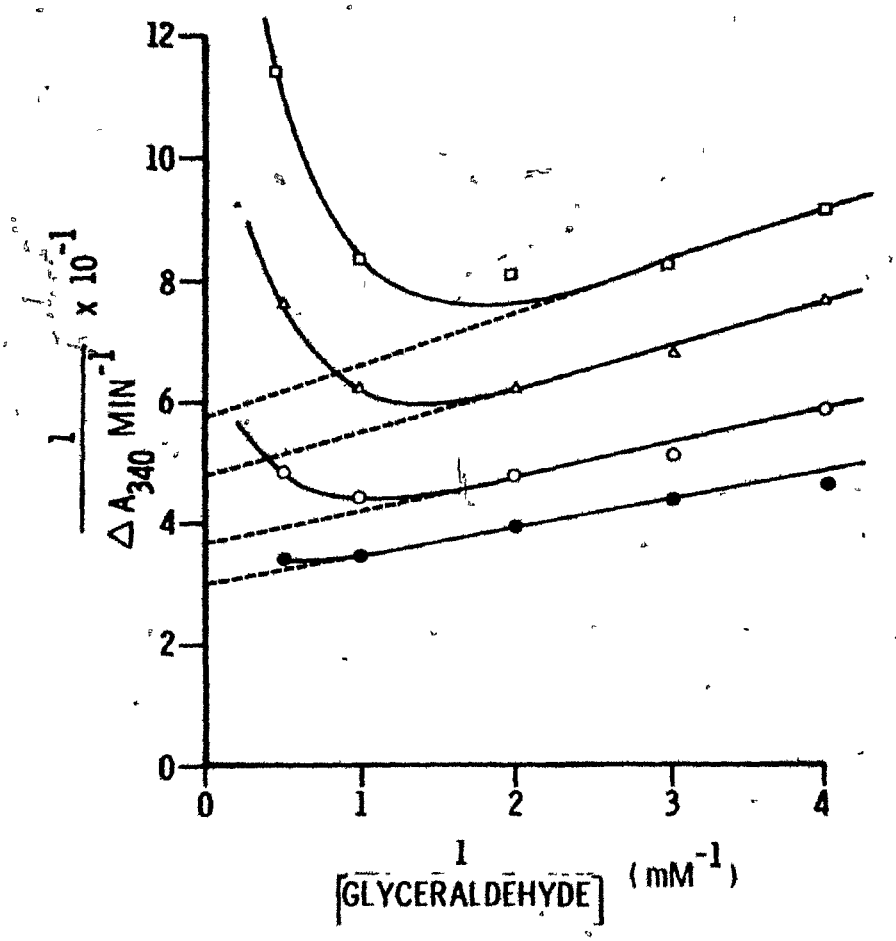

FIGURE 5

Double reciprocal plot with glyceraldehyde as the variable substrate and NAD^+ as the changing fixed substrate at pH 7.3. Reaction mixtures contained: 33 mM sodium pyrophosphate, pH 7.0; 0.08 unit of enzyme; glyceraldehyde as indicated and NAD^+: (□) 0.25 mM; (Δ) 0.4 mM; (○) 0.8 mM; (●) 2.0 mM. Total volume one ml.

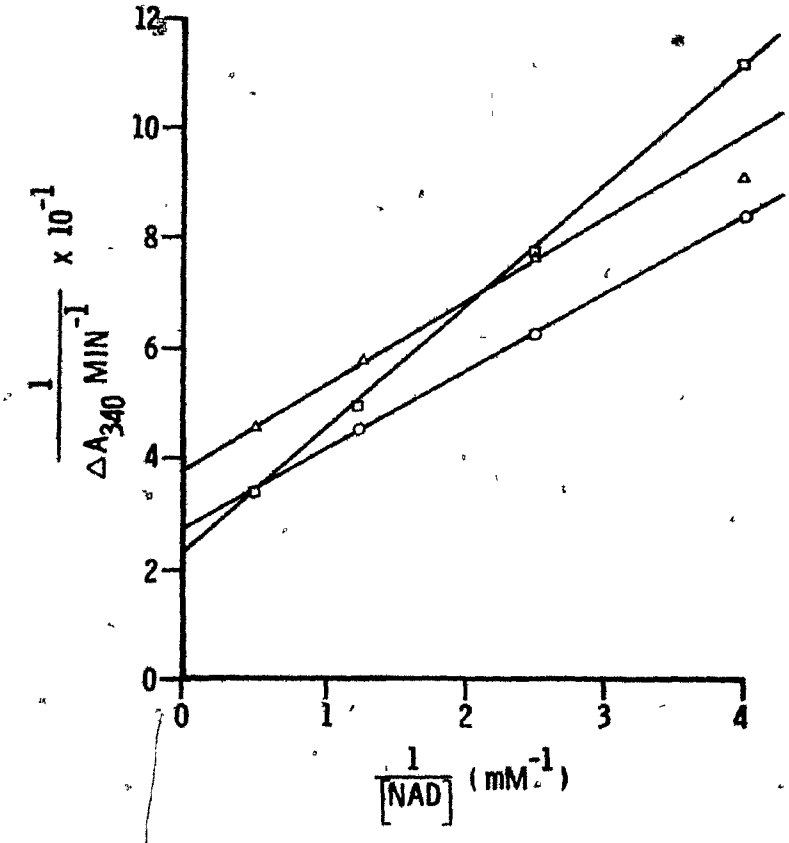

FIGURE 6

Double reciprocal plot with NAD^+ as the variable substrate and glyceraldehyde as the changing fixed substrate at pH 7.3. Reaction mixtures contained: 33 mM sodium pyrophosphate, pH 7.0; 0.08 unit of enzyme; NAD^+ as indicated and glyceraldehyde: (Δ) 0.25 mM; (o) 1.0 mM; (□) 2.0 mM. Total volume one ml.

where the $K_{ia}K_b$ term is very small in comparison to the K_aB and K_bA terms, the sequential rate equation becomes similar to that for a ping pong mechanism. Therefore, the initial velocity pattern would appear parallel rather than clearly converging. A dead-end inhibitor may be employed to aid in making a distinction between these mechanisms. The addition of a constant amount of a competitive inhibitor in the initial velocity studies does not change the actual mechanism (e.g., sequential or ping pong). This is because both the intercept and slope terms in the sequential rate equation, but only the intercept term in the ping pong rate equation, are multiplied by an inhibition factor $(1 + I/K_i)$. In a ping pong mechanism one of the substrate terms will be multiplied by an appropriate $(1 + I/K_i)$ factor but no new constant term will be introduced in the process, i.e., no change in slope occurs. Under certain conditions in a sequential mechanism where the $K_{ia}K_b$ term of the rate equation is very small, the presence of an inhibitor, competitive with respect to the variable substrate, would bring the intersecting point of the double reciprocal plot closer to the intercept-axis. This will occur when the $K_{ia}K_b$ term is multiplied by a $(1 + I/K_i)$ factor. In contrast, the parallel pattern given by a ping pong mechanism will remain parallel in the presence of an inhibitor competitive with respect to a variable substrate.

Therefore, to confirm the sequential nature of substrate addition to the human enzyme, initial velocity

studies were carried out in the presence of a constant amount of a competitive inhibitor. Figures 7 and 8 represent initial velocity patterns in the presence of two inhibitors, thionicotinamide-AD^+ (competitive with respect to NAD^+) and chloral hydrate (competitive with respect to glyceraldehyde) respectively. Inspection of these patterns obtained in the presence of inhibitors indicates that the lines are distinctly convergent, ruling out a ping pong mechanism. Further implications of these data with respect to mechanism are discussed below.

c. Dead-end Inhibition Studies

Various compounds such as adenine, adenosine, inosine, uridine, caffeine, cytidine, hypoxanthine, guanosine, ADP-ribose, N^1-methylnicotinamide, nicotinamide mononucleotide, N'-methylnicotinamide, thionicotinamide-AD^+ and chloral hydrate were tested for their effect on the dehydrogenase activity. Among compounds related to NAD^+, adenine, adenosine, thionicotinamide-AD^+, N'-methylnicotinamide, and ADP-ribose were found to be inhibitory. Chloral hydrate, an aldehyde analogue was also found to inhibit the dehydrogenase reaction.

i. NAD^+-analogues

As illustrated in Figures 9, 11, 13, 15 and 17, adenine, adenosine, thionicotinamide-AD^+, N'-methylnicotinamide and ADP-ribose gave competitive inhibition when NAD^+ was used as the variable substrate at a constant concen- of acetaldehyde equal to 2000 times its K_m value. The secon-

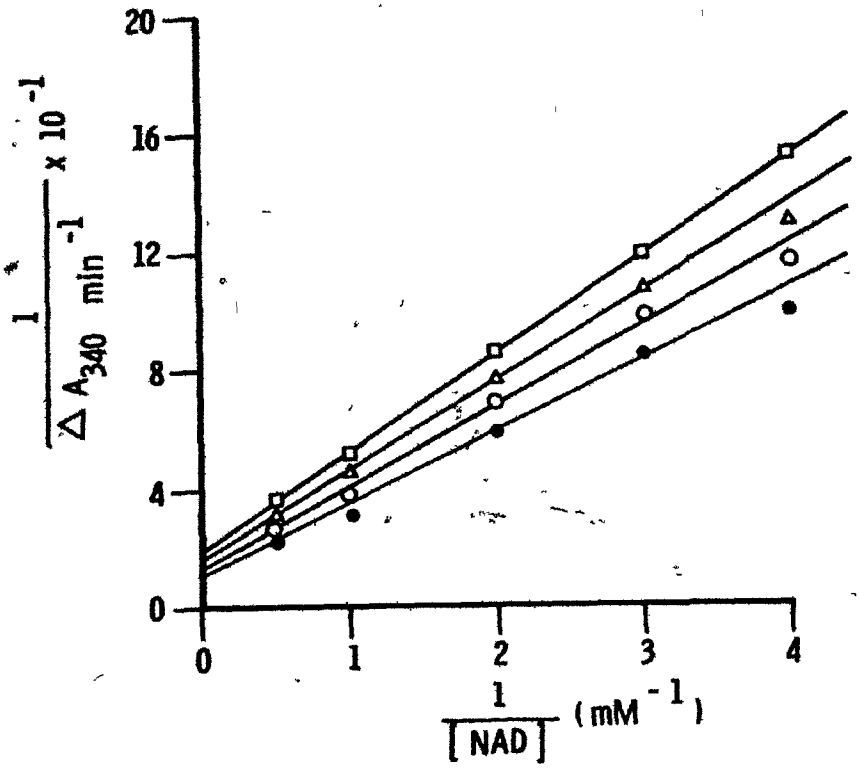

FIGURE 7

Double reciprocal plot with NAD^+ as the variable substrate and glyceraldehyde as the changing fixed substrate in the presence of thionicotinamide-AD^+. Reaction mixtures contained: 33 mM sodium pyrophosphate, pH 9.3; 1.0 mg BSA; 0.05 mM thionicotinamide-AD^+; 0.056 unit of enzyme; NAD^+ as indicated and glyceraldehyde: (□) 0.25 mM; (△) 0.4 mM; (○) 0.8 mM; (●) 2.0 mM. Total volume one ml.

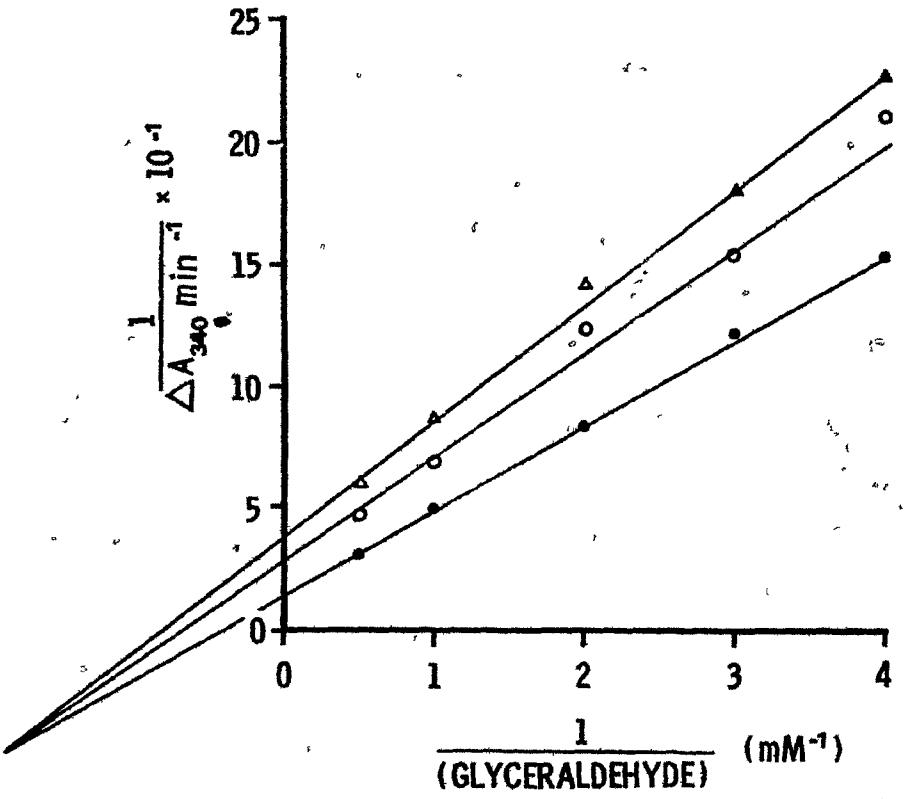

FIGURE 8

Double reciprocal plot with glyceraldehyde as the variable substrate and NAD^+ as the changing fixed substrate in the presence of chloral hydrate. Reaction mixtures contained: 33 mM sodium pyrophosphate, pH 9.3; 0.1 unit of enzyme; 25 µM chloral hydrate; glyceraldehyde as indicated and NAD^+: (Δ) 0.4 mM; (o) 0.6 mM; (•) 2.0 mM. Total volume one ml.

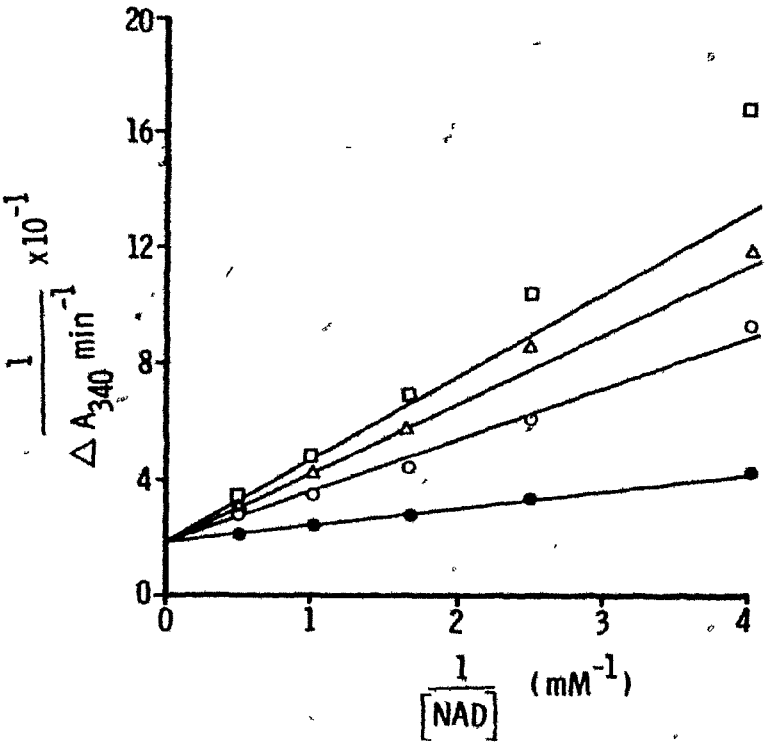

FIGURE 9

Double reciprocal plot with NAD^+ as the variable substrate and adenine as the inhibitor. Reaction mixtures contained: 33 mM sodium pyrophosphate, pH 9.3; 0.022 unit of enzyme; 1.0 mg BSA; 2.0 mM acetaldehyde; NAD^+ as indicated and adenine: (●) absent; (○) 4.0 mM; (△) 6.0 mM; (□) 8.0 mM. Total volume one ml. Solid lines were calculated from fits to equation (c).

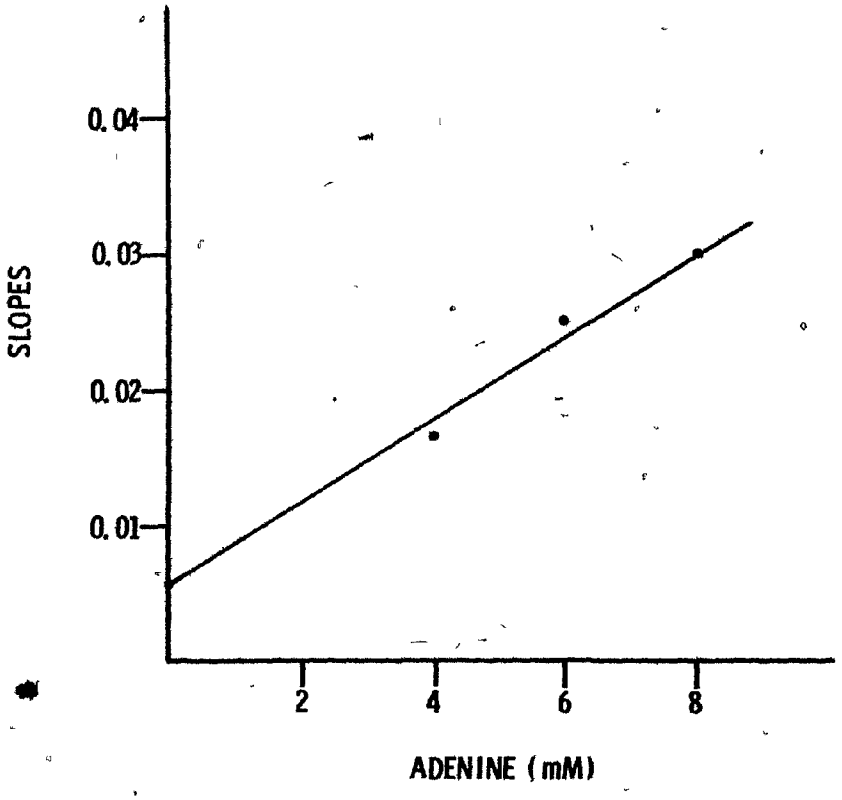

FIGURE 10

Secondary plot of slopes versus adenine concentration. Data taken from Figure 9.

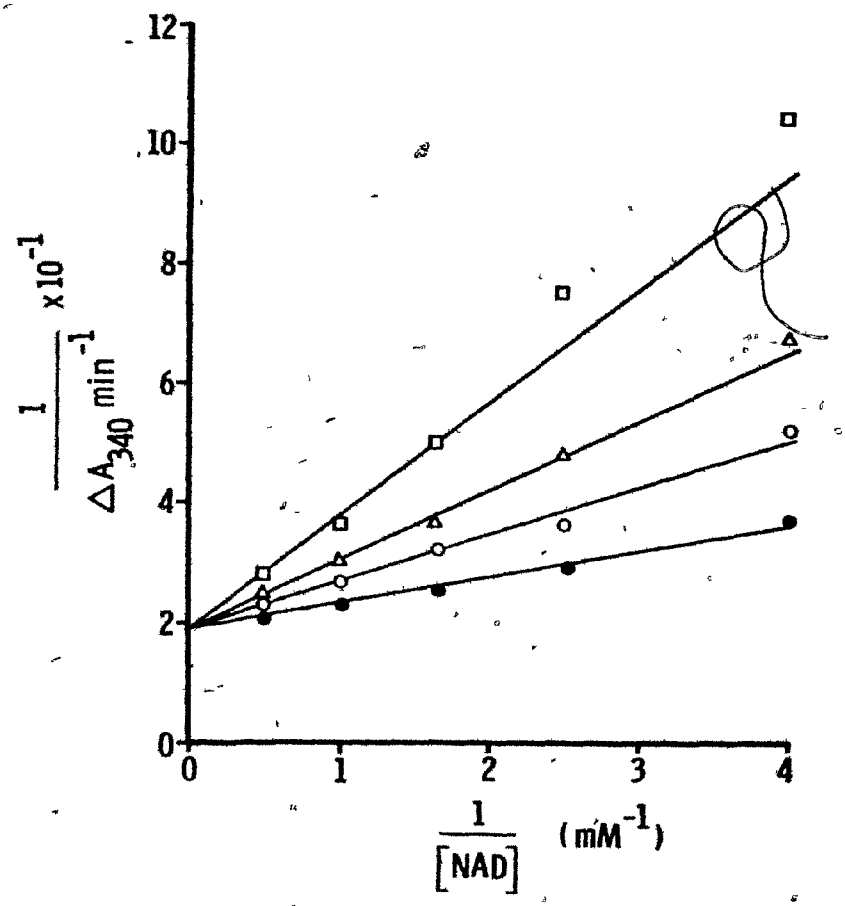

FIGURE 11

Double reciprocal plot with NAD^+ as the variable substrate and adenosine as the inhibitor. Reaction mixtures contained: 33 mM sodium pyrophosphate, pH 9.3; 0.023 unit of enzyme; 1.0 mg BSA; 2.0 mM acetaldehyde; NAD^+ as indicated and adenosine: (●) absent; (○) 0.5 mM; (△) 1.0 mM; (□) 2.0 mM. Total volume one ml. Solid lines were calculated from fits to equation (c).

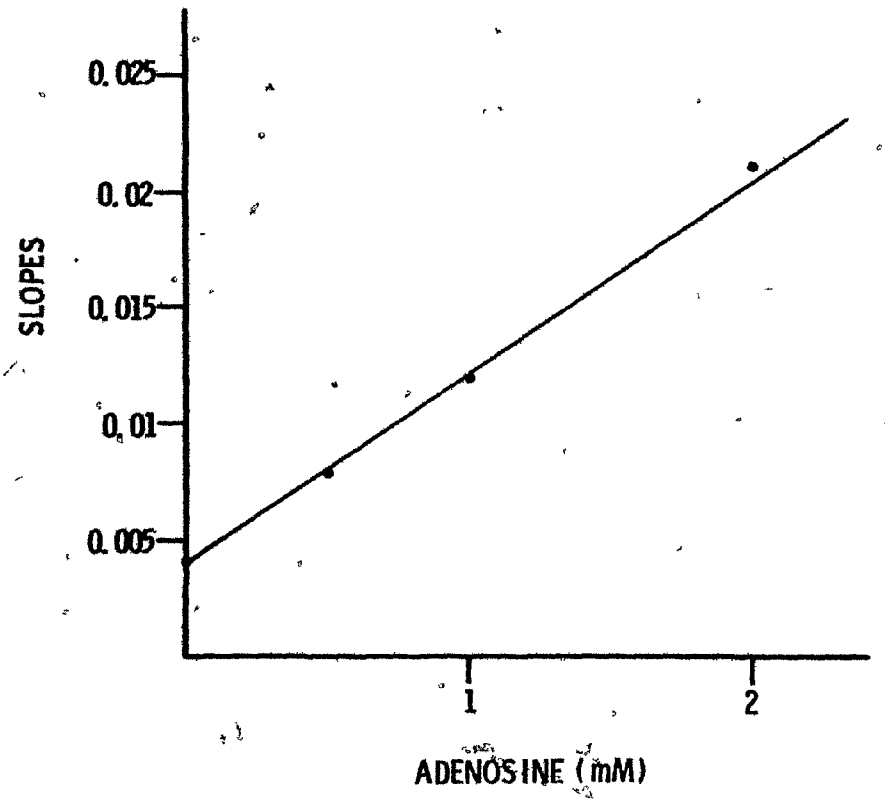

FIGURE 12

Secondary plot of slopes versus adenosine concentration. Data taken from Figure 11.

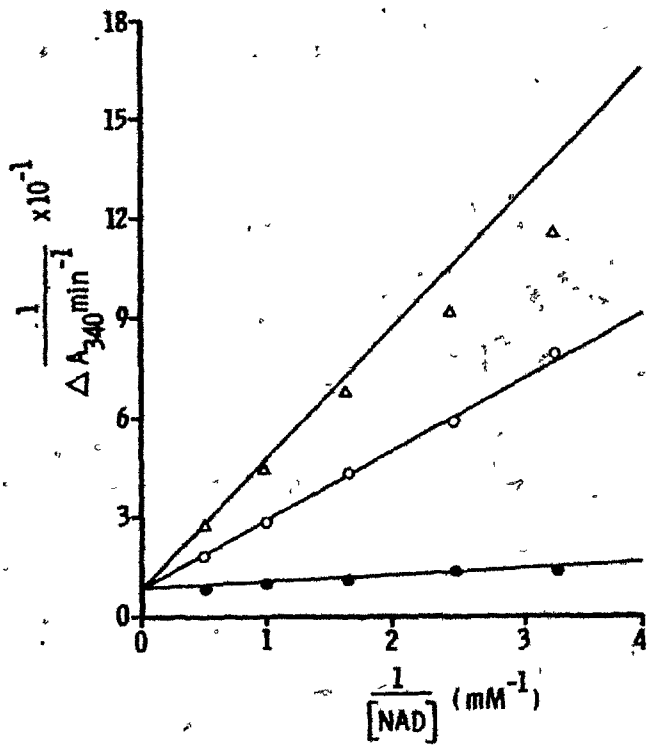

FIGURE 13

Double reciprocal plot with NAD^+ as the variable substrate and thionicotinamide-AD^+ as the inhibitor. Reaction mixtures contained: 33 mM sodium pyrophosphate, pH 9.3; 0.12 unit of enzyme; 2.0 mM acetaldehyde; NAD^+ as indicated and thionicotinamide-AD^+: (●) absent; (o) 0.1 mM; (Δ) 0.2 mM. Total volume one ml. Solid lines were calculated from fits to equation (c).

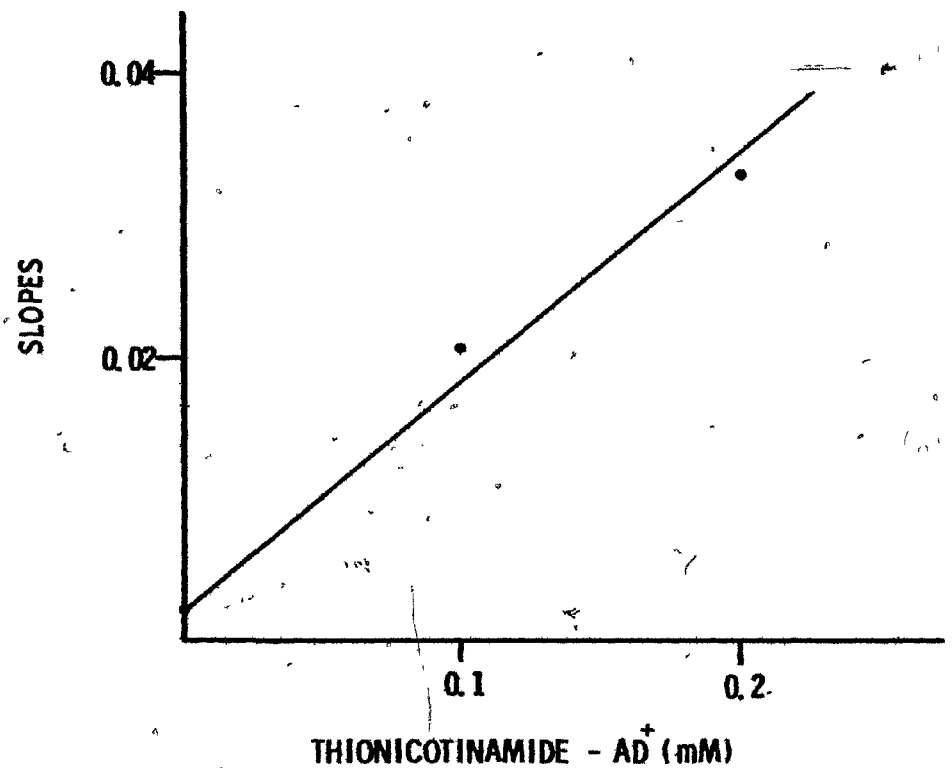

FIGURE 14

Secondary plot of slopes versus thionicotinamide-AD^+ concentration. Data taken from Figure 13.

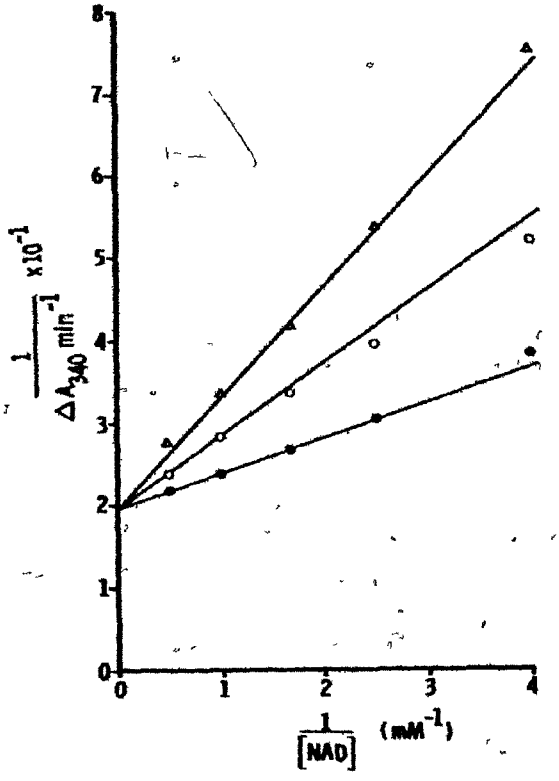

FIGURE 15

Double reciprocal plot with NAD^+ as the variable substrate and N´-methylnicotinamide as the inhibitor. Reaction mixtures contained: 33 mM sodium pyrophosphate, pH 9.3; 0.045 unit of enzyme; 2.0 mM acetaldehyde; NAD^+ as indicated and N´-methylnicotinamide; (●) absent; (○) 10 mM; (△) 20 mM. Total volume one ml. Solid lines were calculated from fits to equation (c).

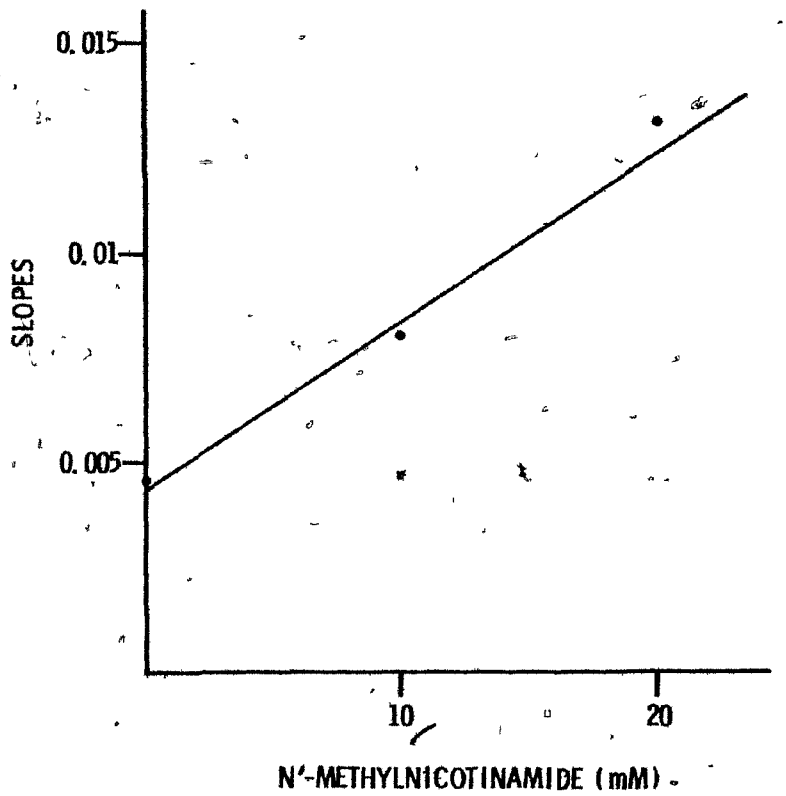

FIGURE 16

Secondary plot of slopes versus N'-methylnicotinamide concentration. Data taken from Figure 15.

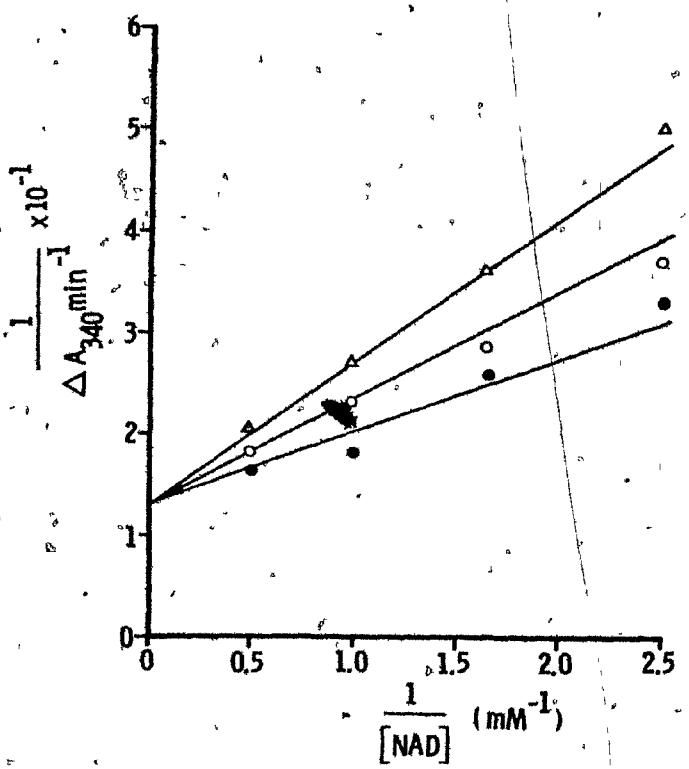

FIGURE 17

Double reciprocal plot with NAD^+ as the variable substrate and ADP-ribose as the inhibitor. Reaction mixtures contained: 33 mM sodium pyrophosphate, pH 9.3; 2.0 mM acetaldehyde; 0.057 unit of enzyme; NAD^+ as indicated and ADP-ribose: (●) absent; (○) 5 mM; (Δ) 10 mM. Total volume one ml. Solid lines were calculated from fits to equation (c).

dary plots of slopes versus the appropriate inhibitor concentrations were linear (Figures 10, 12, 14 and 16). K_i values (slope) for adenine, adenosine, N´-methylnicotinamide and thionicotinamide-AD^+ were calculated to be 1.92 ± 0.16 mM, 0.58 ± 0.06 mM, 9.28 ± 0 98 mM and 11.6 ± 0.8 µM, respectively.

Inhibition by N´-methylnicotinamide and thionicotinamide-AD^+ was noncompetitive with respect to glyceraldehyde when NAD^+ was the fixed substrate at a concentration equal to 5 times K_m, as shown in Figures 18 and 20. Both inhibitors gave linear secondary plots of slopes and intercepts against inhibitor concentration (Figures 19 and 21). K_i values for N´-methylnicotinamide were 11.6 ± 2.1 mM (slope) and 42.3 ± 11.1 mM (intercept). K_i values for thionicotinamide-AD^+ were 59.4 ± 11.9 µM (slope) and 0.177 ± 0.026 mM (intercept).

Adenine and adenosine showed uncompetitive inhibition with respect to glyceraldehyde when NAD^+ was present at a constant concentration equal to 5 times its K_m value (Figures 22 and 24). The secondary plots of intercepts versus inhibitor concentration were linear, as represented in Figures 23 and 25. K_i values (intercept) for adenine and adenosine were 7.68 ± 0.36 mM and 2.16 ± 0.12 mM, respectively.

11. Aldehyde analogues

Chloral hydrate, an analogue of acetaldehyde which is not oxidized by the enzyme gave a competitive inhibition pattern when glyceraldehyde was the variable substrate and NAD^+ the fixed substrate (concentration equal

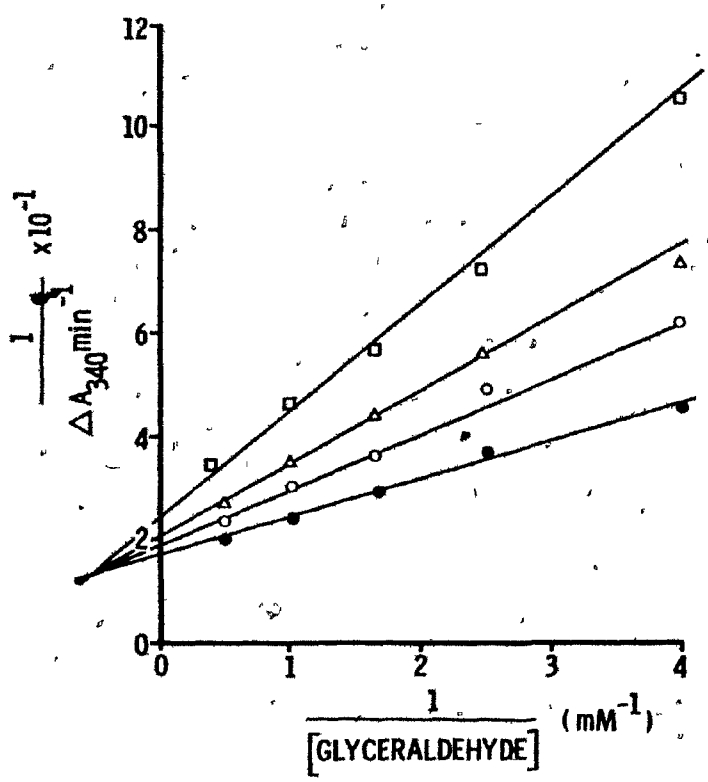

FIGURE 18

Double reciprocal plot with glyceraldehyde as the variable substrate and N'-methylnicotinamide as the inhibitor. Reaction mixtures contained: 33 mM sodium pyrophosphate, pH 9.3; 0.045 unit of enzyme; 2.0 mM NAD^+; glyceraldehyde as indicated and N'-methylnicotinamide: (●) absent; (○) 5 mM; (△) 10 mM; (□) 20 mM. Total volume one ml. Solid lines were calculated from fits to equation (d).

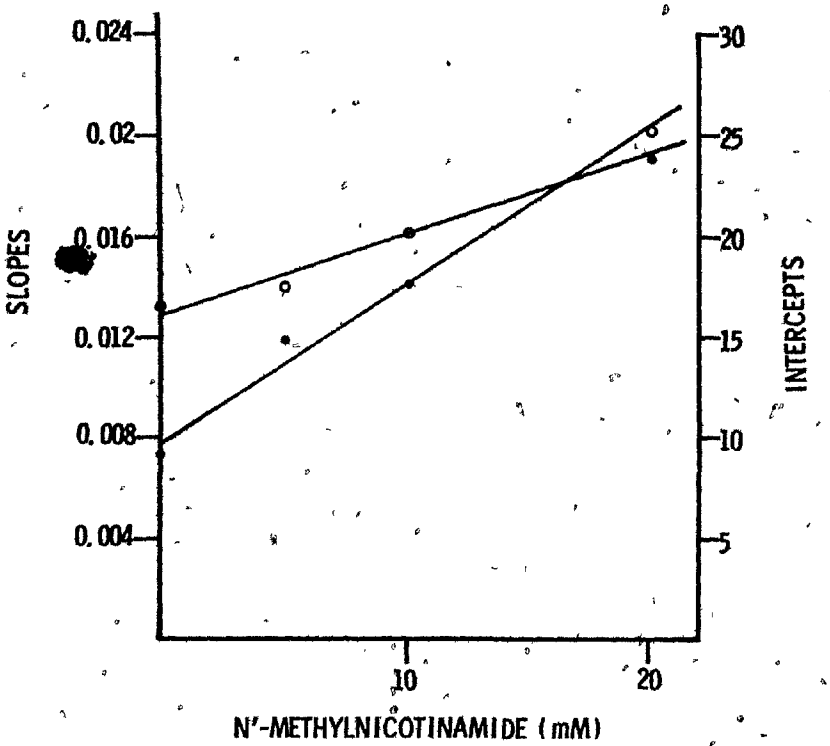

FIGURE 19

Secondary plot of slopes and intercepts versus N'-methylnicotinamide concentration. (●) slope; (○) intercept. Data taken from Figure 18.

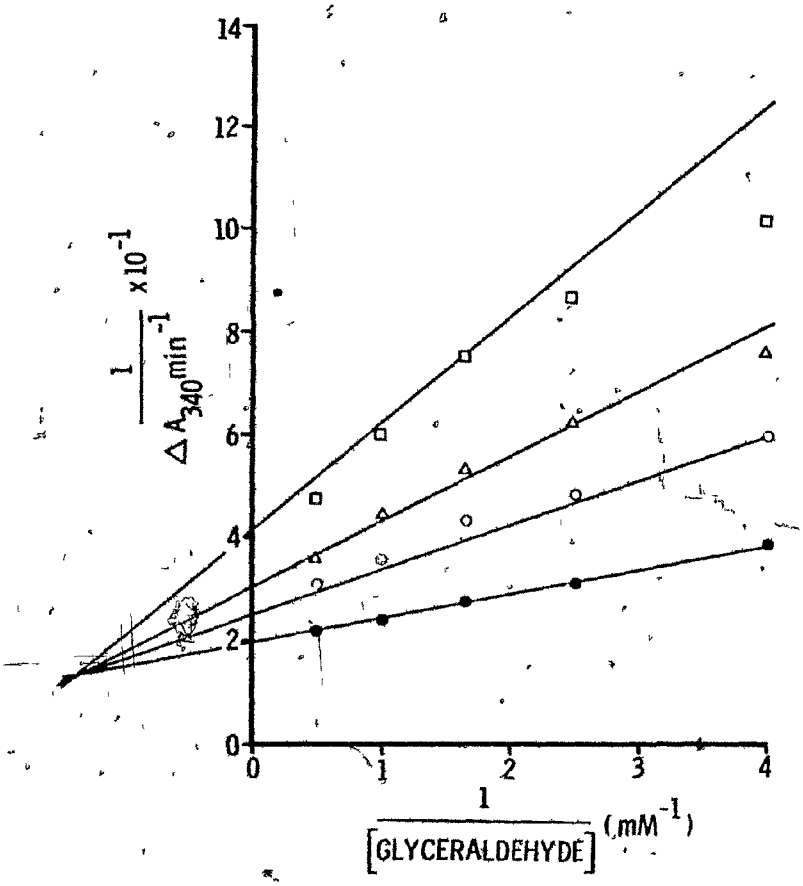

FIGURE 20

Double reciprocal plot with glyceraldehyde as the variable substrate and thionicotinamide-AD^+ as the inhibitor. Reaction mixtures contained: 33 mM sodium pyrophosphate; 0.054 unit of enzyme; 2.0 mM NAD^+; glyceraldehyde as indicated and thionicotinamide-AD^+: (●) absent; (○) 0.05 mM; (△) 0.1 mM; (□) 0.2 mM. Total volume one ml. Solid lines were calculated from fits to equation (d).

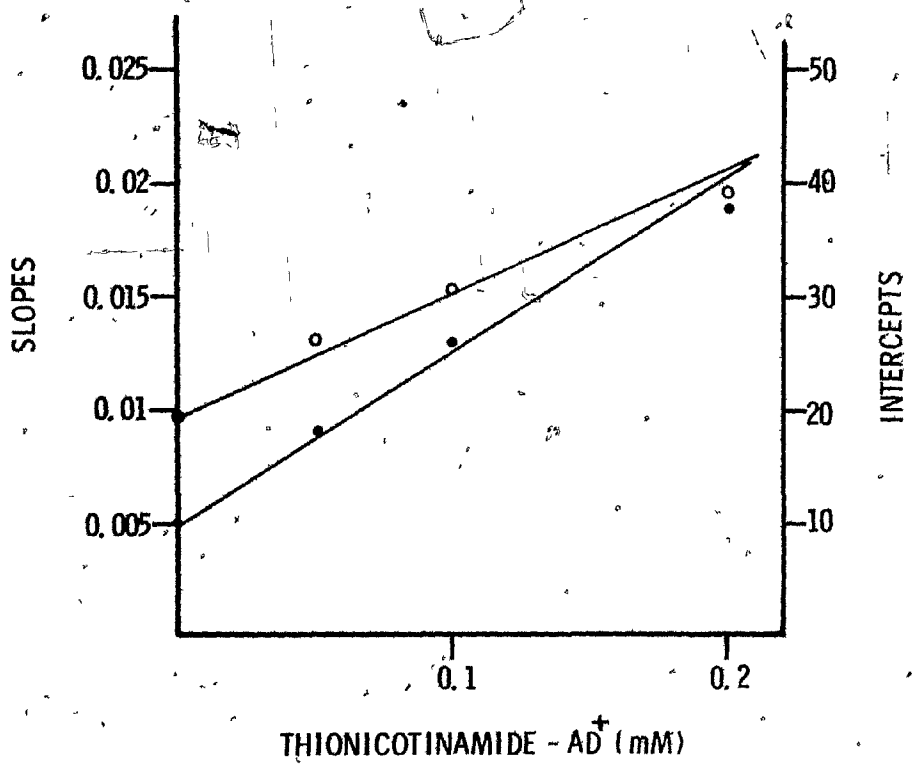

FIGURE 21

Secondary plot of slopes and intercepts versus thionicotinamide-AD^+ concentration. (●) slope; (○) intercept. Data taken from Figure 20.

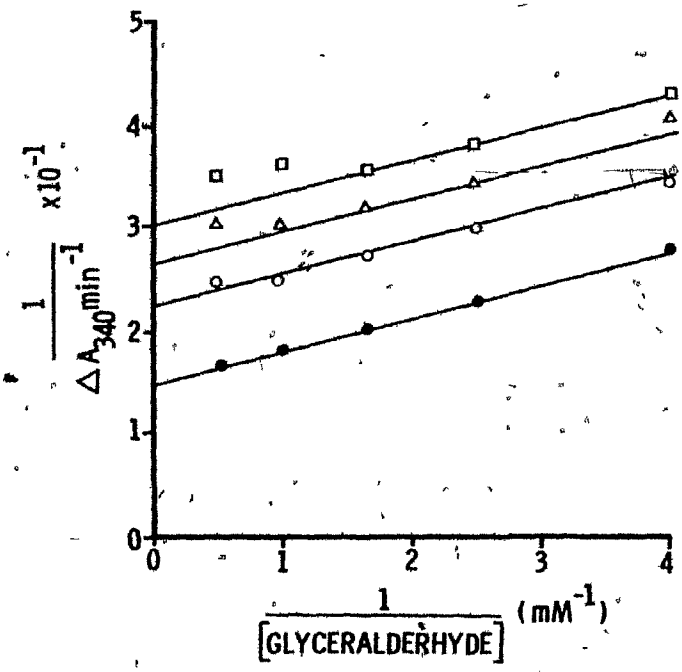

FIGURE 22

Double reciprocal plot with glyceraldehyde as the variable substrate and adenine as the inhibitor. Reaction mixtures contained: 33 mM sodium pyrophosphate, pH 9.3; 0.022 unit of enzyme; 1.0 mg BSA; 2.0 mM NAD^+; glyceraldehyde as indicated and adenine: (●) absent; (○) 4.0 mM; (△) 6.0 mM; (□) 7.6. Total volume one ml. Solid lines were calculated from fits to equation (e).

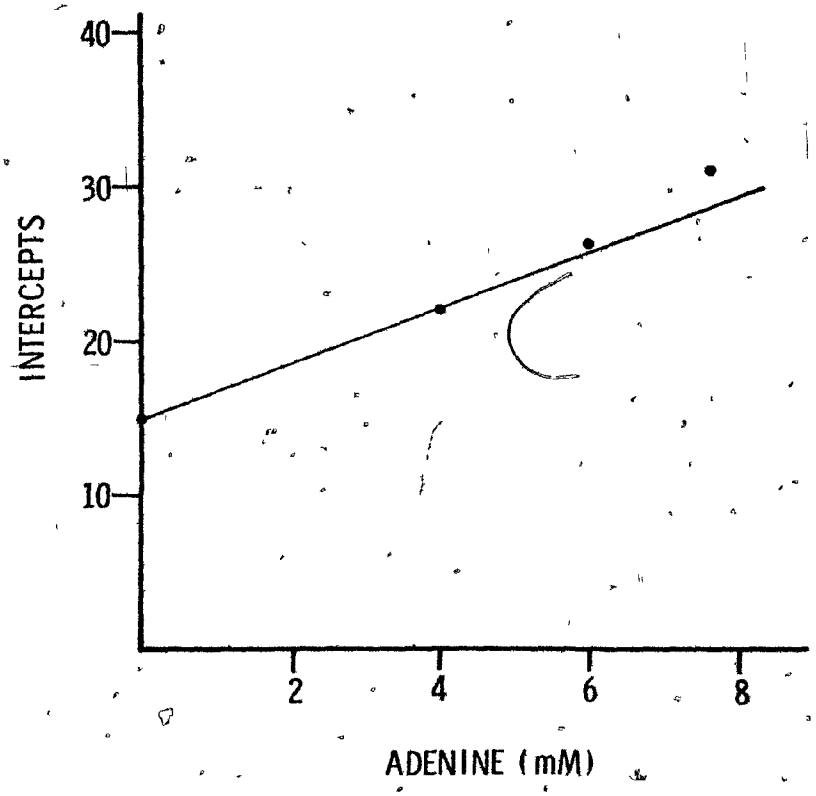

FIGURE 23

Secondary plot of intercepts versus adenine concentration. Data taken from Figure 22.

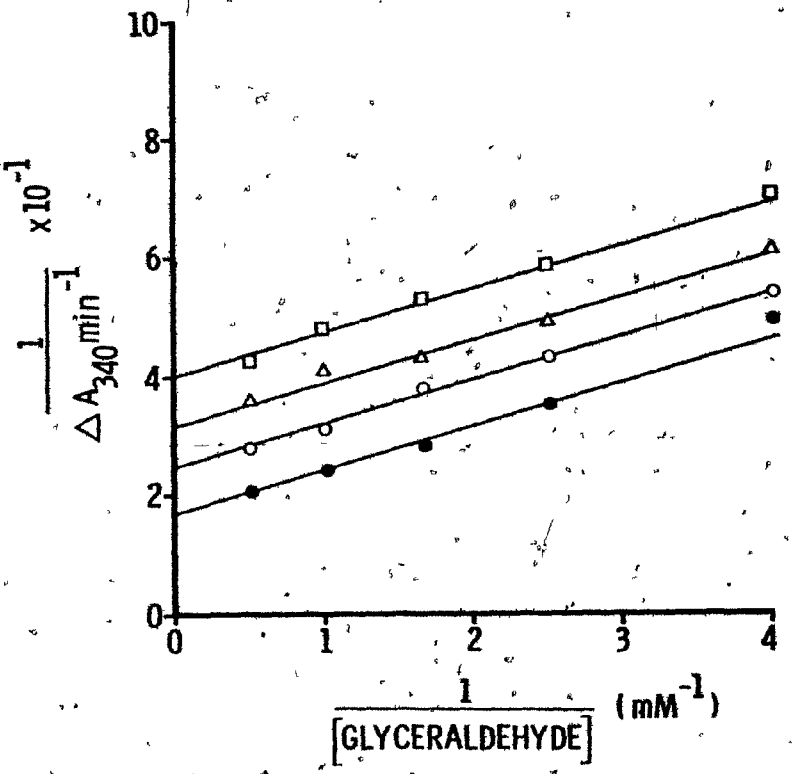

FIGURE 24

Double reciprocal plot with glyceraldehyde as the variable substrate and adenosine as the inhibitor. Reaction mixtures contained: 33 mM sodium pyrophosphate, pH 9.3; 0.037 unit of enzyme; 2.0 mM NAD^+; glyceraldehyde as indicated and adenosine: (●) absent; (○) 1.0 mM; (△) 2.0 mM; (□) 3.0 mM. Total volume one ml. Solid lines were calculated from fits to equation (e).

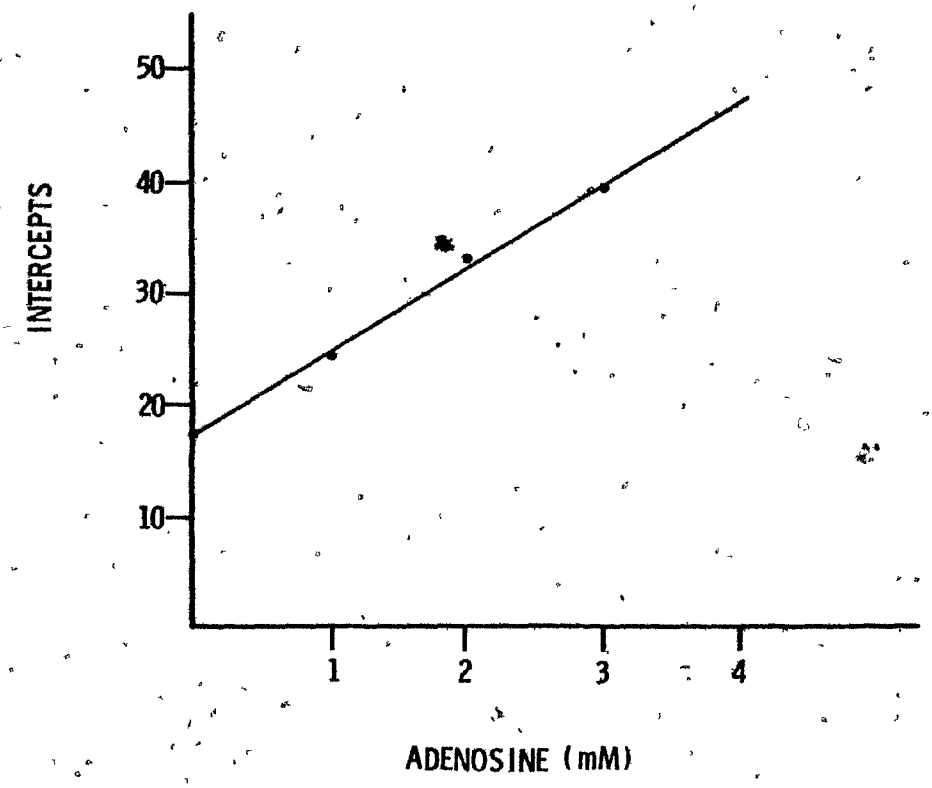

FIGURE 25

Secondary plot of intercepts versus adenosine concentration. Data taken from Figure 24.

to 5 times the K_m), as shown in Figure 26. The replot of slopes versus varying concentration of inhibitor was linear (Figure 27). The K_1 value (slope) was found to be 4.3 ± 0.3 μM. Inhibition by chloral hydrate was noncompetitive with respect to NAD^+ when acetaldehyde at 2 mM was used as the fixed substrate (Figure 28). The secondary plots of slopes and intercepts versus inhibitor concentration were also linear (Figure 29). K_1 values were determined to be 64.2 ± 11.5 μM (slope) and 0.49 ± 0.16 mM (intercept). A similar pattern for chloral hydrate inhibition with respect to NAD^+ was obtained when glyceraldehyde was used in place of acetaldehyde as the fixed substrate at a concentration of 0.6 mM (Figure 30). The secondary plots of slopes and intercepts versus inhibitor concentration were also linear (Figure 31). K_i values were determined to be 32.4 ± 12.4 μM (slope) and 23.3 ± 3.3 μM (intercept).

d. Product inhibition studies

i. NADH inhibition

Acid products (e.g., acetic acid from acetaldehyde) were not inhibitory. NADH was found to be a competitive inhibitor with respect to NAD^+ in the presence of a saturating concentration of acetaldehyde and a noncompetitive inhibitor with respect to glyceraldehyde when the fixed concentration of NAD^+ was less than saturating (0.6 mM). The inhibition patterns are shown in Figures 32 and 33. The K_i value (slope; variable NAD^+) was determined to be 0.133 ± 0.025 mM.

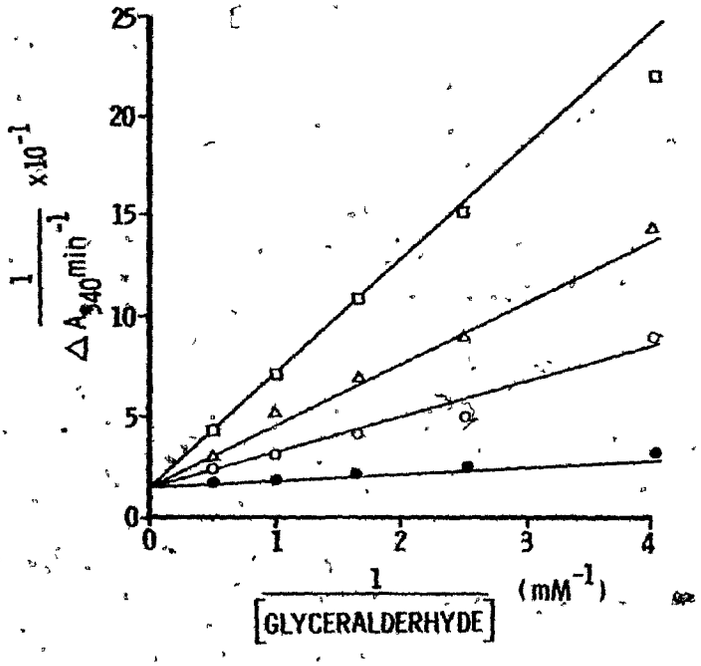

FIGURE 26

Double reciprocal plot with glyceraldehyde as the variable substrate and chloral hydrate as the inhibitor. Reaction mixtures contained: 33 mM sodium pyrophosphate, pH 9.3; 0.025 unit of enzyme; 2 0 mM NAD^+; glyceraldehyde as indicated and chloral hydrate: (●) absent; (o) 12.5 μM; (Δ) 25.0 μM; (□) 50.0 μM. Total volume one ml. Solid lines were calculated from fits to equation (c).

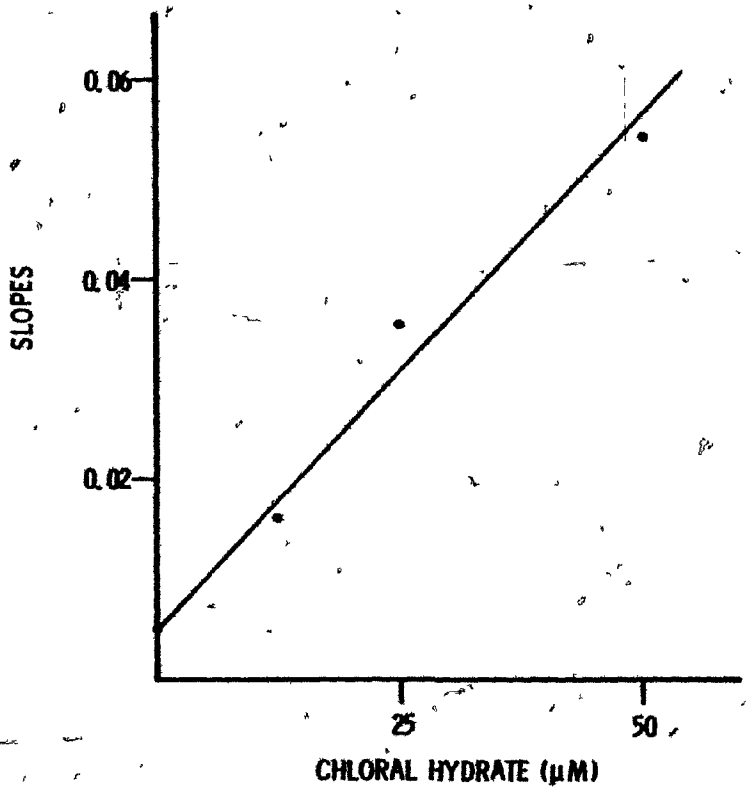

FIGURE 27

Secondary plot of slopes versus chloral hydrate concentration. Data taken from Figure 26.

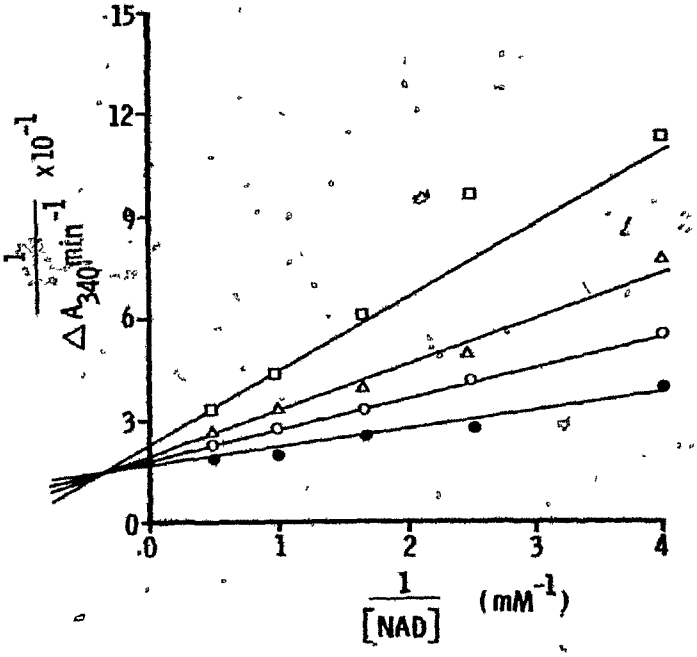

FIGURE 28

Double reciprocal plot with NAD^+ as the variable substrate and chloral hydrate as the inhibitor. Reaction mixtures contained: 33 mM sodium pyrophosphate, pH 9.3; 0.025 unit of enzyme; 2.0 mM acetaldehyde; NAD^+ as indicated and chloral hydrate: (●) absent; (○) 0.05 mM; (Δ) 0.1 mM; (□) 0.2 mM. Total volume one ml. Solid lines were calculated from fits to equation (d).

2 3

OF/DE

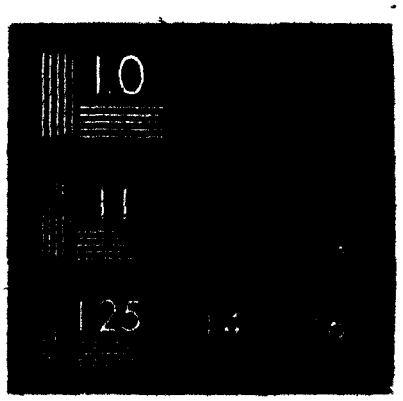

ARC - 374

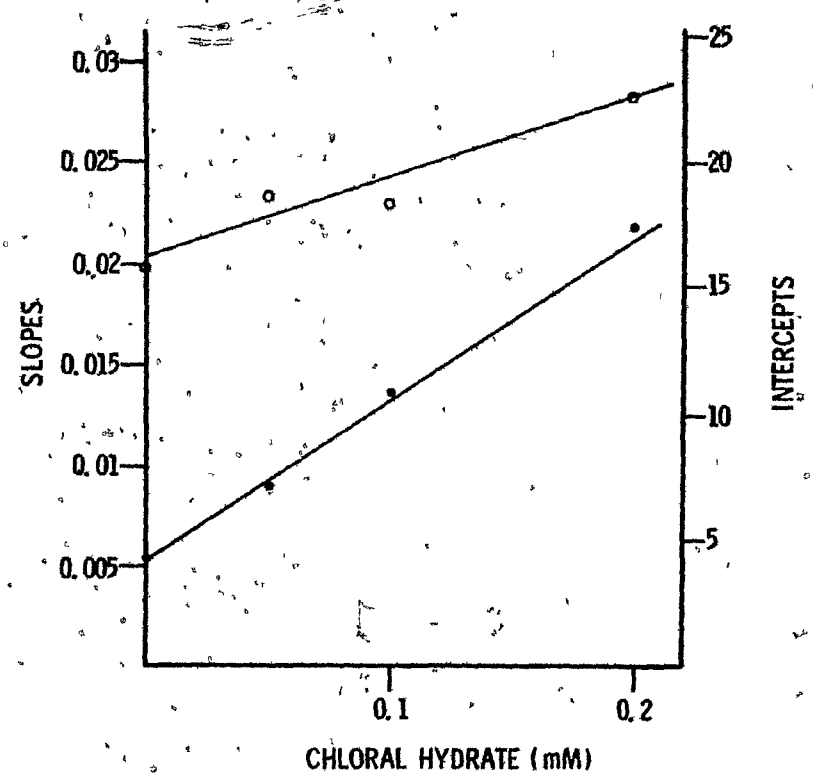

FIGURE 29

Secondary plot of slopes and intercepts versus chloral hydrate concentration. (●) slope; (o) intercept. Data taken from Figure 28.

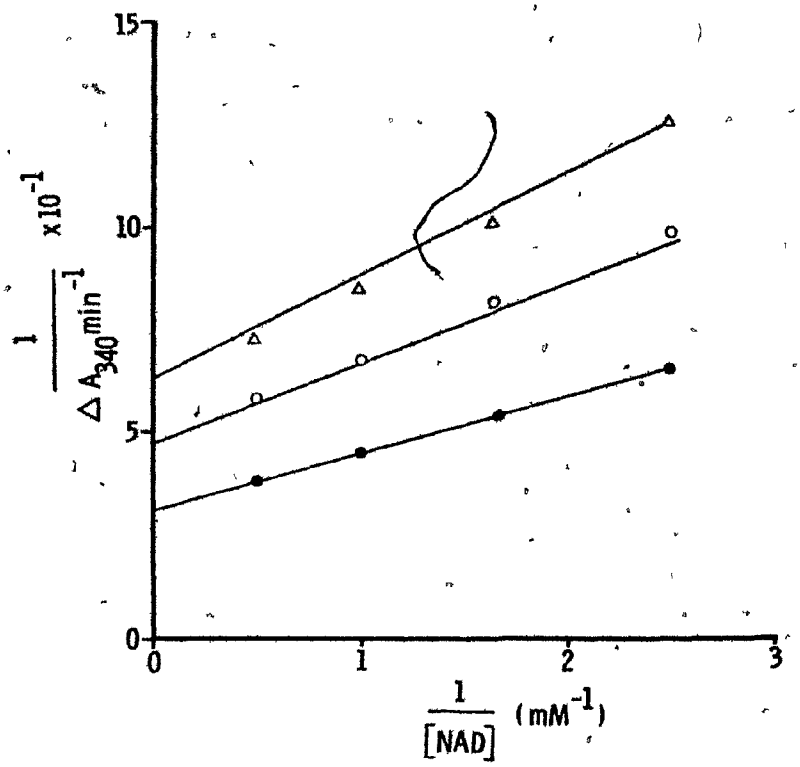

FIGURE 30

Double reciprocal plot with NAD^+ as the variable substrate and chloral hydrate as the inhibitor. Reaction mixtures contained: 33 mM sodium pyrophosphate, pH 9.3; 0.096 unit of enzyme; 0.6 mM glyceraldehyde; NAD^+ as indicated and chloral hydrate: (●) absent; (○) 0.0125 mM; (△) 0.025 mM. Total volume one ml. Solid lines were calculated from fits to equation (d).

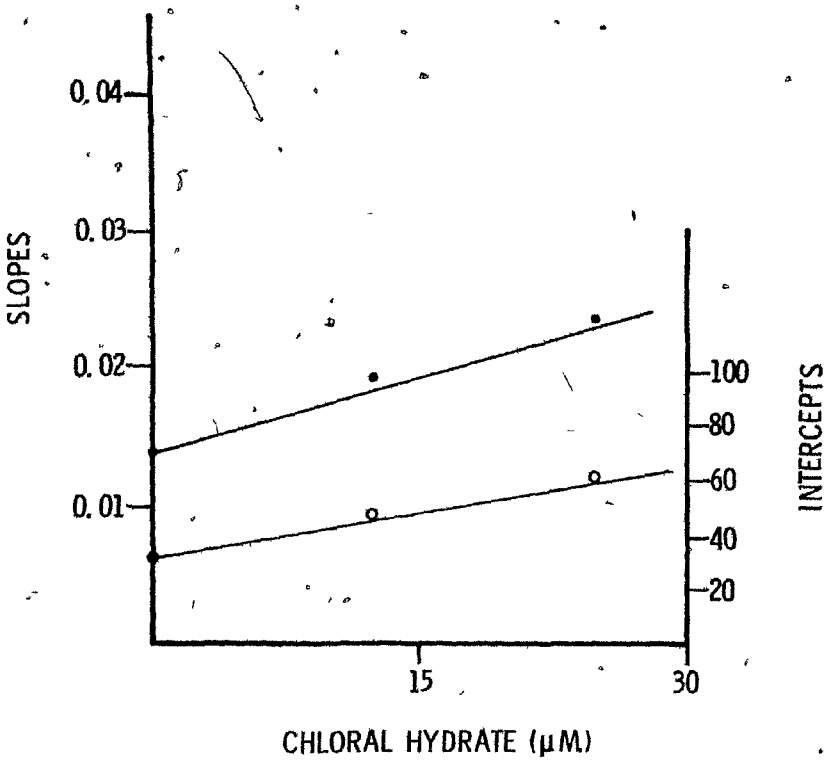

FIGURE 31

Secondary plot of slopes and intercepts versus chloral hydrate concentration. (●) slope; (o) intercept. Data taken from Figure 30.

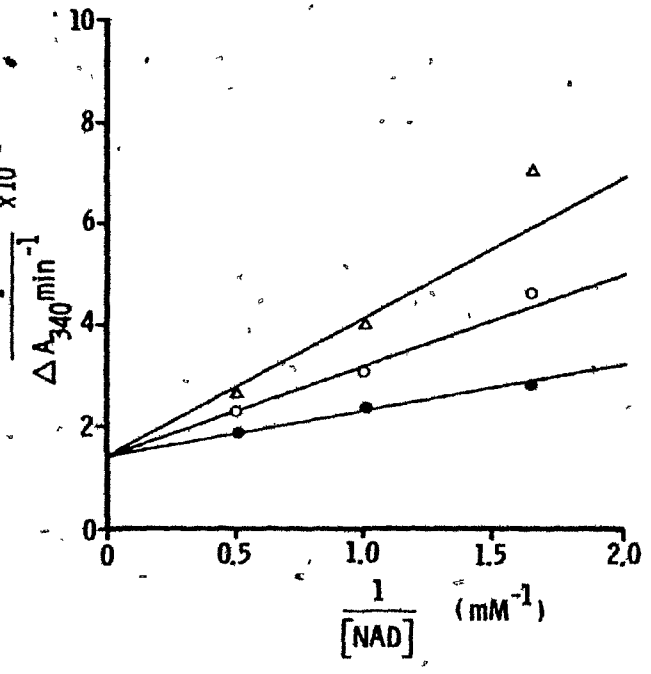

FIGURE 32

Double reciprocal plot with NAD^+ as the variable substrate and NADH as the inhibitor. Reaction mixtures contained: 33 mM sodium pyrophosphate, pH 9.3; 0.054 unit of enzyme; 2.0 mM acetaldehyde; NAD^+ as indicated and NADH: (●) absent; (○) 0.12 mM; (Δ) 0.25 mM. Total volume one ml. Solid lines were calculated from fits to equation (c).

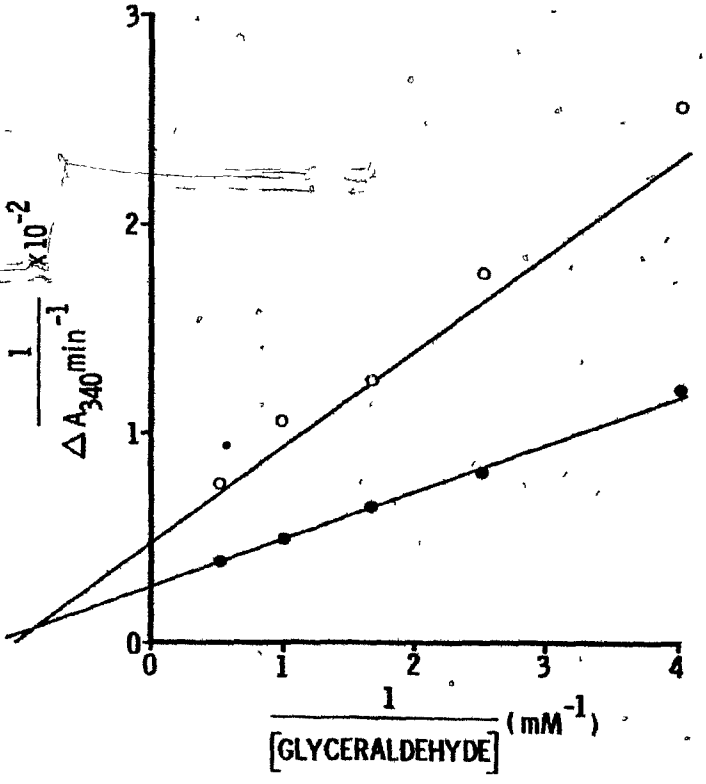

FIGURE 33

Double reciprocal plot with glyceraldehyde as the variable substraae and NADH as the inhibitor. Reaction mixtures contained: 33 mM sodium pyrophosphate, pH 9.3; 0.3 unit of enzyme; 0.6 mM NAD^+; glyceraldehyde as indicated and NADH: (●) absent; (○) 0.12 mM. Total volume one ml. Solid lines were calculated from fits to equation (d).

e. Kinetic studies in the presence of bovine serum albumin

Most of the kinetic experiments were also carried out in the presence of bovine serum albumin. As illustrated in Figures 34-50, bovine serum albumin did not change the inhibition patterns but it had some effect on the inhibition constants (Table VI).

f. Chelating agents as inhibitors

Attempts to demonstrate zinc in human liver aldehyde dehydrogenase have failed (Blair, unpublished data). Nevertheless, this enzyme is inhibited by various metal chelating agents, e.g., 1,10-phenanthroline, 2,9-dimethyl-1,10-phenanthroline and α,α′-dipyridyl. Figure 51 illustrates the inhibition pattern obtained with 1,10-phenanthroline when NAD^+ was used as the variable substrate. As is evident from the plot, 1,10-phenanthroline competitively inhibits the dehydrogenase reaction. Similar inhibition patterns were obtained with 2,9-dimethyl-1,10-phenanthroline, quinoline, α,α′-dipyridyl and γ,γ′-dipyridyl, as shown in Figures 52-55. Inhibition constants calculated from double reciprocal plots for each inhibitor are presented in Table VII. Comparison among inhibition constants indicated that the K_i value for 1,10-phenanthroline was close to its analogue, 2,9-dimethyl-1,10-phenanthroline. Similarly, the K_i values for α,α′-dipyridyl and γ,γ′-dipyridyl were almost identical. Benzoic acid was also found to be a competitive inhibitor of dehydrogenase reaction with respect to NAD^+ (Figure 56). The K_i value calcualted by Lineweaver-Burke method (131) was 2.29 ± 0.15 mM.

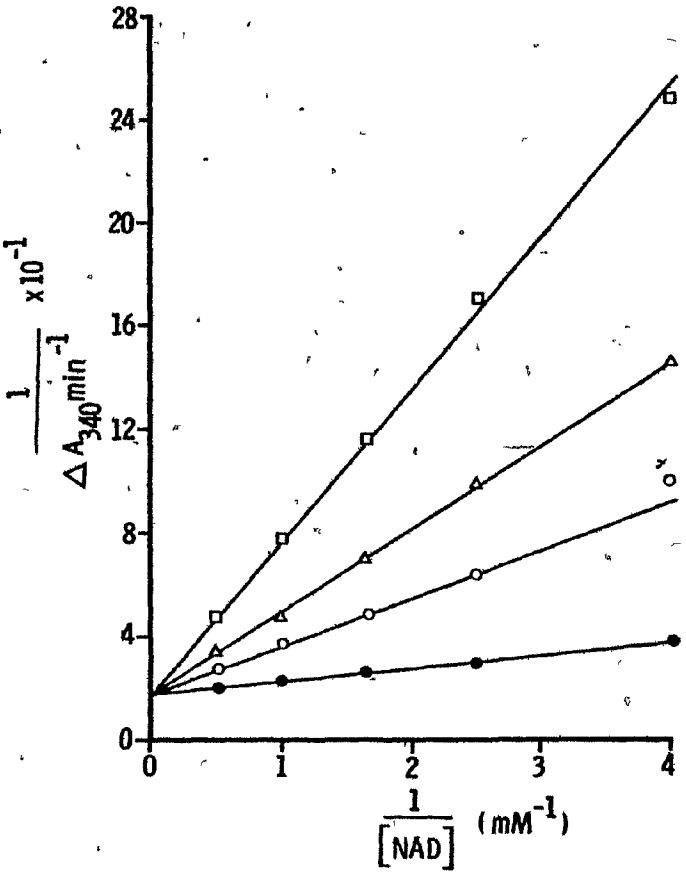

FIGURE 34

Double reciprocal plot with NAD^+ as the variable substrate and thionicotinamide-AD^+ as the inhibitor in the presence of bovine serum albumin. Reaction mixtures contained: 33 mM sodium pyrophosphate, pH 9.3; 0.045 unit of enzyme; 2.0 mM acetaldehyde; 1.0 mg albumin; NAD^+ as indicated and thionicotinamide-AD^+: (●) absent; (○) 0.025 mM; (△) 0.05 mM; (□) 0.1 mM. Total volume one ml. Solid lines were calculated from fits to equation (c).

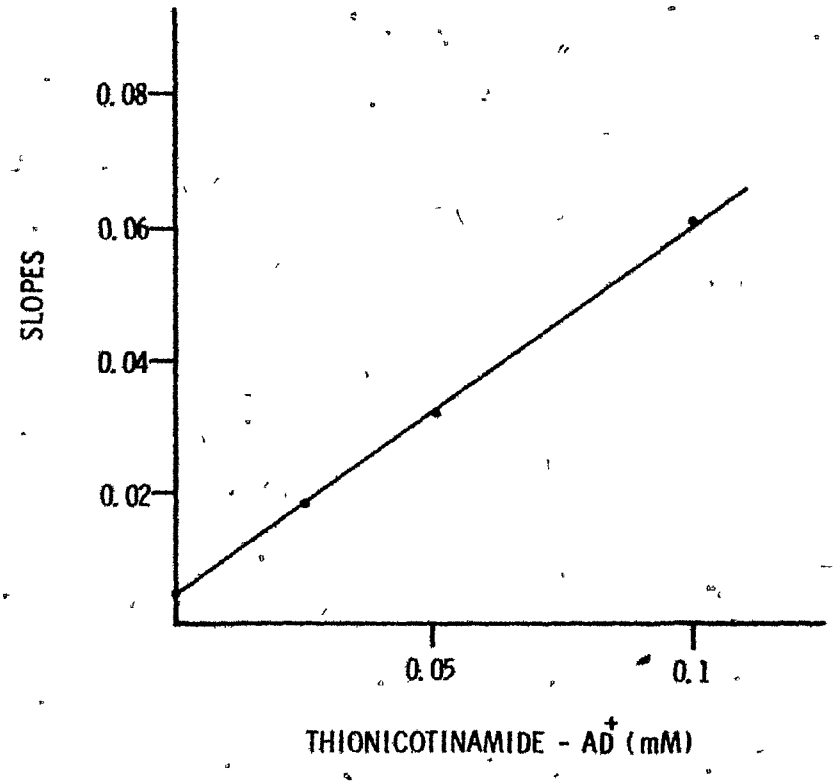

FIGURE 35

Secondary plot of slopes versus thionicotinamide-AD^+ concentration. Data taken from Figure 34.

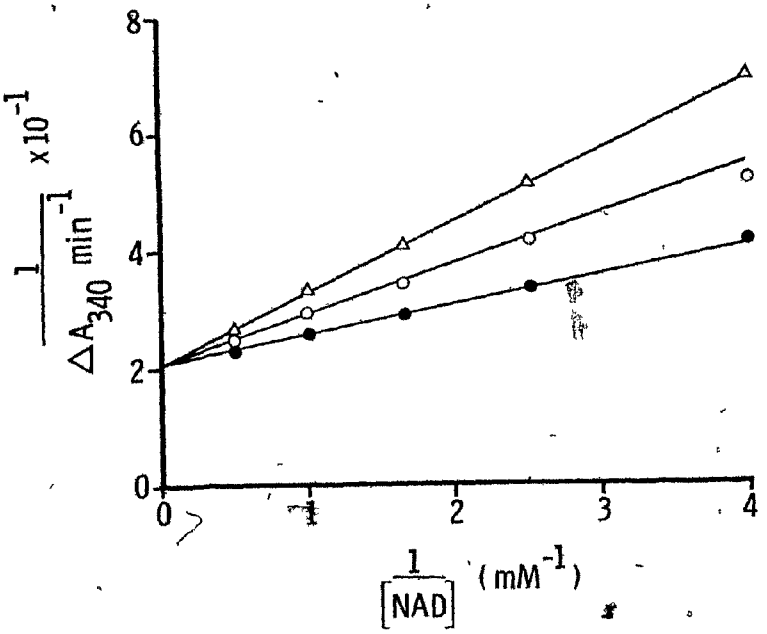

FIGURE 36

Double reciprocal plot with NAD^+ as the variable substrate and N'-methylnicotinamide as the inhibitor in the presence of bovine serum albumin. Reaction mixtures contained: 33 mM sodium pyrophosphate, pH 9.3; 0.04 unit of enzyme; 2.0 mM acetaldehyde; 1.0 mg albumin; NAD^+ as indicated and N'-methylnicotinamide: (●) absent; (○) 10.0 mM; (Δ) 20.0 mM. Total volume one ml. Solid lines were calculated from fits to equation (c).

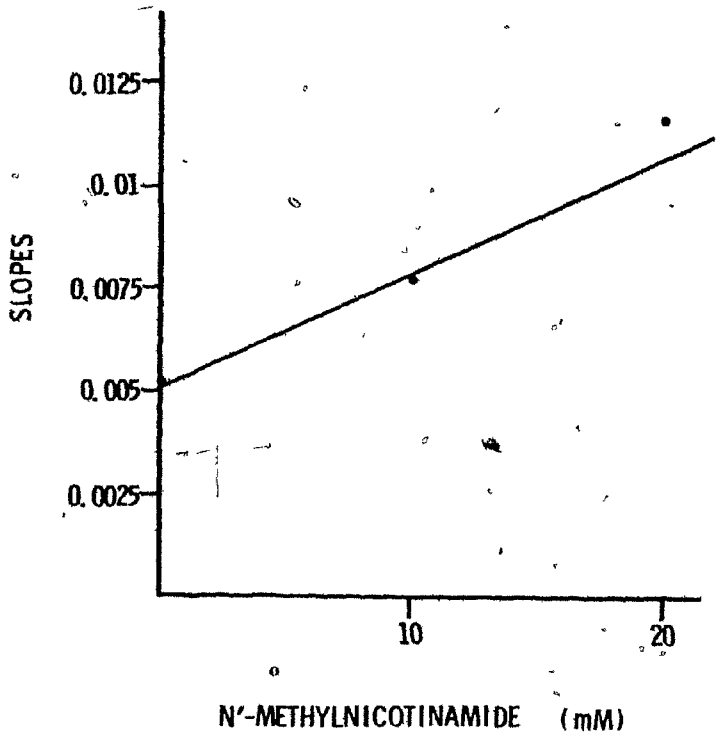

FIGURE 37

Secondary plot of slopes versus N'-methylnicotinamide concentration. Data taken from Figure 36.

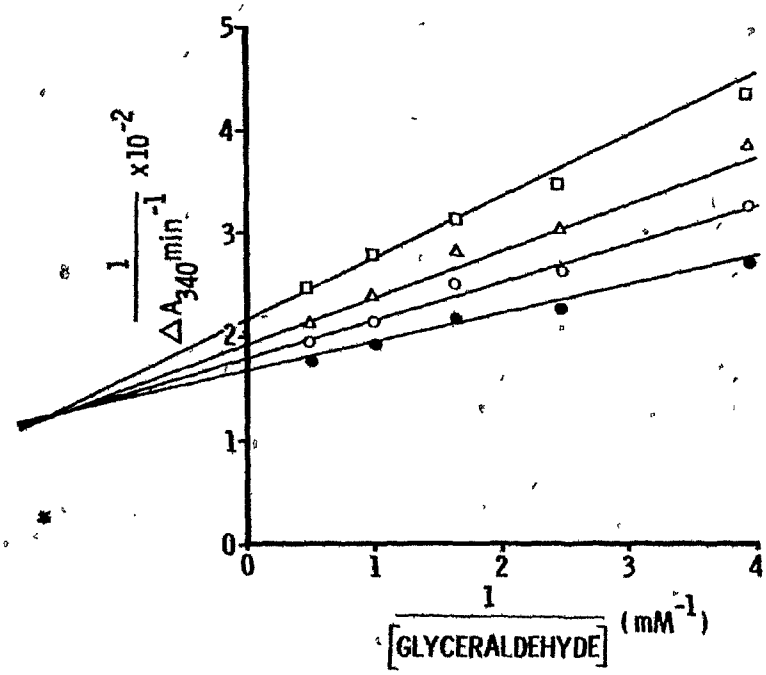

FIGURE 38

Double reciprocal plot with glyceraldehyde as the variable substrate and N′-methylnicotinamide as the inhibitor in the presence of bovine serum albumin. Reaction mixtures contained: 33 mM sodium pyrophosphate, pH 9.3; 0.035 unit of enzyme; 2.0 mM NAD^+; 1.0 mg albumin; glyceraldehyde as indicated, and N′-methylnicotinamide: (●) absent; (o) 5.0 mM; (Δ) 10.0 mM; (□) 19.0 mM. Total volume one ml. Solid lines were calculated from fits to equation (d).

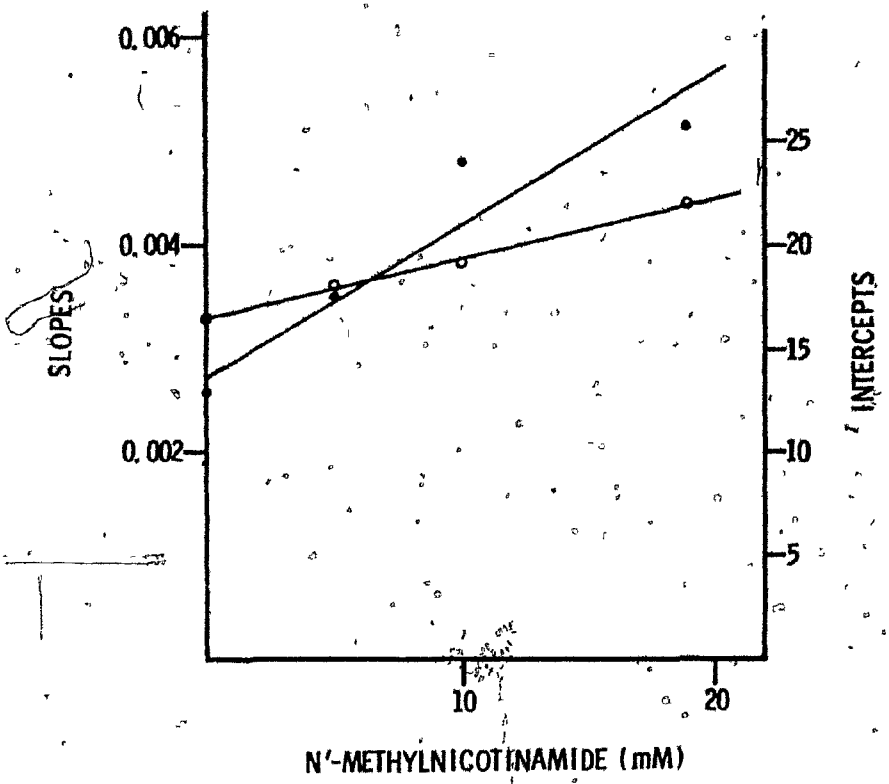

FIGURE 39

Secondary plot of slopes and intercepts versus N'-methylnicotinamide concentration. (●) slope; (○) intercept. Data taken from Figure 38.

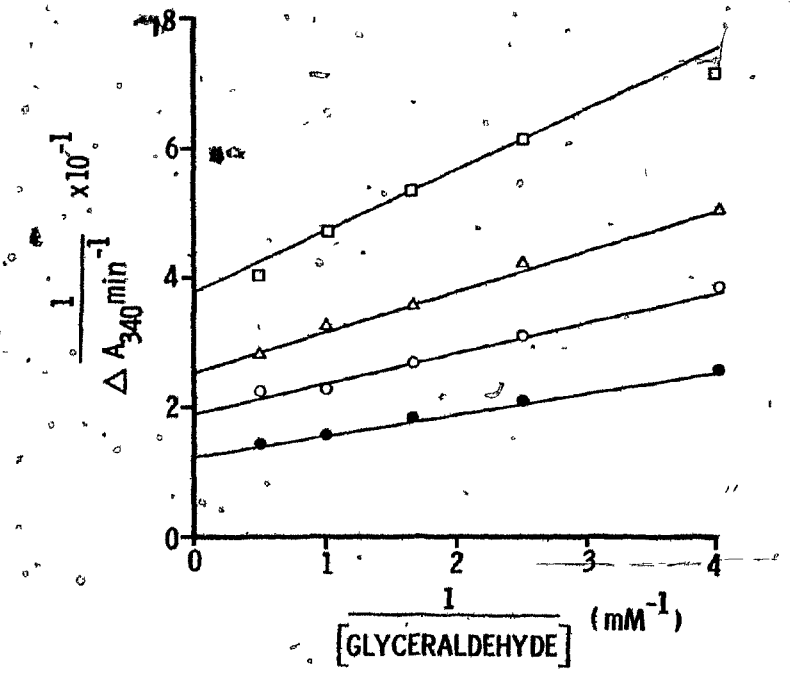

FIGURE 40

Double reciprocal plot with glyceraldehyde as the variable substrate and thionicotinamide-AD^+ as the inhibitor in the presence of bovine serum albumin. Reaction mixtures contained: 33 mM sodium pyrophosphate, pH 9.3; 0.042 unit of enzyme; 2.0 mM NAD^+; 1.0 mg albumin; glyceraldehyde as indicated and thionicotinamide-AD^+: (●) absent; (○) 0.05 mM; (Δ) 0.1 mM; (□) 0.2 mM. Total volume one ml. Solid lines were calcualted from fits to equation (d).

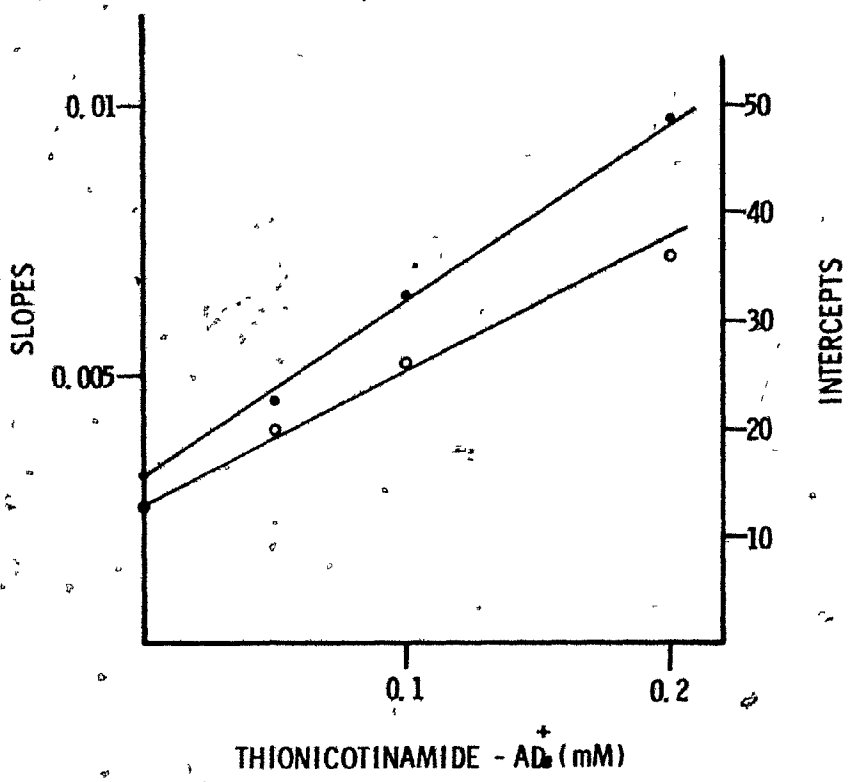

FIGURE 41

Secondary plot of slopes and intercepts versus thionicotinamide-AD^+ concentration. (●) slope; (○) intercept. Data taken from Figure 40.

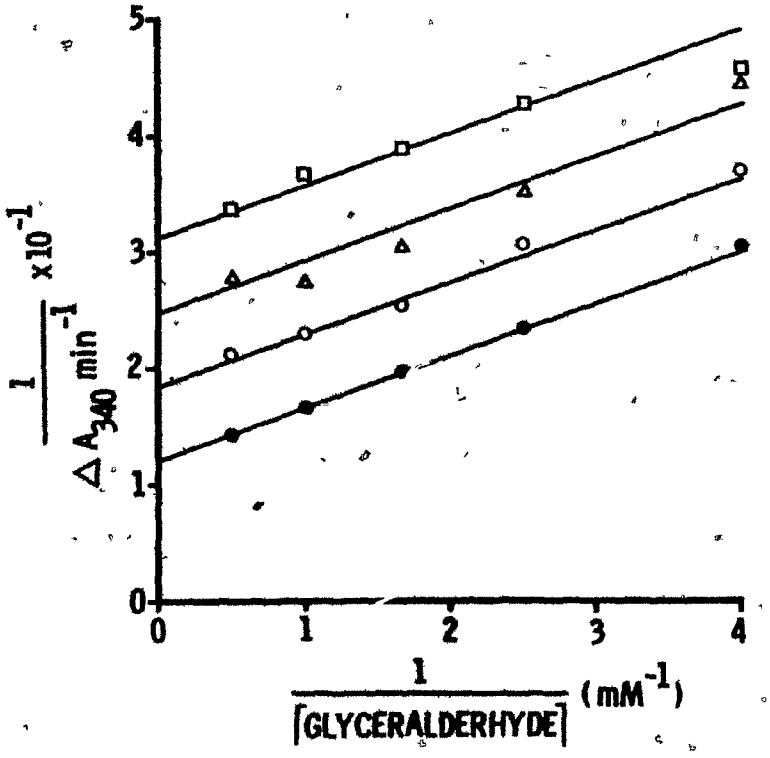

FIGURE 42

Double reciprocal plot with glyceraldehyde as the variable substrate and adenosine as the inhibitor in the presence of bovine serum albumin. Reaction mixtures contained: 33 mM sodium pyrophosphate, pH 9.3; 0.025 unit of enzyme; 2.0 mM NAD^+; 1.0 mg albumin; glyceraldehyde as indicated and adenosine: (●) absent; (○) 1.0 mM; (△) 2.0 mM; (□) 3.0 mM. Total volume one ml. Solid lines were calculated from fits to equation (e).

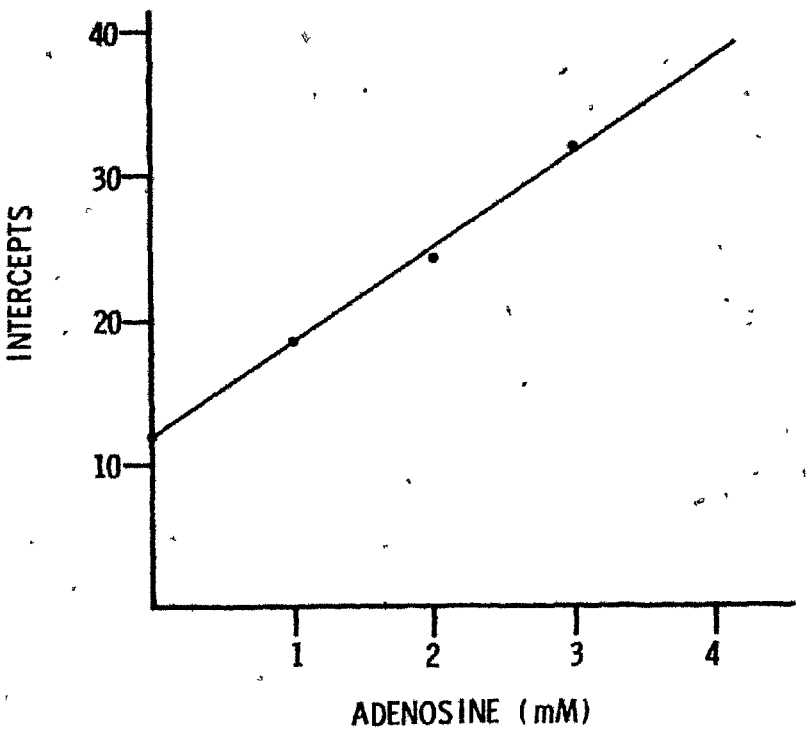

FIGURE 43

Secondary plot of intercepts versus adenosine concentration. Data taken from Figure 42.

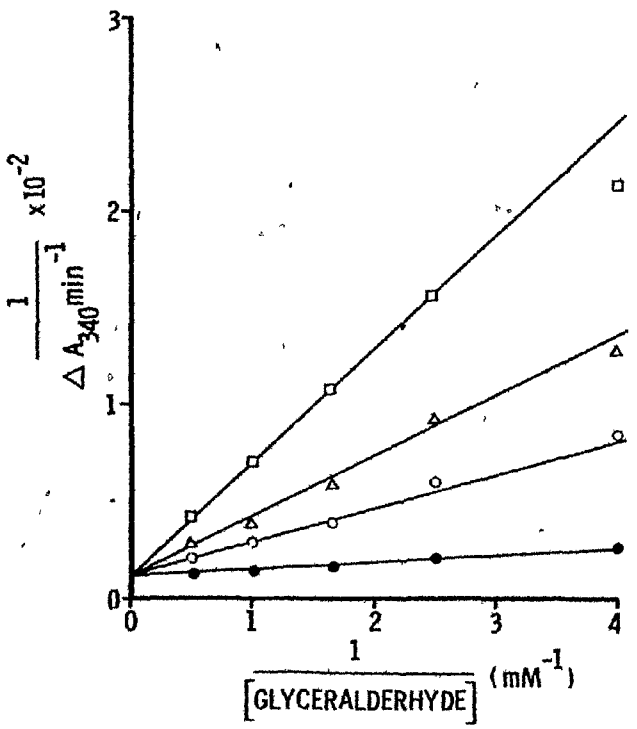

FIGURE 44

Double reciprocal plot with glyceraldehyde as the variable substrate and chloral hydrate as the inhibitor in the presence of bovine serum albumin. Reaction mixtures contained: 33 mM sodium pyrophosphate, pH 9.3; 0.05 unit of enzyme; 2.0 mM NAD^+; 1.0 mg albumin; glyceraldehyde as indicated and chloral hydrate: (●) absent; (○) 0.0125 mM; (△) 0.025 mM; (□) 0.05 mM. Total volume one ml. Solid lines were calculated from fits to equation (c).

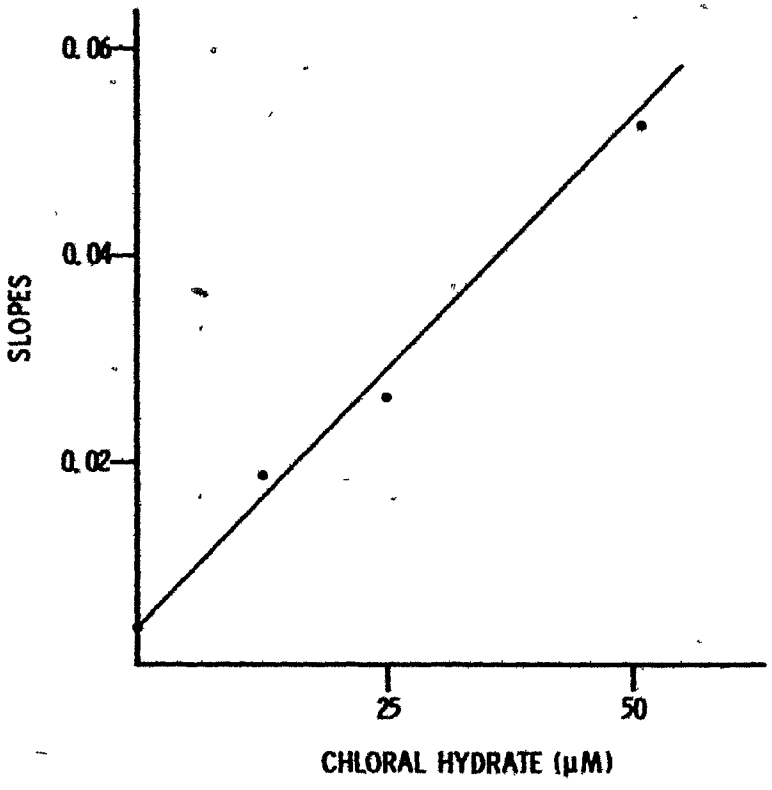

FIGURE 45

Secondary plot of slopes versus chloral hydrate concentration. Data taken from Figure 44.

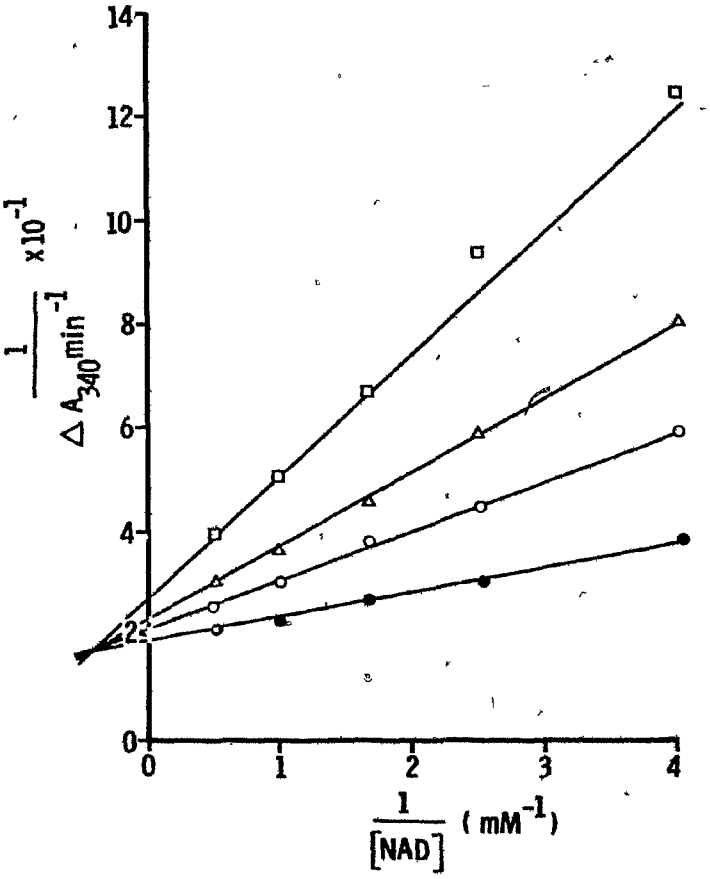

FIGURE 46

Double reciprocal plot with NAD^+ as the variable substrate and chloral hydrate as the inhibitor in the presence of bovine serum albumin. Reaction mixtures contained: 33 mM sodium pyrophosphate, pH 9.3; 0.03 unit of enzyme; 2.0 mM acetaldehyde; 1.0 mg albumin; NAD^+ as indicated and chloral hydrate; (o) absent; (o) 0.05 mM; (Δ) 0.1 mM; (□) 0.2 mM. Total volume one ml. Solid lines were calculated from fits to equation (d).

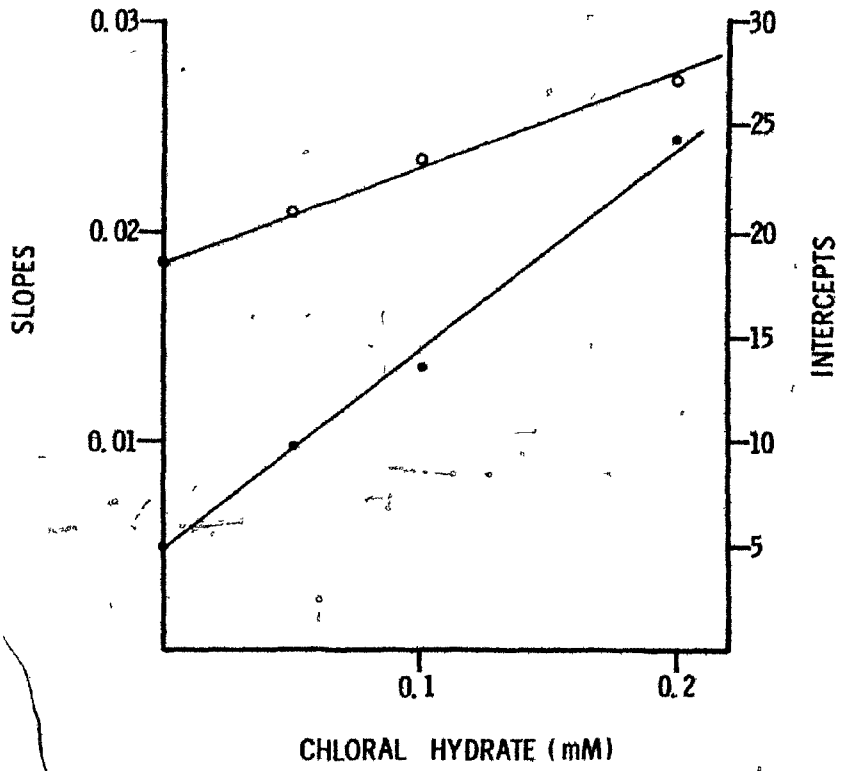

FIGURE 47

Secondary plot of slopes and intercepts versus chloral hydrate concentration. (●) slope; (○) intercept. Data taken from Figure 46.

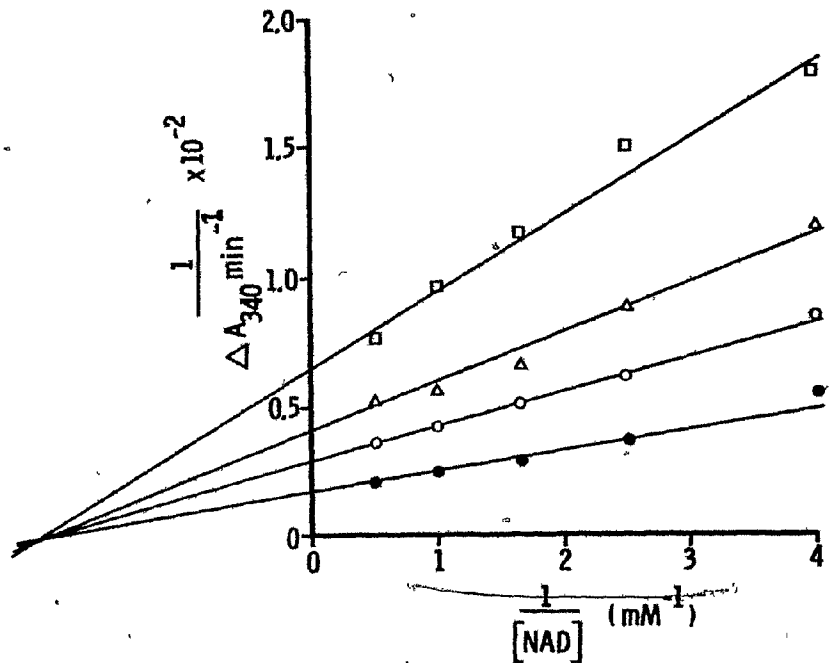

FIGURE 48

Double reciprocal plot with NAD^+ as the variable substrate and chloral hydrate as the inhibitor in the presence of bovine serum albumin. Reaction mixtures contained: 33 mM sodium pyrophosphate, pH 9.3; 0.048 unit of enzyme; 0.6 mM glyceraldehyde; 1.0 mg albumin; NAD^+ as indicated and chloral hydrate: (●) absent; (○) 0.0125 mM; (△) 0.025 mM; (□) 0.05 mM. Total volume one ml. Solid lines were calculated from fits to equation (d).

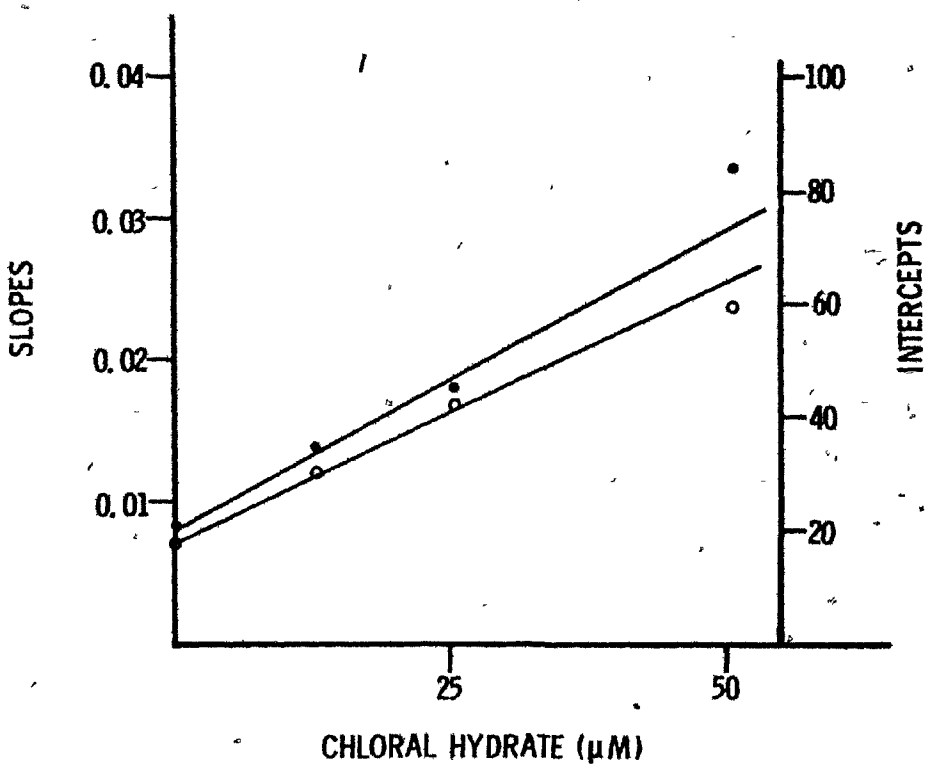

FIGURE 49

Secondary plot of slopes and intercepts versus chloral hydrate concentration. (●) slope; (○) intercept. Data taken from Figure 48.

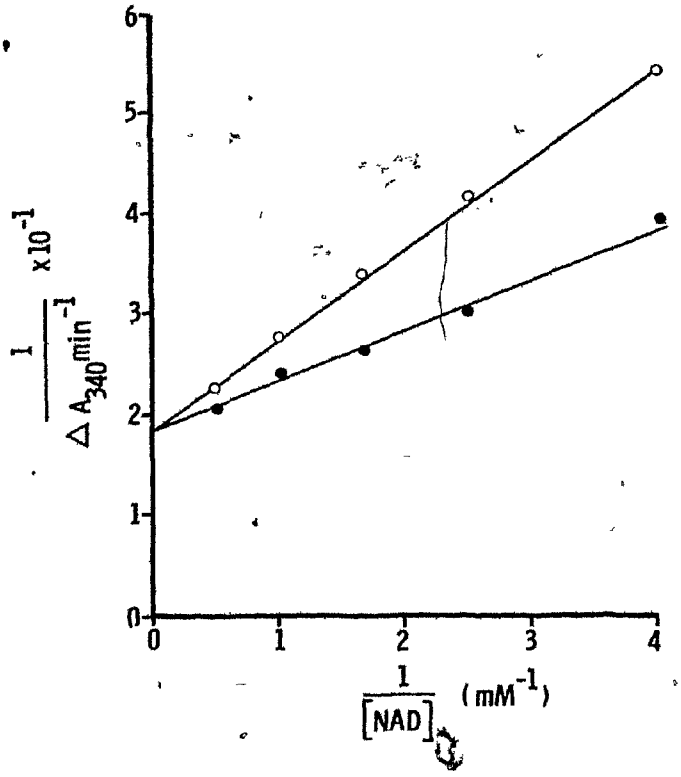

FIGURE 50

Double reciprocal plot with NAD^+ as the variable substrate and NADH as the inhibitor in the presence of bovine serum albumin. Reaction mixtures contained: 33 mM sodium pyrophosphate, pH 9.3; 0.023 unit of enzyme; 2.0 mM acetaldehyde; 1.0 mg albumin; NAD^+ as indicated and NADH: (●) absent; (○) 0.12 mM. Total volume one ml. Solid lines were calculated from fits to equation (c).

TABLE VI

COMPARISON OF INHIBITION CONSTANTS DETERMINED IN THE PRESENCE AND ABSENCE OF BOVINE SERUM ALBUMIN FOR VARIOUS DEAD-END INHIBITORS OF HUMAN LIVER ALDEHYDE DEHYDROGENASE

Inhibitor	Variable Substrate	Inhibition Constants			
		Bovine Serum Albumin(-)		Bovine Serum Albumin(+)	
		K_{is}	K_{ii}	K_{is}	K_{ii}
Adenosine uncompetitive	glyceraldehyde		2.16±0.12mM		1.89±0.08mM
Thionicotinamide-AD^+ competitive	NAD^+	11.6±0.8 μM		8.8±0.5 μM	
noncompetitive	glyceraldehyde	59.4±11.9μM	0.177±0.026mM	99.0±18.1μM	0.104±0.00[illegible]mM
N'-Methylnicotinamide competitive	NAD^+	9.28±0.98mM		14.24±2.17mM	
noncompetitive	glyceraldehyde	11.56±2.11mM	42.30±11.12mM	16.47±4.94mM	58.41±12.50mM
Chloral hydrate competitive	glyceraldehyde	4.3 ± 0.3μM		3.2 ±0.3 μM	
noncompetitive	NAD^+	64.2±11.5μM	0.49±0.16mM	52.3 ±5.6 μM	0.40±0.07mM
Chloral hydrate (low fixed concentration of glyceraldehyde) noncompetitive	NAD^+	32.4±12.4μM	23.3±3.3μM	19.0 ±3.9 μM	18.3±2.0μM
NADH competitive	NAD^+	0.133±0.025		0.148±0.019mM	

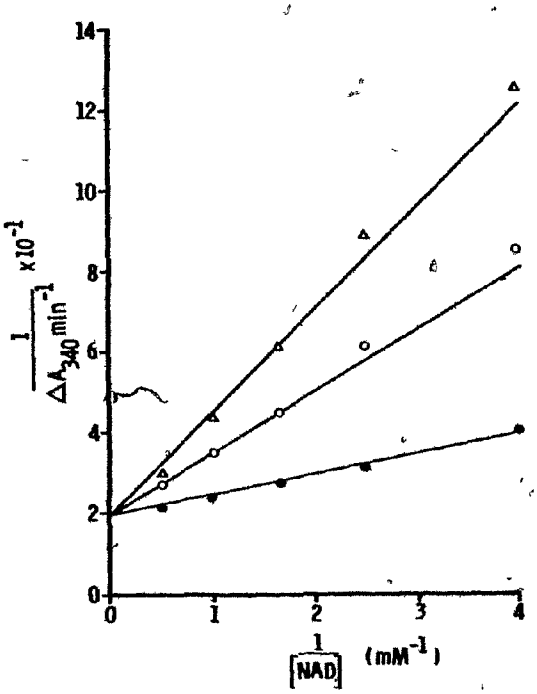

FIGURE 51

Double reciprocal plot with NAD^+ as the variable substrate and 1,10-phenanthroline as the inhibitor. Reaction mixtures contained: 33 mM sodium pyrophosphate, pH 9.3; 0.045 unit of enzyme; 2.0 mM acetaldehyde; 1.0 mg BSA; NAD^+ as indicated and 1,10-phenanthroline: (●) absent; (○) 0.25 mM; (Δ) 0.5 mM. Total volume one ml.

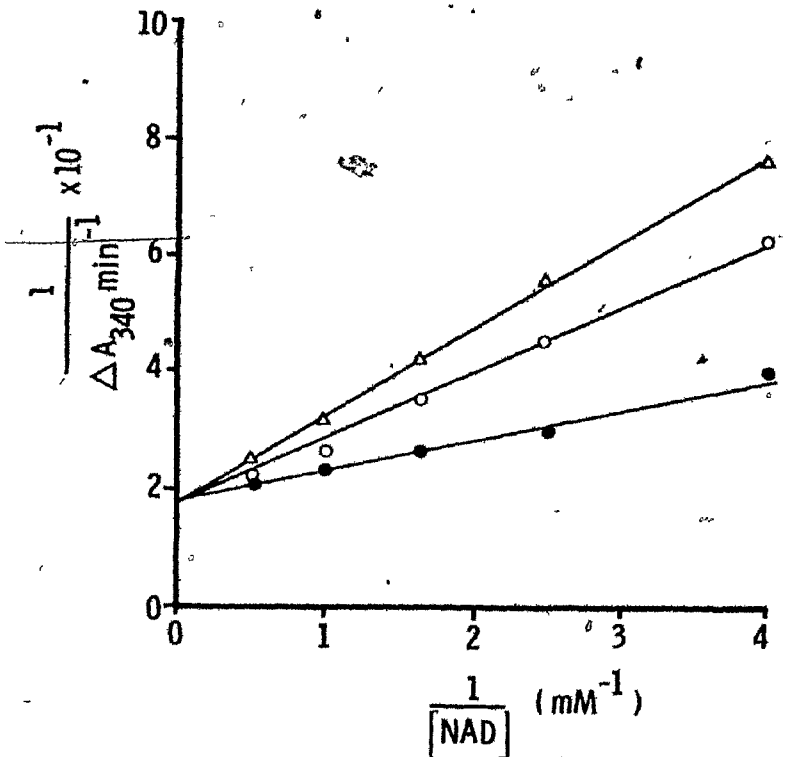

FIGURE 52

Double reciprocal plot with NAD^+ as the variable substrate and 2,9-dimethyl-1,10-phenanthroline as the inhibitor. Reaction mixtures contained: 33 mM sodium pyrophosphate, pH 9.3; 0.046 unit of enzyme; 2.0 mM acetaldehyde; 1.0 mg BSA; NAD^+ as indicated and 2,9-dimethyl-1,10-phenanthroline: (●) absent; (○) 0.125; (Δ) 0.25 mM. Total volume one ml.

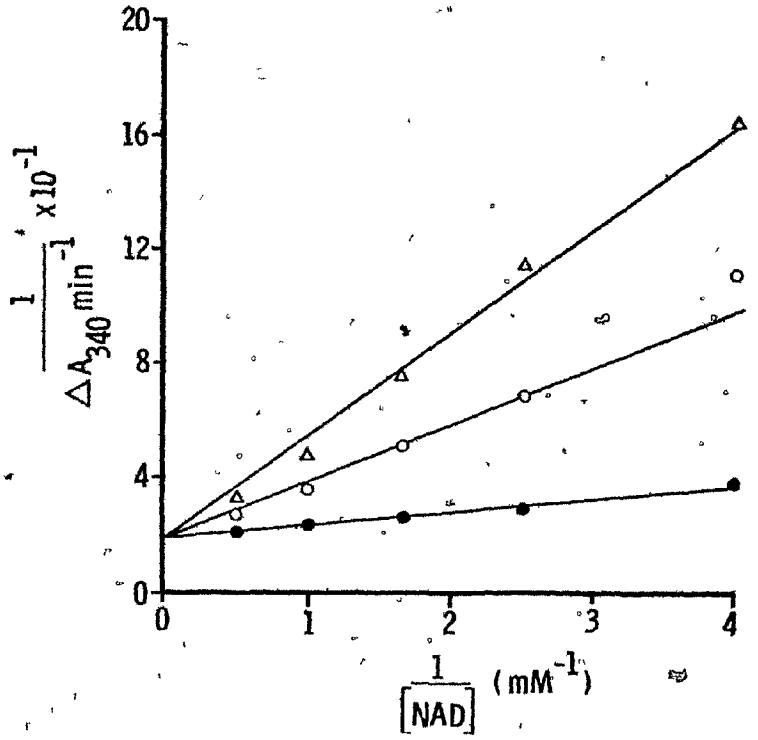

FIGURE 53

Double reciprocal plot with NAD^+ as the variable substrate and α,α´-dipyridyl as the inhibitor. Reaction mixtures contained: 33 mM sodium pyrophosphate, pH 9.3; 0.044 unit of enzyme; 2.0 mM acetaldehyde; 1.0 mg BSA; NAD^+ as indicated and α,α´-dipyridyl: (●) absent; (○) 3.0 mM; (Δ) 5.0 mM. Total volume one ml.

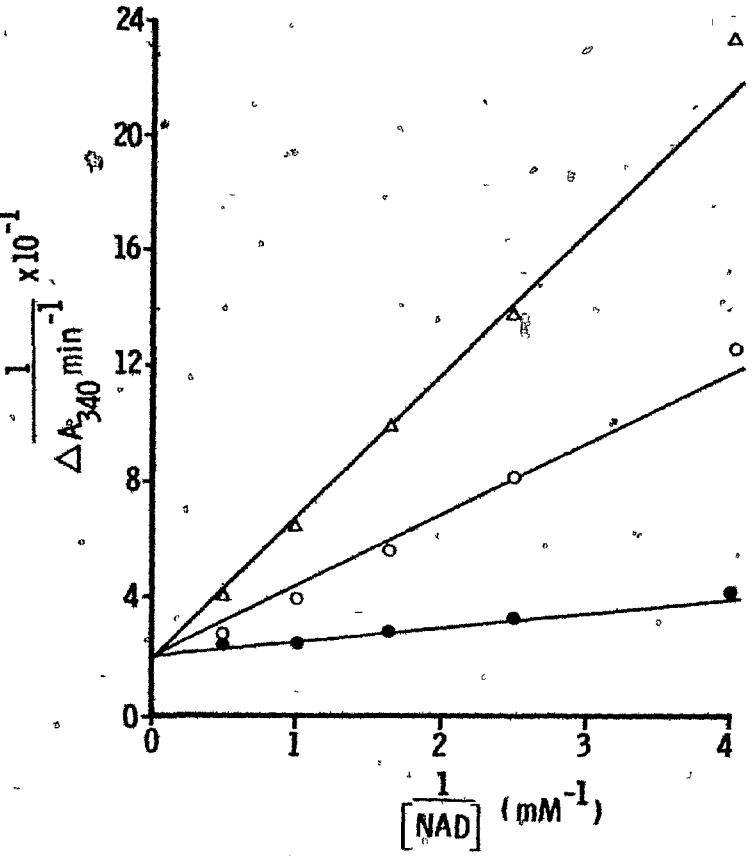

FIGURE 54

Double reciprocal plot with NAD^+ as the variable substrate and γ,γ′-dipyridyl as the inhibitor. Reaction mixtures contained: 33 mM sodium pyrophosphate, pH 9.3; 0.043 unit of enzyme; 2.0 mM acetaldehyde; 1.0 mg BSA; NAD^+ as indicated and γ,γ′-dipyridyl: (●) absent; (○) 4.0 mM; (Δ) 7.0 mM. Total volume one ml.

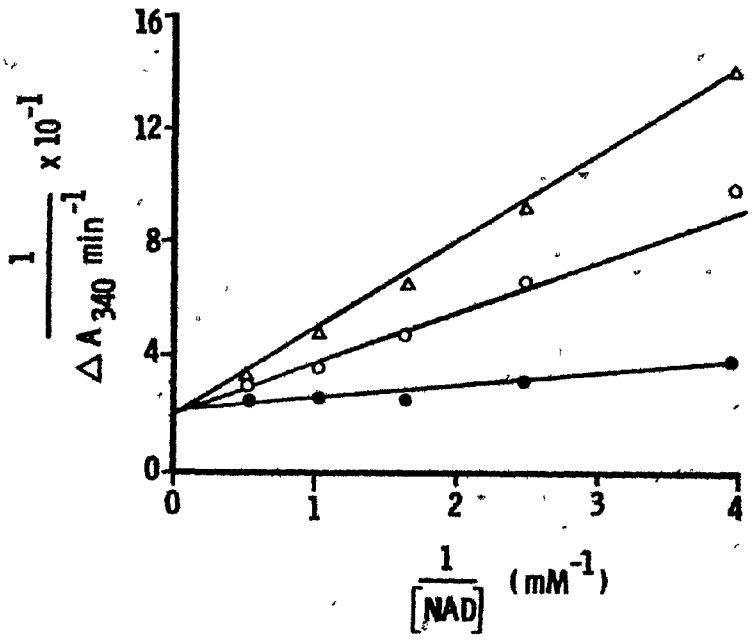

FIGURE 55

Double reciprocal plot with NAD^+ as the variable substrate and quinoline as the inhibitor. Reaction mixtures contained: 33 mM sodium pyrophosphate, pH 9.3; 0.045 unit of enzyme; 2.0 mM acetaldehyde; 1.0 mg BSA; NAD^+ as indicated and quinoline: (●) absent; (○) 0.5 mM; (△) 1.0 mM. Total volume one ml.

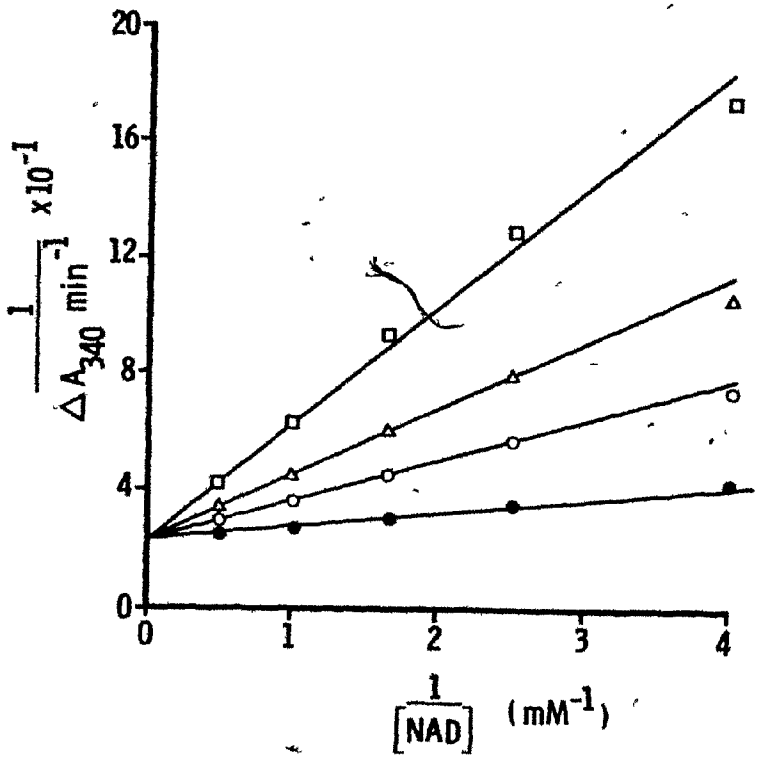

FIGURE 56

Double reciprocal plot with NAD^+ as the variable substrate and benzoic acid as the inhibitor. Reaction mixtures contained: 33 mM sodium pyrophosphate, pH 9.3; 0.04 unit of enzyme; 2.0 mM acetaldehyde; 1.0 mg BSA; NAD^+ as indicated and benzoic acid: (●) absent; (○) 5 mM; (Δ) 10 mM; (□) 20 mM. Total volume one ml.

TABLE VII

INHIBITION CONSTANTS FOR DIFFERENT CHELATING AGENTS

The K_i (slope) values were calculated from data presented in Figures 51 - 56

Chelating Agent	K_1
	M
1,10-Phenanthroline	$1.29 \pm 0.14 \times 10^{-4}$
2,9-Dimethyl-1,10-phenanthroline	$1.38 \pm 0.18 \times 10^{-4}$
α,α'-Dipyridyl	$1.04 \pm 0.10 \times 10^{-3}$
γ,γ'-Dipyridyl	$1.26 \pm 0.21 \times 10^{-3}$
Quinoline	$2.29 \pm 0.22 \times 10^{-4}$
Benzoic acid	$2.29 \pm 0.15 \times 10^{-3}$

2. Esterase Reaction

a. Non-hyperbolic relationship between initial velocity and ester concentration

Human liver aldehyde dehydrogenase was also found to catalyze the hydrolysis of p-nitrophenyl acetate, a well studied substrate of esterases. The initial rate of hydrolysis of p-nitrophenyl acetate as a function of its concentration is shown in Figure 57. It can be seen that the curve continues to rise instead of falling off at very high substrate concentrations. The double reciprocal plot of the same data (Figure 57) shows a downward curvature at high substrate concentrations (Figure 58) rather than remaining linear as required by simple Michaelis-Menten kinetic behavior. The data were fitted to rate equation 5 by a least squares method, assuming equal variance for the experimental velocities.

$$v = \frac{V_2 + V_1K_2/(1 - V_2/V_2)S}{1 + K_2/(1 - V_1/V_2)S + K_1K_2/(1 - V_1/V_2)S^2} \qquad (5)$$

S is the substrate concentration and v the initial velocity; V_1 and K_1 are the maximal velocity and apparent Michaelis constant for low substrate concentrations and V_2 and K_2 are the maximal velocity

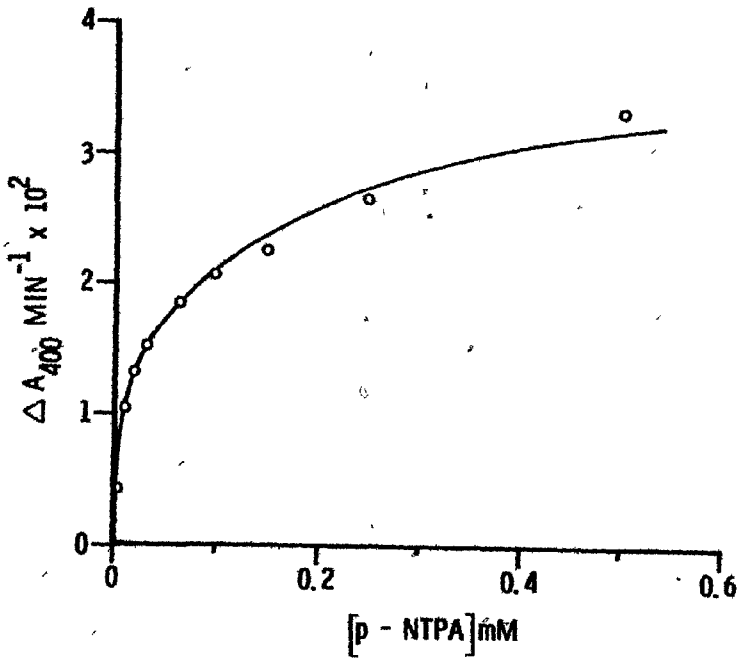

FIGURE 57

Plot of initial velocity versus p-nitrophenyl acetate concentration. Reaction mixtures contained: 33 mM sodium pyrophosphate, pH 7.0; 0.6 unit of enzyme and p-nitrophenyl acetate as indicated. Circles represent experimental values; the solid line was calculated from a fit of the data to equation (f). Constants: V_1 = 0.014; V_2 = 0.04; K_1 = 3.75 x 10^{-6}; K_2 = 1.5 x 10^{-4}.

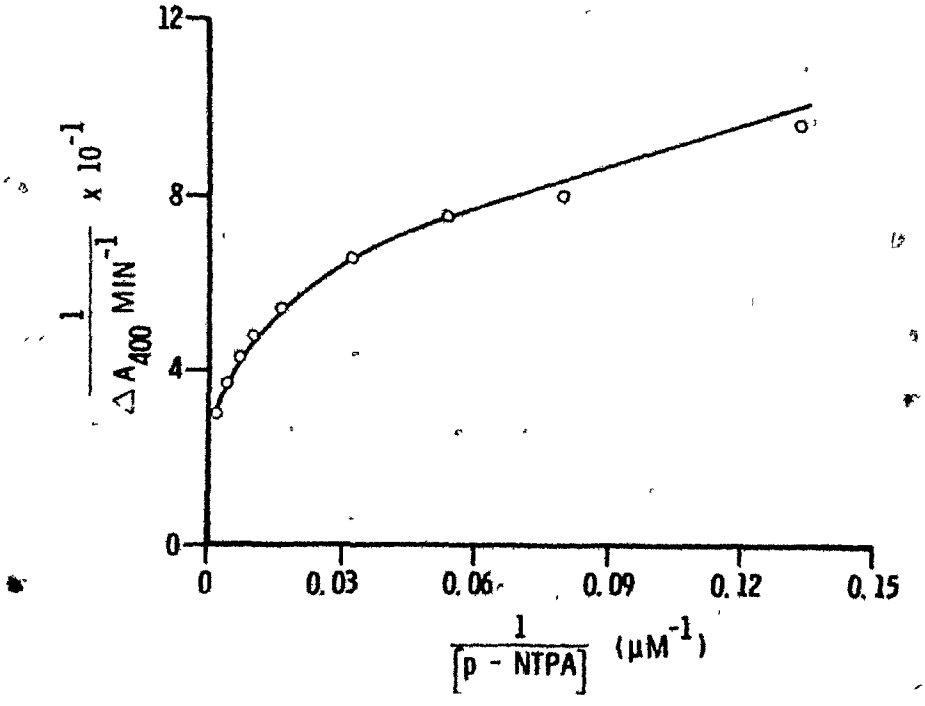

FIGURE 58

Double reciprocal plot of initial velocity versus p-nitrophenyl acetate concentration. Circles represent experimental values from Figure 57; the solid line was calculated as in Figure 57.

and apparent Michaelis constant for high substrate concentrations.

The preliminary values for V_1, V_2, K_1 and K_2 were calculated from the double reciprocal plot of initial rate of hydrolysis versus p-nitrophenyl acetate concentration. Apparent K_m and V_{max} values at high and low substrate concentrations are given in Table VIII.

b. Chromatographic elution pattern of dehydrogenase and esterase activities

Aldehyde dehydrogenase, purified through the DEAE-cellulose step, was subjected to column chromatography on DEAE-sephadex (see Methods). Figure 59 shows the elution pattern from this DEAE-sephadex column subjected to a linear salt gradient. Fractions obtained were assayed for dehydrogenase activity, esterase activity and esterase activity measured in the presence of NAD^+. Esterase activity followed a similar elution pattern to dehydrogenase activity, indicating that a single enzyme was responsible for both.

c. Ester specificity

In addition to p-nitrophenyl acetate, two other p-nitrophenyl esters, i.e., p-nitrophenyl propionate and p-nitrophenyl butyrate were found to be hydrolyzed by the human enzyme. Reciprocal plots of the initial rate of hydrolysis of these esters are shown in Figures 60 and 61. The downward curvature observed in the reciprocal plot for p-nitrophenyl acetate was also evident in these reciprocal

TABLE VIII

KINETIC CONSTANTS FOR p-NITROPHENYL ACETATE, p-NITROPHENYL PROPIONATE AND p-NITROPHENYL BUTYRATE

K_m and V_{max} values were calculated from data presented in Figures 58, 60 and 61.

Ester concentration range	p-Nitrophenyl Acetate		p-Nitrophenyl Propionate		p-Nitrophenyl Butyrate	
	K_m	V_{max}	K_m	V_{max}	K_m	V_{max}
	μM	ΔA_{400} min^{-1}	μM	ΔA_{400} min^{-1}	μM	ΔA_{400} min^{-1}
4 μM to 25 μM	3.8	0.014	8.4	0.022	14.3	0.021
0.1 mM to 0.6 mM	150.0	0.040	121.0	0.074	195.0	0.065

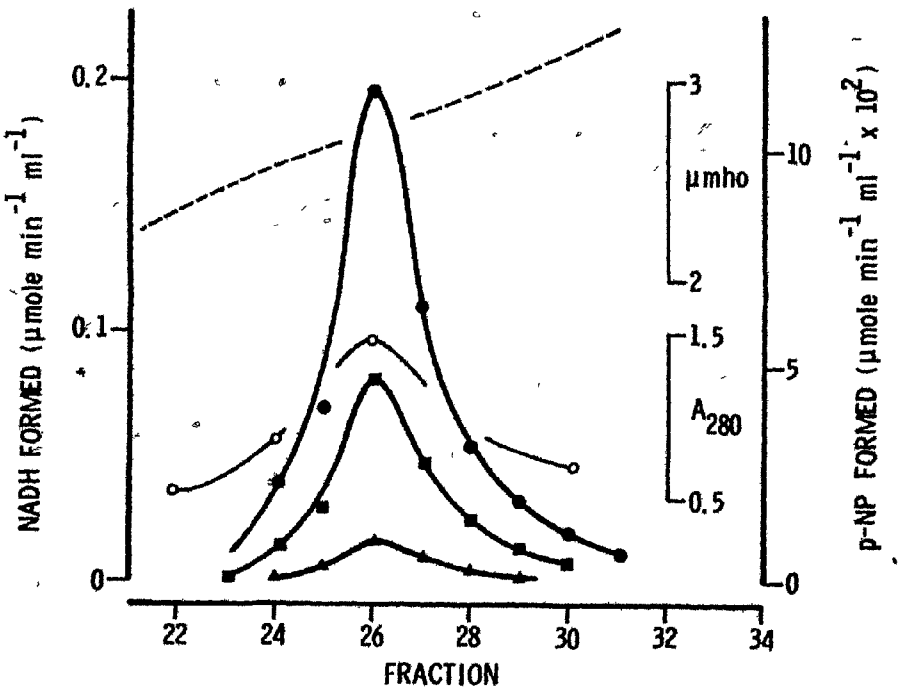

FIGURE 59

DEAE-sephadex column chromatography of human liver aldehyde dehydrogenase. Pooled fractions from DEAE-cellulose column were applied to the DEAE-sephadex column (2x35 cm), previously equilibrated with 0.04 mM sodium phosphate, pH 6.8, containing 1.0 mM GSH and 1.0 mM EDTA. Enzyme activity was eluted with a linear gradient between 0.04 M sodium phosphate, pH 6.8, and 0.2 M sodium phosphate, pH 6.8. Both buffers contained 1.0 mM GSH and 1.0 mM EDTA. The assay method for dehydrogenase and esterase activities is described under "Methods". Dehydrogenase activity (●); Esterase activity (▲); esterase activity in the presence of 1.0 mM NAD^+ (■); absorbance at 280 nm (○); conductivity (---).

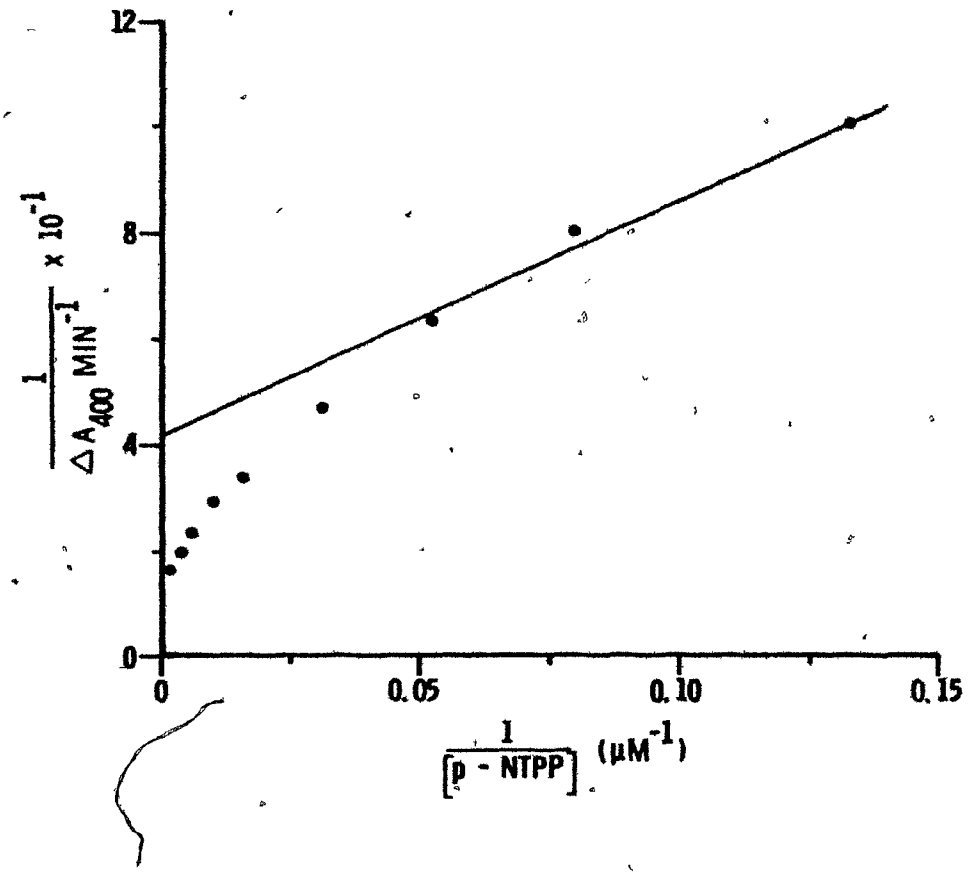

FIGURE 60

Double reciprocal plot of initial velocity versus p-nitrophenyl propionate concentration. Reaction mixtures contained: 33 mM sodium pyrophosphate, pH 7.0; 0.1 unit of enzyme and p-nitrophenyl propionate as indicated. Total volume one ml.

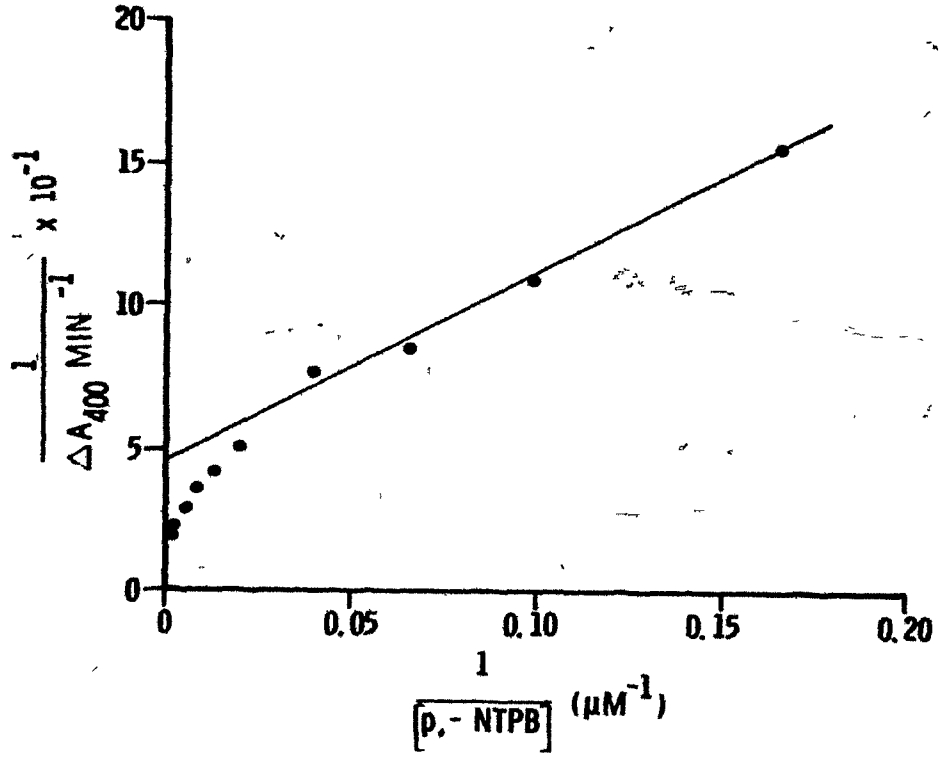

FIGURE 61

Double reciprocal plot of initial velocity versus p-nitrophenyl butyrate concentration. Reaction mixtures contained: 33 mM sodium pyrophosphate, pH 7.0; 0.12 unit of enzyme and p-nitrophenyl butyrate as indicated. Total volume one ml.

plots. K_m and V_{max} values calculated from Lineweaver-Burke plots at high and low ester concentrations are listed in Table VIII. It was apparent that an increase in the length of the aliphatic chain of the esters increased the Michaelis constant.

d. Activation by NAD^+ and NADH

NAD^+, a co-factor for the dehydrogenase reaction, stimulated the hydrolysis of p-nitrophenyl acetate. The plot of esterase activity as a function of NAD^+ concentration gave a hyperbolic curve (Figure 62). At very high concentrations (>0.01M) NAD^+ became inhibitory. Similar data, plotted in double reciprocal form, gave a straight line, indicating the binding of a single molecule of NAD^+ per active center (Figure 63). The activation constant calculated from these data was 75 μM.

NADH, a product of the dehydrogenase reaction, was also an activator of the esterase reaction. The initial rate of hydrolysis with respect to varying NADH concentration gave a hyperbolic relationship (Figure 64). At high concentrations NADH was also inhibitory. The double reciprocal plot of accelerated hydrolysis of p-nitrophenyl acetate versus NADH concentration was also linear, indicating the binding of one molecule of NADH per active center (Figure 65). The activation constant was determined to be 4 μM. The maximal extent of activation with NADH was somewhat less than half that observed with NAD^+.

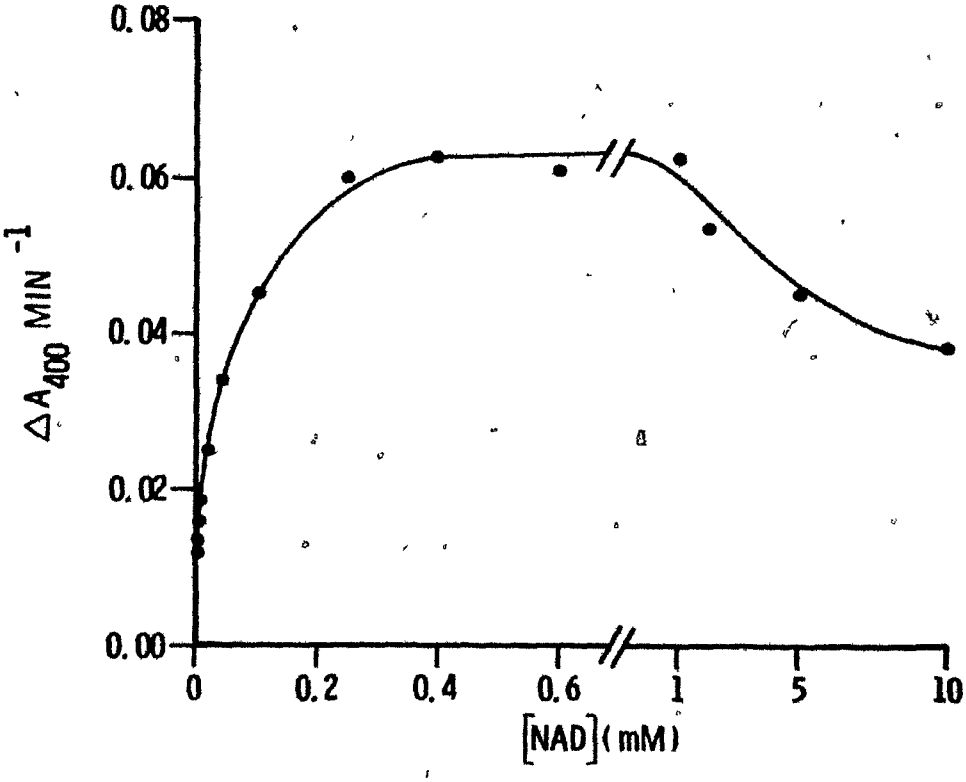

FIGURE 62

Activation of esterase activity by NAD^+. Reaction mixtures contained: 33 mM sodium pyrophosphate, pH 7.0; 0.06 unit of enzyme; 30 μM p-nitrophenyl acetate and the indicated concentrations of NAD^+. Total volume one ml.

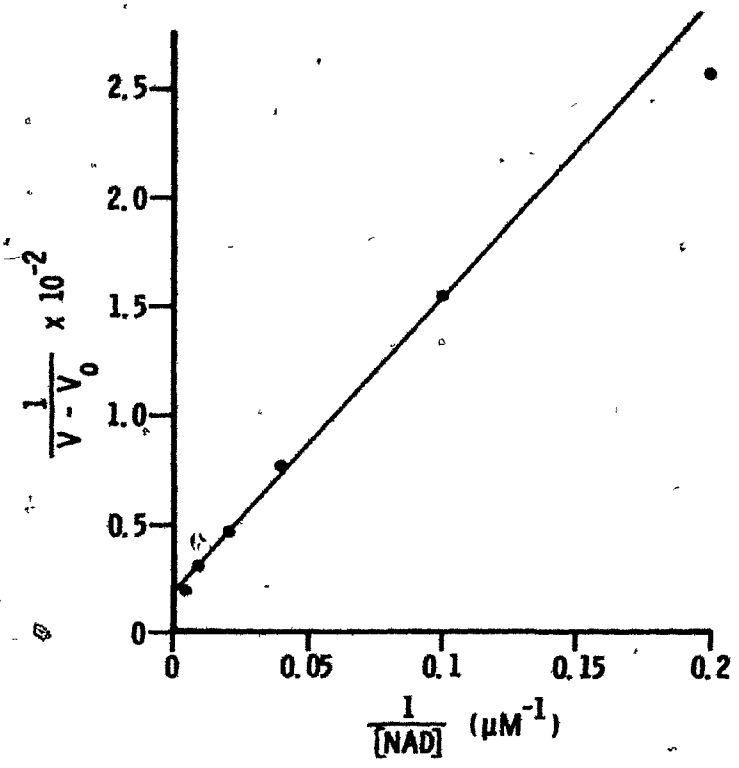

FIGURE 63

Double reciprocal plot of accelerated hydrolysis of p-nitrophenyl acetate versus NAD^+ concentration. Reaction mixtures as described in Figure 62. V, the absorbance change per min in the presence of NAD^+; V_o, the absorbance change per min in the absence of NAD^+.

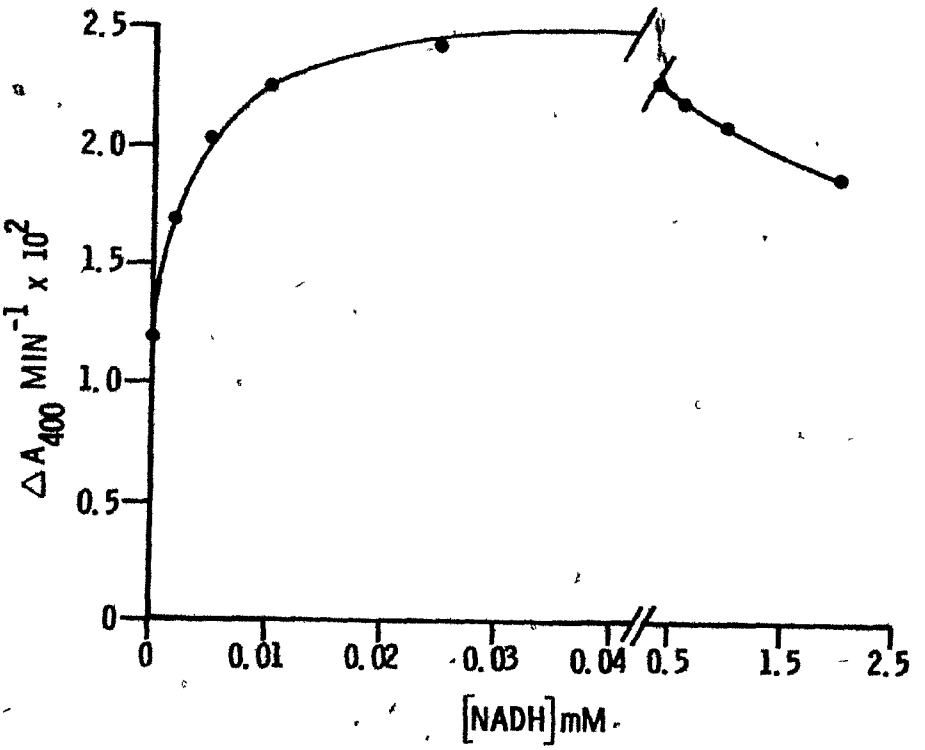

FIGURE 64

Activation of esterase activity by NADH. Reaction mixtures contained: 33 mM sodium pyrophosphate, pH 7.0; 0.045 unit of enzyme; 30 µM p-nitrophenyl acetate and the indicated concentrations of NADH. Total volume one ml.

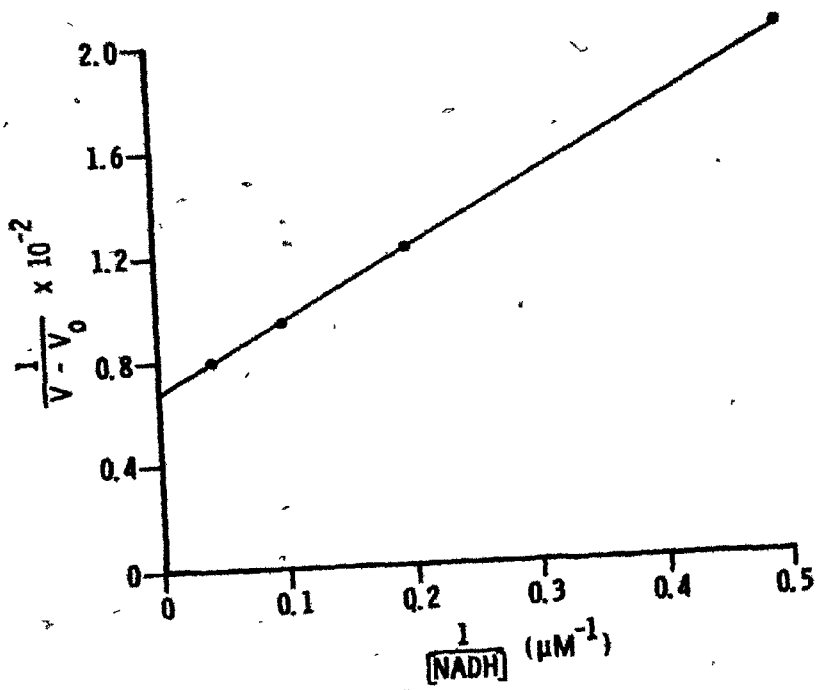

FIGURE 65

Double reciprocal plot of accelerated hydrolysis of p-nitrophenyl acetate versus NADH concentration. Reaction mixtures as described in Figure 64. V, the absorbance change per min in the presence of NADH; V_o, the absorbance change per min in the absence of NADH.

e. Effect of NAD^+ on the initial velocity versus ester concentration curve

A plot of initial rate of hydrolysis versus p-nitrophenyl acetate concentration in the presence of a saturating concentration of NAD^+ (i.e., a concentration which gave maximal stimulation) is shown in Figure 66. NAD^+ shifted the velocity versus substrate concentration plot to a normal hyperbolic curve. The double reciprocal plot of data from Figure 66 gave a linear relationship as required by Michaelis-Menten kinetics (Figure 67).

f. Effect of NAD^+ and NADH on K_m and V_{max} values for p-nitrophenyl acetate

Figure 68 illustrates double reciprocal plots of initial rate of hydrolysis versus p-nitrophenyl acetate concentration in the presence and absence of fixed levels of NAD^+ and NADH. The p-nitrophenyl acetate concentration range was below that where substrate activation became evident. It was clear from the reciprocal plots that K_m and V_{max} values for p-nitrophenyl acetate were increased by both NAD^+ and NADH. K_m and V_{max} values for p-nitrophenyl acetate in the presence and absence of NAD^+ and NADH are tabulated in Table IX.

g. Effect of NAD^+ on the double reciprocal plot at high ester concentration

Figure 69 shows the double reciprocal plot of initial rate of hydrolysis versus p-nitrophenyl acetate con-

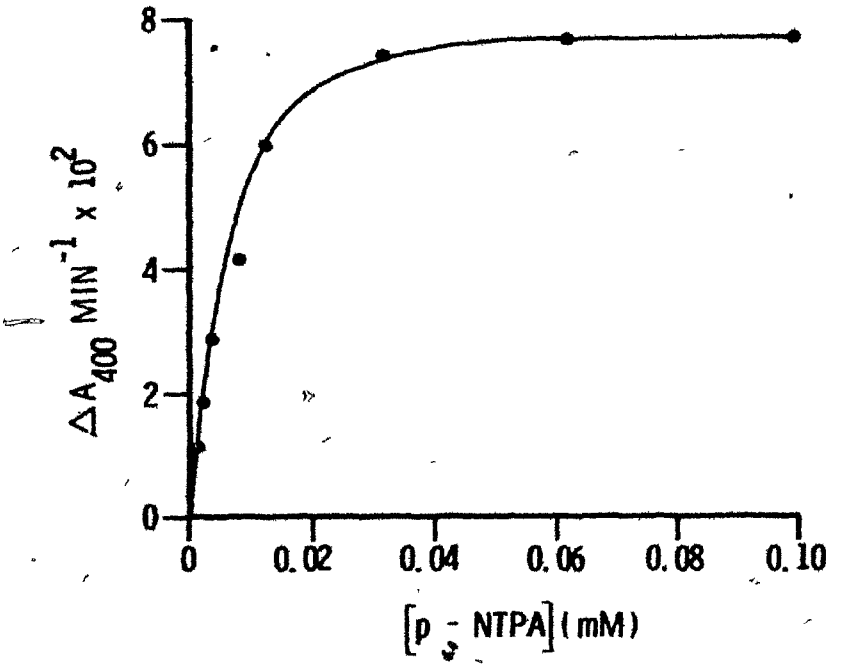

FIGURE 66

Plot of initial velocity versus p-nitrophenyl acetate concentration in the presence of NAD^+. Reaction mixtures contained: 33 mM sodium pyrophosphate, pH 7.0; 0.045 unit of enzyme; 1.0 mM NAD^+ and p-nitrophenyl acetate as indicated. Total volume one ml.

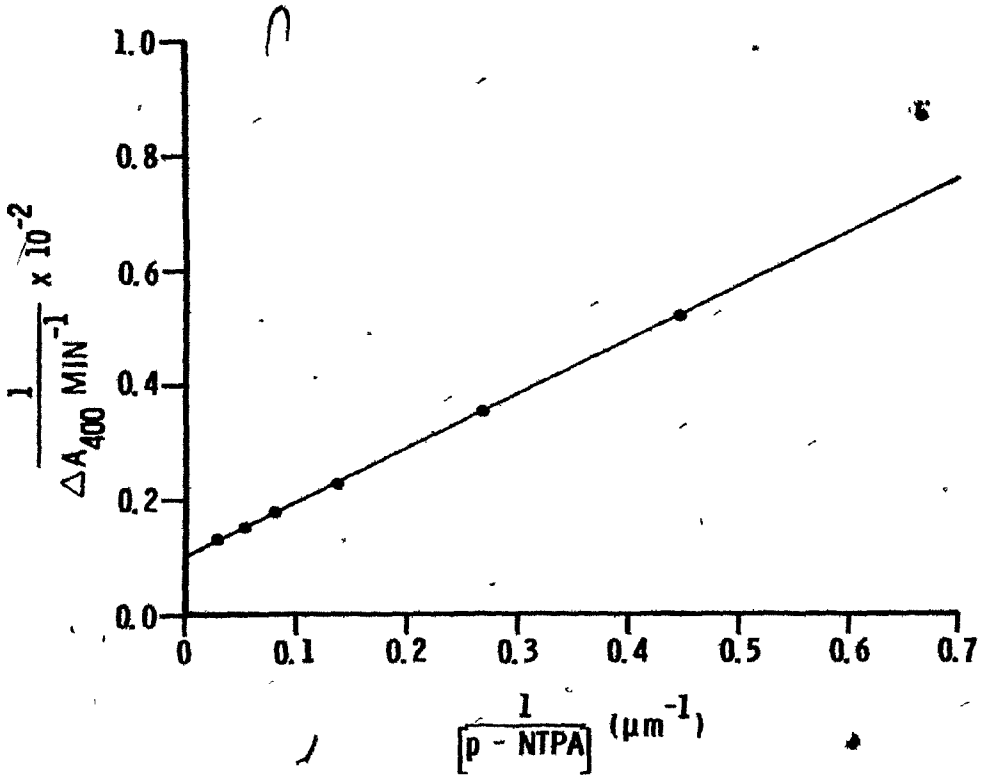

FIGURE 67

Double reciprocal plot of initial velocity versus p-nitrophenyl acetate concentration in the presence of NAD^+. Data taken from Figure 66.

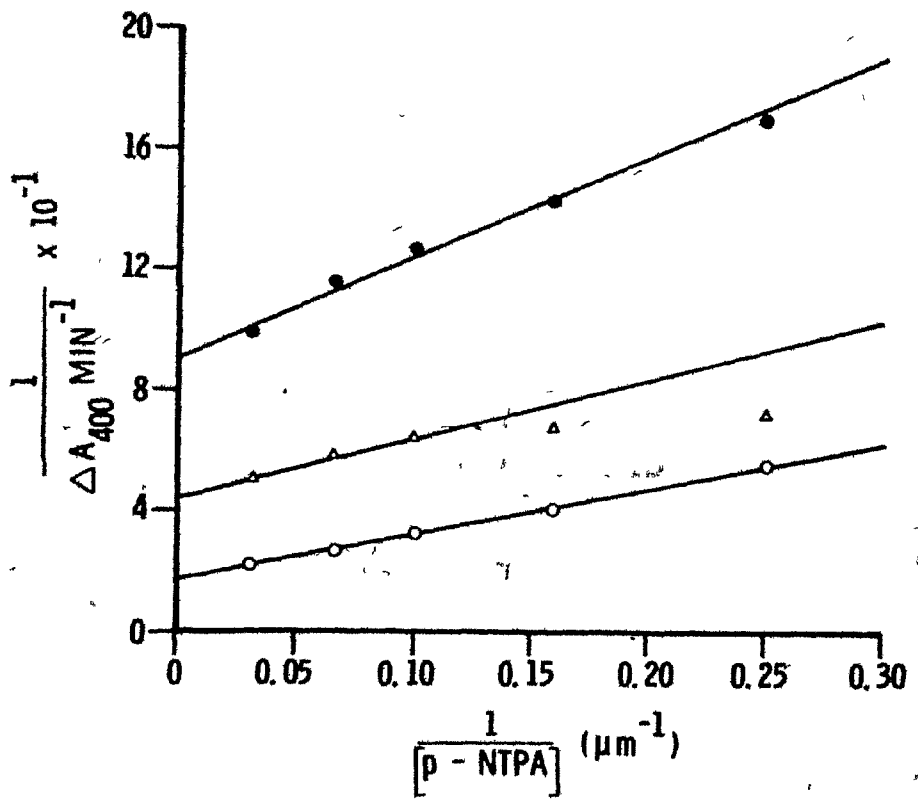

FIGURE 68

Double reciprocal plot of initial velocity versus p-nitrophenyl acetate concentration in the presence and absence of NAD^+ and NADH. Reaction mixtures contained: 33 mM sodium pyrophosphate, pH 7.0; 0.23 unit of enzyme; p-nitrophenyl acetate as indicated and NAD^+: (○) 1.0 mM; NADH: (△) 0.08 mM; (●) absent. Total volume one ml.

TABLE IX

COMPARISON OF KINETIC CONSTANTS FOR DEHYDROGENASE AND ESTERASE REACTIONS IN THE PRESENCE AND ABSENCE OF NAD^+ AND NADH

K_m and V_{max} values were calculated from data presented in Figure 68. V_{max} for esterase activity was calculated as micromoles of p-nitrophenol formed per min. V_{max} for dehydrogenase activity was calculated as micromoles of NADH formed per min.

Reaction	Activator	K_m	Relative V_{max} [a]
		μM	
Esterase	none	3.7	1.0
	NADH	4.4	2.0
	NAD^+	8.3	5.2
Dehydrogenase, pH 7.3	—	—	2.6

a V_{max} determined for esterase activity in the absence of modifier set equal to 1.0 as standard.

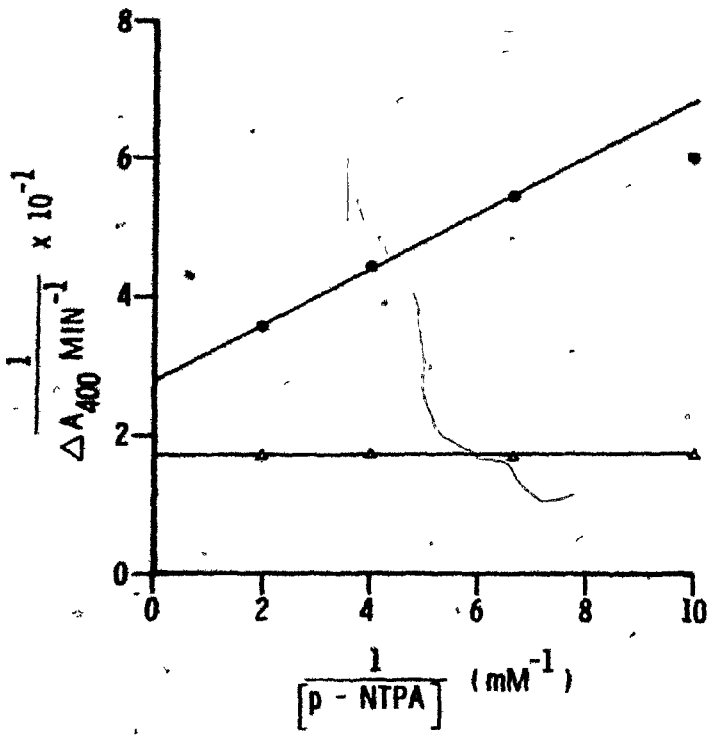

FIGURE 69

Double reciprocal plot of initial velocity versus high concentrations of p-nitrophenyl acetate in the presence and absence of NAD^+. Reaction mixtures contained: 33 mM sodium pyrophosphate, pH 7.0; 0.045 unit of enzyme and the indicated concentrations of p-nitrophenyl acetate. The concentrations of NAD^+ were: (●) none; (Δ) 2.0 mM. Total volume one ml.

centration in the presence and absence of a fixed level of NAD^+. In this experiment, p-nitrophenyl acetate was present at concentrations giving pronounced substrate activation in the absence of NAD^+. NAD^+ altered the double reciprocal plot to give a horizontal line (i.e., zero slope), consistent with the inference that the NAD^+-binding site may be identical with a second site for the binding of ester at high ester concentration (see Discussion).

h. Dead-end inhibition by glyceraldehyde and chloral hydrate

Glyceraldehyde, a substrate for the dehydrogenase reaction, competitively inhibited ester hydrolysis in the absence of NAD^+. The double reciprocal plot of initial rate of hydrolysis versus p-nitrophenyl acetate concentration in the presence of a constant concentration of glyceraldehyde is shown in Figure 70. The inhibition constant for glyceraldehyde was calculated to be 7 mM.

Chloral hydrate, a competitive inhibitor of the dehydrogenase reaction with respect to aldehyde, also competitively inhibited esterase activity in the absence of NAD^+, as shown in Figure 71. The inhibition constant for chloral hydrate was 0.86 mM. The inhibition patterns observed for chloral hydrate and glyceraldehyde are consistent with ester hydrolysis taking place at the aldehyde site.

Since NAD^+ was an activator of esterase reaction, it was of interest to determine the nature of chloral

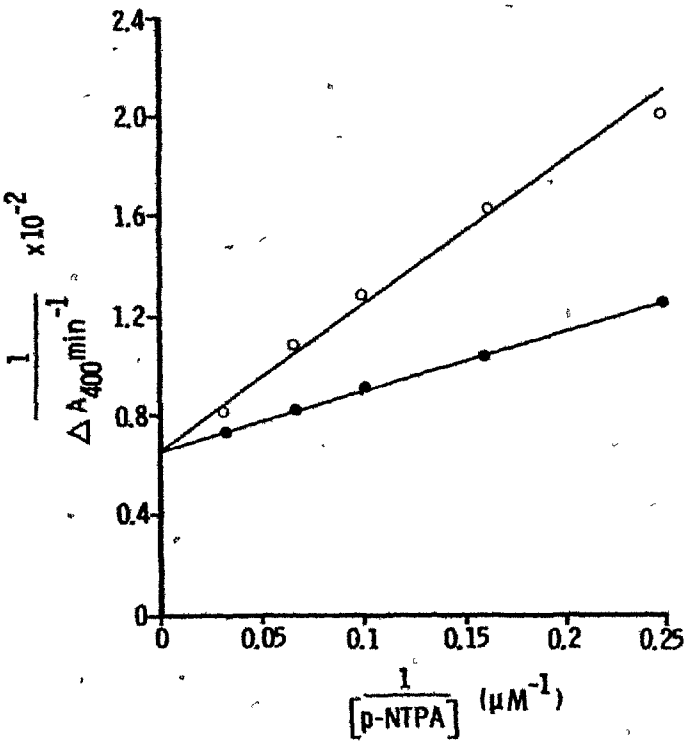

FIGURE 70

Inhibition of esterase activity by glyceraldehyde. Reaction mixtures contained: 33 mM sodium pyrophosphate, pH 7.0; 0.05 unit of enzyme and p-nitrophenyl acetate as indicated. The concentrations of glyceraldehyde were: (●) none; (○) 10 mM. Total volume one ml.

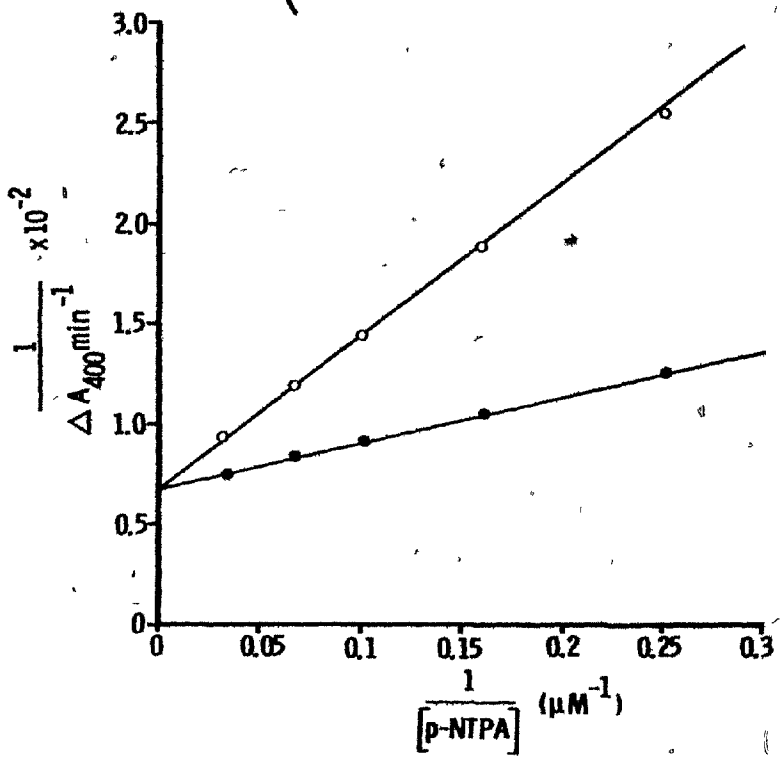

FIGURE 71

Inhibition of esterase activity by chloral hydrate. Reaction mixtures contained: 33 mM sodium pyrophosphate, pH 7.0; 0.05 unit of enzyme and p-nitrophenyl acetate as indicated. The concentrations of chloral hydrate were: (●) none; (○) 2.0 mM. Total volume one ml.

hydrate and glyceraldehyde inhibition in the presence of NAD^+. Figure 72 shows inhibition of ester hydrolysis by chloral hydrate in the presence of a fixed level of NAD^+ (the concentration which gave maximal stimulation). The presence of NAD^+ in the assay system did not change the inhibition pattern. However, it did lower the inhibition constant to 5 μM, as calculated from this data. A similar experiment with glyceraldehyde as an inhibitor in the presence of NAD^+ was found to be impossible to conduct owing to the fact that both the dehydrogenase and esterase reactions were taking place simultaneously and the product of the esterase reaction had a small absorption peak which overlapped the absorption maximum of NADH.

C. PROTEIN-PROTEIN INTERACTIONS

During kinetic investigations of human liver aldehyde dehydrogenase bovine serum albumin was observed to increase dehydrogenase activity as measured in the standard assay system. The following studies were carried out in order to delineate this activation effect.

1. Effect of Different Proteins on Dehydrogenase Activity

A survey of various proteins was carried out in the hope of correlating particular chemical or physical properties with the capacity of a protein to activate the dehydrogenase reaction. The results are presented in Table X, which

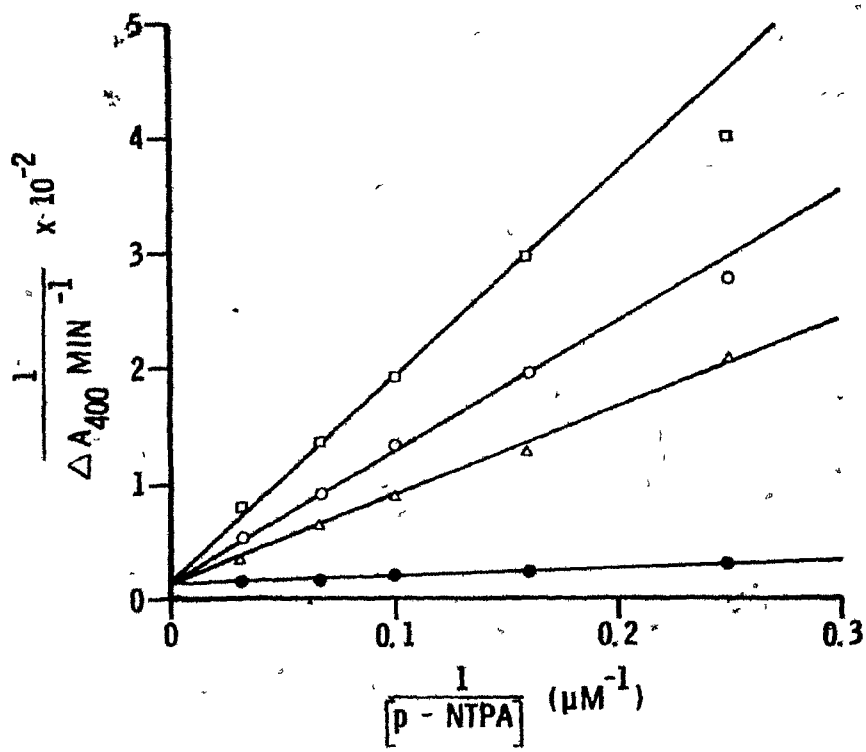

FIGURE 72

Inhibition of esterase activity by chloral hydrate in the presence of NAD^+. Reaction mixtures contained: 33 mM sodium pyrophosphate, pH 7.0; 0.088 unit of enzyme: p-nitrophenyl acetate as indicated and chloral hydrate: (●) absent; (Δ) 0.05 mM; (○) 0.1 mM; (□) 0.2 mM. Total volume one ml.

TABLE X

EFFECT OF VARIOUS PROTEINS ON HUMAN LIVER ALDEHYDE DEHYDROGENASE ACTIVITY

Reaction mixtures contained: 33 mM sodium pyrophosphate, pH 9.3; 2 mM acetaldehyde; 0.25 mM NAD^+; 0.01 unit of enzyme and one mg of the indicated protein. Total volume one ml.

Protein Added	Properties of Each Protein				Activity
	Molecular weight	pI (132)	SH group/ molecule (133)	SS group/ molecule (133)	%
None					100
Bovine Serum Albumin	66,000	4.7	0.7	17	134
Ovalbumin	46,000	4.59	3,4	1	103
Ribonuclease	13,700	9.6	0	4	105
Lysozyme	14,800	11.0, 11.2	0	4	109
Gelatin	-	4.7, 5.0	-	-	109
Cytochrome c	13,000	9.8, 10.1	0	0	110
Myoglobin	17,500	6.99	0	0	116

also includes selected physical and chemical properties of the proteins tested. Maximal activation occurred with bovine serum albumin under the reaction conditions employed and the activating effect did not correlate with any of the physical or chemical properties listed in the table.

2. Effect of Serum Albumins on the Dehydrogenase Activity

Serum albumins of different mammalian origins were analyzed for their effect on enzyme activity and the results are given in Table XI. Of all the albumins tested, bovine serum albumin exhibited the greatest activating effect on dehydrogenase activity. Since most commercially available serum albumins contain bound fatty acids, albumins free from fatty acids were also included in the trial in order to examine this parameter. The removal of free fatty acids from bovine serum albumin reduced the activation.

3. Effect of Bovine Serum Albumin on the pH Activity Curve for Aldehyde Dehydrogenase

Figure 73 shows the effect of BSA on enzyme activity as a function of pH when acetaldehyde was saturating and the NAD^+ concentration was 5 times its K_m value. Activity was optimal at pH values above 9 both with and without albumin. However, activation by bovine serum albumin increases as the pH decreases. Below pH 7.5 enzyme activity was very low in the absence of albumin under the reaction conditions used.

TABLE XI

EFFECT OF SERUM ALBUMINS ON HUMAN LIVER

ALDEHYDE DEHYDROGENASE ACTIVITY

Reaction mixtures contained: 33 mM sodium pyrophosphate, pH 9.3; 2 mM acetaldehyde; 0.25 mM NAD^+; 0.042 unit of enzyme and one mg of the indicated albumin. Total volume one ml.

Type of Serum Albumin Added	Activity %
None	100
Bovine	218
Human	88
Horse	77
Rabbit	149
Bovine, Fatty Acid Free	132
Human, Fatty Acid Free	84

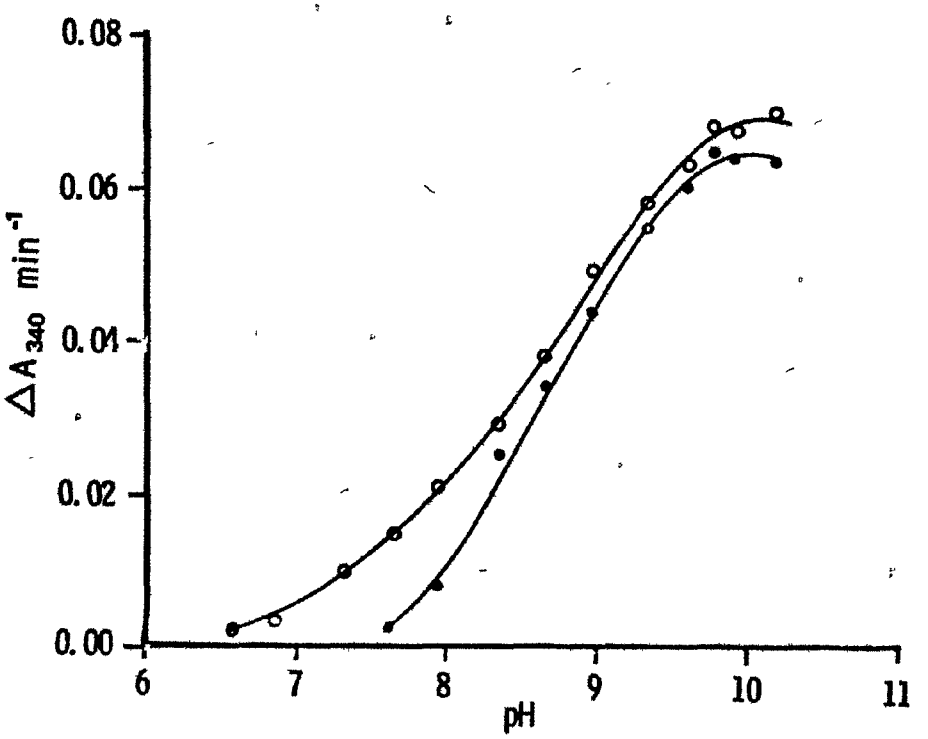

FIGURE 73

Effect of bovine serum albumin on the pH-activity curve for aldehyde dehydrogenase at high NAD^+ concentration. Reaction mixtures contained: 33 mM sodium pyrophosphate; 0.06 unit of enzyme; 2.0 mM acetaldehyde; 2.0 mM NAD^+ and albumin; (●) absent; (○) 1.0 mg. Total volume one ml.

Figure 74 shows the effect of bovine serum albumin on the pH dependence of dehydrogenase activity when acetaldehyde was saturating but the NAD^+ concentration was approximately equal to its K_m value. Here also, the BSA activation was most pronounced over the low pH range. Furthermore, the change in the pH activity curve produced by bovine serum albumin was much greater at the low NAD^+ concentration (Figure 74).

4. Effect of Bovine Serum Albumin on Kinetic Constants For the Dehydrogenase Reaction

Double reciprocal plots of initial velocity against varying concentrations of glyceraldehyde in the presence and absence of bovine serum albumin at pH 9.5 and 7.3 are shown in Figures 75 and 76. At both pH values, bovine serum albumin increased the apparent V_{max} for glyceraldehyde to approximately 1.3 times the control value (absence of albumin) whereas the Michaelis constant was unaffected at either pH value. Figure 77 and 78 show the effect of bovine serum albumin on K_m and V_{max} for NAD^+ at pH 9.5 and 7.3. In this case, bovine serum albumin decreased the Michaelis constant but did not affect the observed V_{max} value. The results are summarized in Table XII.

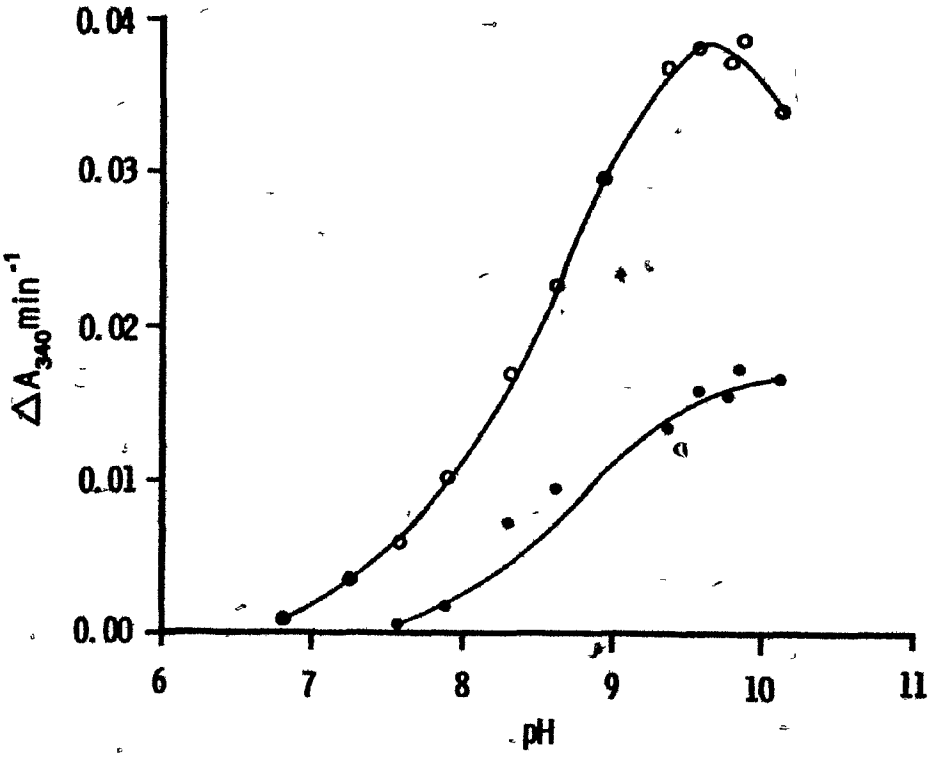

FIGURE 74

Effect of bovine serum albumin on the pH-activity curve for aldehyde dehydrogenase at low NAD^+ concentration. Reaction mixtures contained: 33 mM sodium pyrophosphate; 0.09 unit of enzyme; 2.0 mM acetaldehyde; 0.25 mM NAD^+ and albumin: (●) absent; (O) 1.0 mg. Total volume one ml.

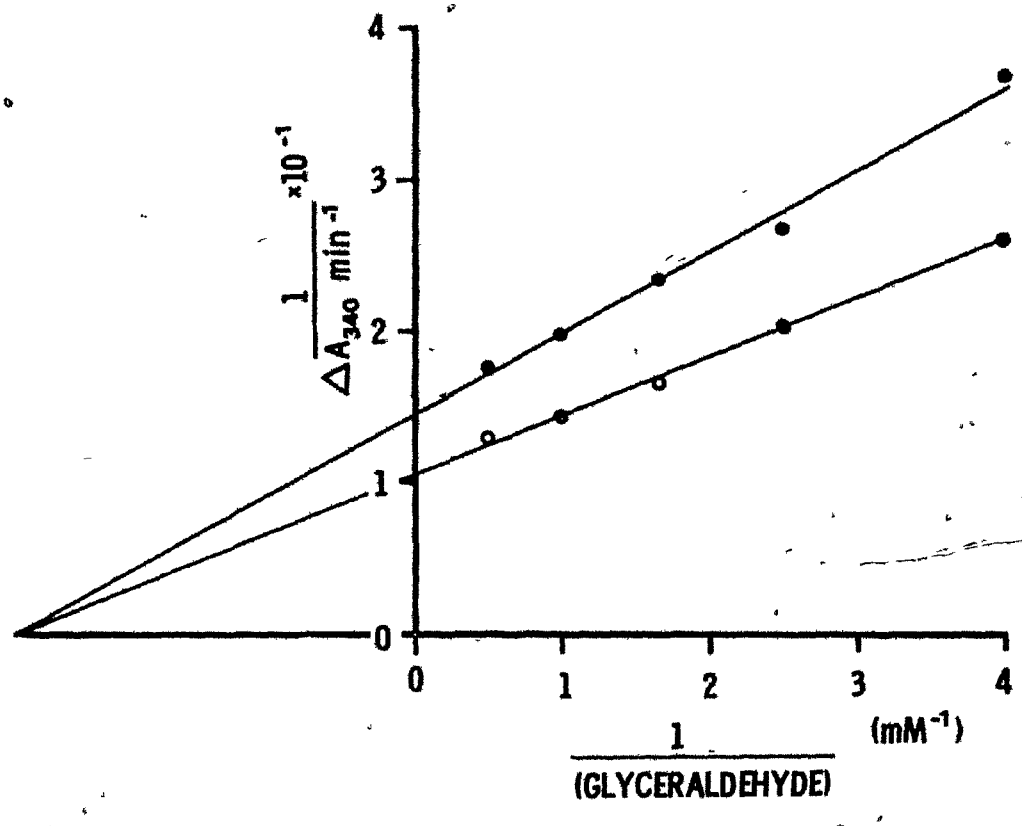

FIGURE 75

Double reciprocal plot of initial velocity versus glyceraldehyde concentration in the presence and absence of bovine serum albumin at pH 9.5. Reaction mixtures contained: 33 mM sodium pyrophosphate, pH 9.3; 0.05 unit of enzyme; 2.0 mM NAD^+; glyceraldehyde as indicated and albumin: (●) absent; (○) 1.0 mg. Total volume one ml.

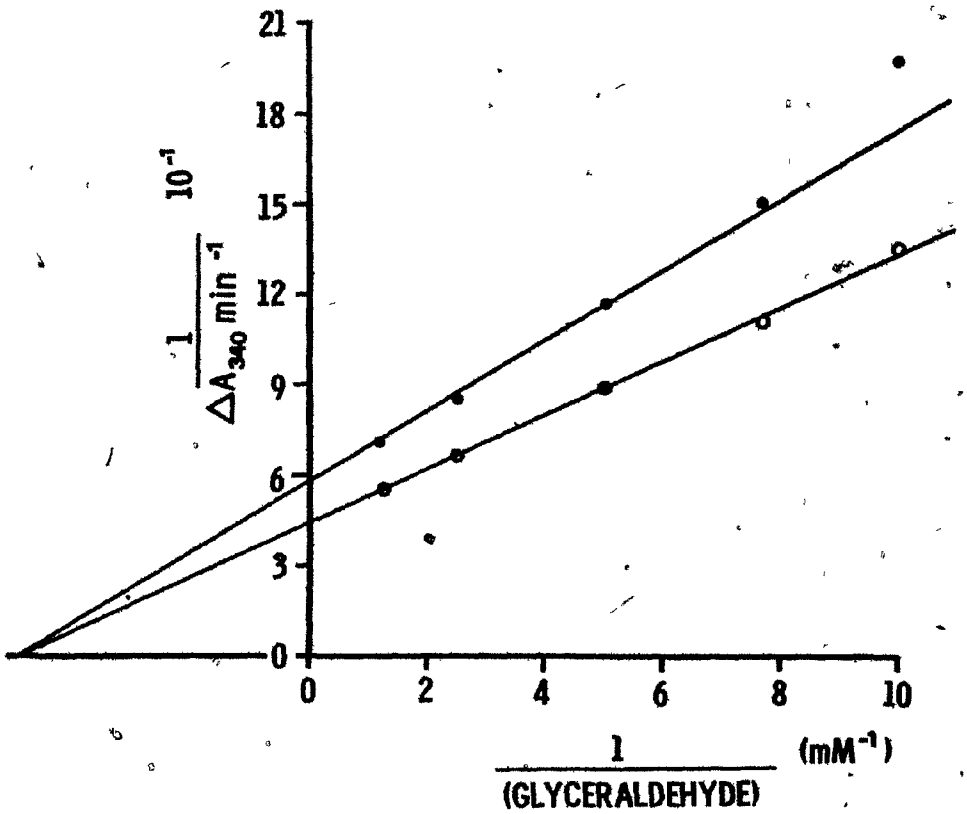

FIGURE 76

Double reciprocal plot of initial velocity versus glyceraldehyde concentration in the presence and absence of bovine serum albumin at pH 7.3. Reaction mixtures contained: 33 mM sodium pyrophosphate, pH 7.0; 0.32 unit of enzyme; 2.0 mM NAD^+; glyceraldehyde as indicated and albumin: (●) absent; (○) 1.0 mg. Total volume one ml.

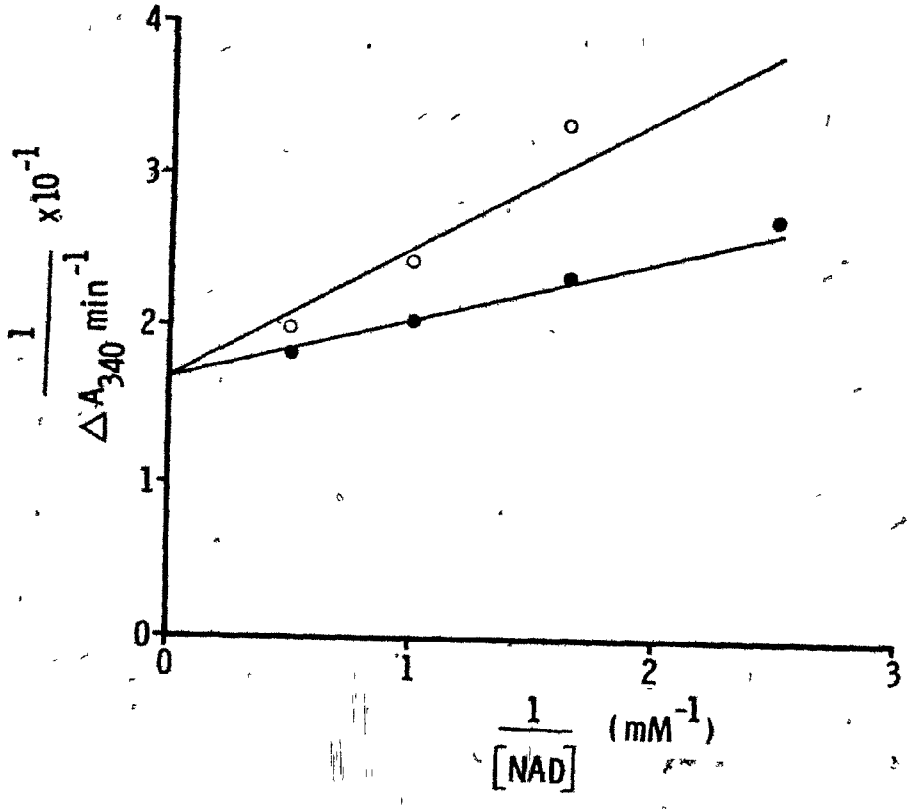

FIGURE 77.

Double reciprocal plot of initial velocity versus NAD^+ concentration in the presence and absence of bovine serum albumin at pH 9.5. Reaction mixtures contained: 33 mM sodium pyrophosphate, pH 9.3; 0.05 unit of enzyme; 2.0 mM acetaldehyde; NAD^+ as indicated and albumin: (O) absent; (●) 1.0 mg. Total volume one ml.

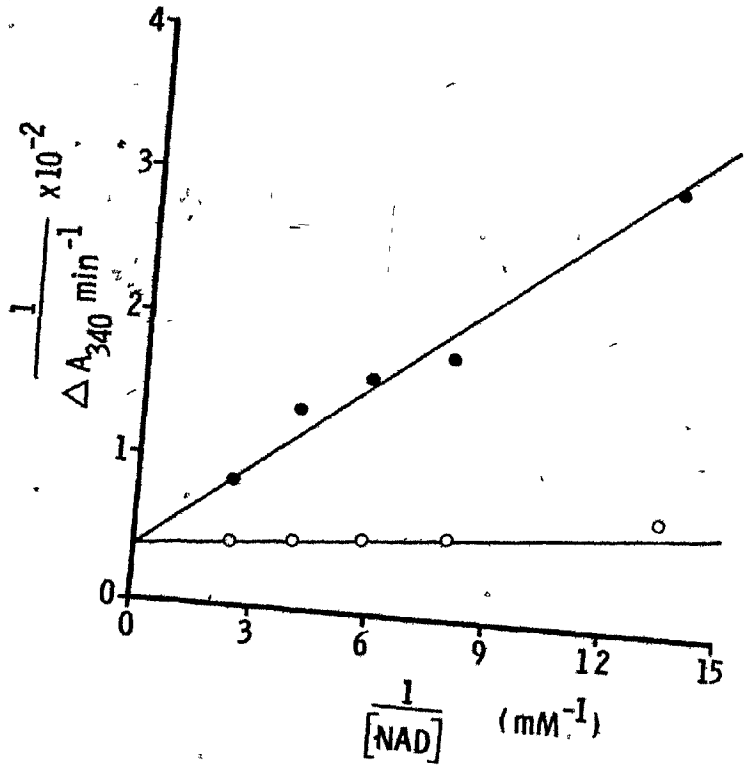

FIGURE 78

Double reciprocal plot of initial velocity versus NAD^+ concentration in the presence and absence of bovine serum albumin at pH 7.3. Reaction mixtures contained: 33 mM sodium pyrophosphate, pH 7.0; 0.4 unit of enzyme; 2.0 mM acetaldehyde; NAD^+ as indicated and albumin: (●) absent; (○) 1.0 mg. Total volume one ml.

TABLE XII

EFFECT OF BOVINE SERUM ALBUMIN ON MICHAELIS CONSTANTS AND MAXIMAL VELOCITIES FOR NAD^+ AND GLYCERALDEHYDE

K_m and V_{max} values were calculated from data presented in Figures 75 - 78.

Substrate	Bovine Serum Albumin	pH 7.3			pH 9.5		
		K_m	V_{max}	% increase in V_{max}	K_m	V_{max}	% increase in V_{max}
		mM	ΔA_{340}/min		mM	ΔA_{340}/min	
NAD^+	-	0.54	0.026	—	0.5	0.059	—
	+	0.053	0.026	0	0.23	0.059	0
Glyceraldehyde	-	0.2	0.015	—	0.37	0.065	—
	+	0.2	0.021	40	0.37	0.091	40

DISCUSSION

A. ENZYME PURIFICATION

In enzymology, the purification of unstable enzymes has remained a difficult task. The use of conventional as well as recently developed techniques for enzyme purification and modifications thereof have not yet brought this enzyme to the crystalline state. However, several improvements over the existing procedure have been achieved. For example, the addition of a sulfhydryl compound and EDTA in the equilibrating and eluting buffers has resulted in higher yields of enzyme from ion-exchange columns. GSH was found to be more effective than mercaptoethanol or cysteine and has been used routinely. Although GSH and EDTA stabilized this enzyme during purification, they did not activate it in the standard assay system. This behavior is in contrast to that observed with yeast and Pseudomonas aldehyde dehydrogenases, where a sulfhydryl compound must be included in the assay system (37,47,80).

The passage of crude extract through the PAB-cellulose column prior to loading on to the DEAE-cellulose column not only removed some of the contaminating proteins but also removed a considerable amount of lipid material which hinders the adsorption of enzyme by DEAE-cellulose. This interference manifests itself by causing channelling in the upper part of the column. The original procedure of removal of lipids and protein impurities by organic solvents such as alcohol

(134) was discontinued because of irreversible losses of activity during the time that the enzyme was exposed to solvent. Thus, the inclusion of a PAB-cellulose treatment early in the purification procedure improves the results obtained with subsequent steps.

The treatment of DEAE-cellulose purified human enzyme with calcium-phosphate gel yielded enzyme of 2.5-fold higher purity. This step is simple and less time consuming than any other step used in the purification of the human enzyme. The reason that this treatment was not used in the standard purification procedure is that no simple method to concentrate fractions obtained from the DEAE-cellulose column was found.

It is not clear why the enzyme could not be eluted from BD-cellulose columns.

Unfortunately, isoelectric focusing, a powerful technique for the separation of proteins differing in isoelectric points by as little as 0.02 pH units, failed to work because of the instability and precipitation of human liver aldehyde dehydrogenase at its isoelectric point. Moreover, incubation studies indicated that ampholine carrier ampholyte solutions, which form the medium usually used for creating a pH gradient in the isoelectric focusing column, were also inhibitory to this enzyme. Presumably, this inhibition also contributed to the failure to achieve success with the technique. Glycerol could protect the enzyme against inhibition by ampholytes in the test tube but not in the isoelectric focusing column. It

should be pointed out that ampholytes may also be inhibitory towards other enzymes.

The precipitation of proteins during an isoelectric focusing run is not a new problem experienced here. It has been a major drawback of this technique in the hands of many workers. However, horse liver aldehyde dehydrogenase has been successfully purified by the isoelectric focusing technique (36).

Attempts made to resolve the discrepancy in the molecular weight reported in the literature (44,62) led to the conclusion that human liver aldehyde dehydrogenase has a molecular weight of 200,000 daltons as reported by Blair and Bodley (44). No evidence at any stage was obtained in favour of a molecular weight of 100,000. Experiments carried out to determine the effect of enzyme concentrations on its elution patterns from sephadex columns demonstrated that a fifteen-fold dilution of the enzyme had no effect on the elution volume. Thus, it was not possible to obtain an explanation for the differing results reported by Deitrich's laboratory. Later, Deitrich indicated in a personal communication that the molecular weight of another enzyme sample determined by ultracentrifugation turned out to be 200,000 daltons.

B. INTERACTION WITH NAD^+-ANALOGUES

The groups on the NAD^+ molecule directly involved in binding to the human enzyme and in the catalytic step may be examined by studying the participation of various analogues in the dehydrogenase reaction. Studies with NAD^+-analogues has indicated that the human enzyme is capable of binding all of the analogues tested and reducing most of them, albeit at very low rates. This observation distinguishes this enzyme from yeast aldehyde dehydrogenase which is totally inactive with pyridine-3-aldehyde-AD^+ and pyridine-3-aldehyde-HD^+, but reduces other analogues at substantial rates (108). The bovine liver enzyme can also utilize certain pyridine-aldehyde analogues but gives generally greater rates than those observed with the human enzyme (107). The most active analogue with the human enzyme was 3-acetylpyridine-AD^+ which gave a maximal rate 6% of that with NAD^+. In contrast, deamino-NAD^+ was reduced at 53% of the rate of NAD^+ by the yeast enzyme and 3-acetylpyridine-AD^+ was reduced at 85% of the rate of NAD^+ by the bovine enzyme (107,108).

The data presented here on the coenzyme activity of NAD^+-analogues with the human enzyme showed that the carboxamide group and 6-amino group of adenine are not absolutely essential for the coenzyme activity of NAD^+, but that both groups are required for optimal activity. The high Michaelis constant for hypoxanthine analogues of NAD^+ suggests that the 6-amino group of adenine is involved in binding of NAD^+ to the human enzyme. The only exception was 3-acetylpyridine-

AD^+ which had a Michaelis constant very close to that for NAD^+.

As expected, the results also indicated that analogues with low coenzyme activity but with significant affinity for the enzyme are inhibitory. However, data for two NAD^+-analogues, 3-acetylpyridine-AD^+ and 3-acetylpyridine-HD^+ did not conform to this expectation. 3-Acetylpyridine-AD^+ was not inhibitory under the conditions employed (both nucleotides present at 0.6 mM) although equation 4 predicted 30% inhibition on the basis of the Michaelis constant measured for this analogue.

The low K_m value for 3-acetylpyridine-HD^+ was not expected for an analogue lacking the 6-amino group of adenine, e.g., by comparison with deamino-NAD^+. It may be that acetyl analogues behave differently because the acetylpyridine ring, unlike the nicotinamide ring in β-NAD^+, is in the anti conformation with respect to the pyrophosphate ribose backbone (110,111). The results obtained with thionicotinamide-AD^+ indicate that the incorporation of a C=S group in the place of a C=O group in the nicotinamide ring of NAD^+ increases the affinity of the analogue for this enzyme. Thionicotinamide-AD^+ was also found to be the strongest inhibitor.

Recent studies of Kaplan on the conformation of NAD^+ and its analogues indicate that deamino-NAD^+ occurs in the open conformation (110,111). Thus, the high K_m obtained for this analogue suggests that the stacked conformation is the preferred one for the human enzyme. It was also found that N^1-methylnicotinamide and nicotinamide mononucleotide were not

inhibitory under the conditions used here. This further suggests that the adenosine moiety of the NAD^+ molecule may make a major contribution in binding of the natural coenzyme.

C. KINETIC REACTION MECHANISM

Kinetic investigations of aldehyde dehydrogenase action are circumscribed by the experimental irreversibility of the reaction. This precludes the use of product inhibition and isotope exchange studies which have proved useful in distinguishing a large number of mechanisms. Furthermore, most aldehyde substrates not only exhibit very low substrate concentrations for half maximal velocity, making initial velocity measurements difficult, but also are chemically reactive. In the present instance, dead-end inhibition studies were included as a means of circumventing these difficulties and providing experimental data on the mode of interaction of substrates with human liver aldehyde dehydrogenase.

The intersecting initial velocity pattern observed with glyceraldehyde as variable substrate and NAD^+ as the changing fixed substrate (Figure 1) is consistent with a sequential mechanism in which all the substrates must bind to the enzyme before any product is released. Secondary plots of slopes and intercepts versus the fixed substrate (of the primary plot) were also linear as required by this mechanism. The data conform to equation 2 which specifies sequential mechanism. However, this rate equation does not distinguish between random or ordered addition of substrates and release

of products.

In the reciprocal plots shown in Figure 1 the lines appear to meet very far to the left of the 1/v axis. The shift in the point of intersection of these lines towards the 1/v axis, observed in the presence of an inhibitor competitive with respect to variable substrate, (Figure 7) indicates that the presence of the inhibitor affects rate constants for those steps which contribute to the estimation of K_{ia}, the inhibition constant for the first substrate. In other words, it can be concluded that a ping pong mechanism which requires the release of product before the addition of the last substrate does not apply for the human enzyme. The parallel appearance of the initial velocity pattern (Figure 1) simply reflects a small contribution by the term, $K_{ia}K_b$, in the sequential rate equation (2).

Initial velocity studies in which an inhibitor competitive with respect to the variable substrate was present, can also provide some information on the order of binding of substrates. In case of an ordered mechanism in which NAD^+ binds first, the K_{ia} value for NAD^+ will increase in the presence of an inhibitor competitive with respect to NAD^+. However, the intersection point of initial velocity patterns with glyceraldehyde as the variable substrate and a competitive inhibitor (with respect to glyceraldehyde) present should not change if the mechanism is ordered, NAD^+-first. In the same way, if aldehyde binding is the obligatory first step then the intersection point of the initial velocity pattern

in which NAD^+ is the variable substrate should remain constant in the presence of a competitive inhibitor (with respect to NAD^+). In the present study (Figures 7 and 8), whether NAD^+ was the variable substrate or glyceraldehyde was the variable substrate, the intersection points of initial velocity patterns changed in the presence of a competitive inhibitor with respect to the variable substrate. Thionicotinamide-AD^+, a competitive inhibitor with respect to NAD^+, increased the K_{ia} value for NAD^+ from 0.24 mM to 1.0 mM. Similarly, chloral hydrate, a competitive inhibitor with respect to aldehyde, increased the value for intersection point from 0.15 mM to 0.81 mM. It should be mentioned here that the K_{ia} value for the second substrate in case of an ordered mechanism can not be calculated from initial velocity data.

Substrate inhibition by glyceraldehyde indicated by the upward curvature in the double reciprocal plot, was more pronounced at pH 7.3 (Figure 5) than at pH 9.5 (Figure 1). This inhibition was overcome by NAD^+ as indicated most clearly by the reciprocal plot in Figure 6 where NAD^+ is the variable substrate and glyceraldehyde the changing fixed substrate. Moreover, the secondary plot of intercepts versus glyceraldehyde was still linear (Figure 4). Substrate inhibition is generally considered to be due either to the binding of a second molecule of substrate at a site other than the catalytic site or to the dead-end combination of substrate with an enzyme form other than the one it is supposed to react

with. The observed competitive substrate inhibition with respect to NAD^+ by glyceraldehyde at high concentrations can be accounted for if glyceraldehyde interacts at the NAD^+ site, perhaps with an amino or -SH group.

As stated above, the initial velocity data do not differentiate between random or ordered addition of substrates and release of products. Dead-end inhibitors may be used to distinguish between these possibilities. In an ordered mechanism, an inhibitor interacting at the A site (first substrate binding site) forms a dead-end complex with a free enzyme and, therefore, the inhibition with respect to second substrate (B) would be noncompetitive (equation 6). On the other hand, an inhibitor which interacts at the B site (second substrate binding site) forms a dead-end complex with a binary complex, EA. Thus, the inhibition with respect to the first substrate (A) would be uncompetitive (equation 7).

$$\frac{1}{v} = \frac{1}{V}\left(\frac{K_{ia}K_b}{A}(1 + I/K_i) + K_b\right)\frac{1}{B} + \left(\frac{K_a}{A}(1 + I/K_i) + 1\right)\frac{1}{V} \quad (6)$$

$$\frac{1}{v} = \left(\frac{K_{ia}K_b}{VB} + \frac{K_a}{V}\right)\frac{1}{A} + \frac{1}{V}\left(\frac{K_b}{B}(1 + I/K_i) + 1\right) \quad (7)$$

A random mechanism predicts that the inhibition by a dead-end inhibitor which is competitive with respect to the first substrate or the second substrate would be noncompetitive with

respect to the non-varied substrate in all cases (equations 11 and 13, see following). A number of patterns for various mechanisms are specified in Table XIII. In the present study, thionicotinamide-AD^+ and N'-methylnicotinamide, competitive inhibitors with respect to NAD^+, showed noncompetitive inhibition when glyceraldehyde was the variable substrate. Conversely, chloral hydrate gave competitive inhibition with respect to glyceraldehyde and noncompetitive with respect to NAD^+. Thus, these inhibition patterns are consistent with a random mechanism in which the interconversion of ternary complexes is the rate limiting step and all other steps are at approximate equilibrium, i.e., rapid equilibrium random mechanism. In a random mechanism either substrate, NAD^+ or aldehyde, can bind to free enzyme as well as to a binary complex (E-ald or E-NAD). The diagramatic representation of a random Bi Bi mechanism describing the interactions of competitive inhibitors, thionicotinamide-AD^+, N'-methylnicotinamide and chloral hydrate, with various enzyme species is shown below:

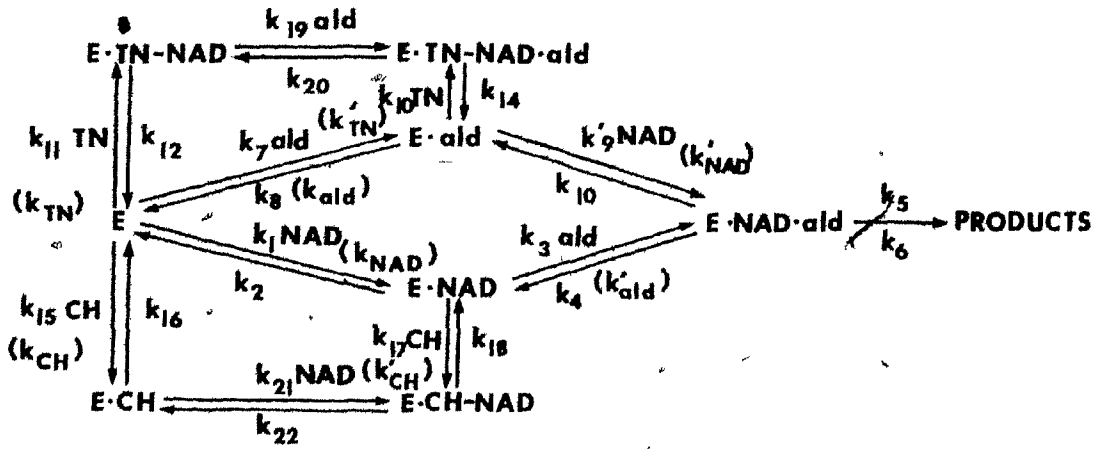

TABLE XIII

DEAD-END INHIBITION PATTERNS

Determined for ordered mechanisms by introducing $(1 + I/K_i)$ factors into equation 2 (equation 6 and 7) as described by Cleland (135). Determined for rapid equilibrium random mechanism by the procedure of Cha, including steps for combination of inhibitors as shown in scheme given on page 158.

Inhibitor	Variable Substrate	Interaction site	Inhibition pattern			
			Predicted			Observed
			Ordered		Random*	
			NAD^+ first	Ald. first		
Thionicotinamide-AD	NAD glyc.	NAD	compet. noncompet.	compet. uncompet.	compet. noncompet.	compet. noncompet.
N'-Methylnicotinamide	NAD glyc.	NAD	compet. noncompet.	compet. uncompet.	compet. noncompet.	compet. noncompet.
Chloral Hydrate	glyc. NAD	alde.	compet uncompet.	compet. noncompet.	compet. noncompet.	compet. noncompet.
Adenine	NAD glyc.	NAD	compet. noncompet.	compet. uncompet.	compet. noncompet.	compet. uncompet.
Adenosine	NAD glyc.	NAD	compet. noncompet.	compet. uncompet.	compet. noncompet.	compet. uncompet.
NADH	NAD glyc.	NAD	compet. noncompet.	compet. uncompet.	compet. noncompet.	compet. noncompet.

* Inhibitor combining with both E and a binery ES complex.

where TN = thionicotinamide-AD^+

CH = chloral hydrate

K_{TN}, K'_{TN}, K_{CH}, K'_{CH} = dissociation constants

K_{NAD}, K'_{NAD}, K_{ald}, K'_{ald}

This formulation was used as the basis for obtaining rate equation 8.

Equation 8 was derived on the basis of rapid equilibrium assumptions by using Cha's procedure (136) and incorporates terms for the dead-end combination of thionicotinamide-AD^+ and chloral hydrate.

$$v = \frac{V_1 NAD.Ald}{K_{NAD}.K'_{ald}(1 + \frac{CH}{K_{CH}} + \frac{TN}{K_{TN}}) + K'_{ald}.NAD(1 + \frac{CH}{K'_{CH}}) + K'_{NAD}.Ald(1 + \frac{TN}{K'_{TN}}) + NAD.Ald} \quad (8)$$

reciprocal form:

$$\frac{1}{v} = \frac{(1 + CH/K_{CH} + TN/K_{TN})K_{NAD}.K'_{ald}}{V_1 NAD.Ald} + \frac{K'_{ald}(1 + CH/K'_{CH})}{V_1 Ald} + \frac{K'_{NAD}(1 + TN/K'_{TN})}{V_1 NAD} + \frac{1}{V} \quad (9)$$

Equation 10 obtained by rearrangement of equation 9 describes the inhibition patterns obtained for thionicotinamide-AD^+ and N'-methylnicotinamide when NAD^+ is the variable substrate:

$$\frac{1}{v} = \frac{1}{V_1}\left[\frac{K_{NAD}K'_{ald}(1 + TN/K_{TN})}{Ald} + K'_{NAD}(1 + TN/K'_{TN})\right]\frac{1}{NAD} + \frac{1}{V} \qquad (10)$$

Thus, competitive inhibition is predicted for these inhibitors and was observed experimentally. (Figures 13 and 15).

Alternative rearrangement of equation 9 to give equation 11, specifies the observed pattern when aldehyde is the variable substrate:

$$\frac{1}{v} = \frac{1}{V}\left[\frac{K_{NAD}K'_{ald}(1 + TN/K_{TN})}{NAD}\right]\frac{1}{Ald} + \frac{1}{V_1}\left[1 + \frac{K'_{NAD}(1 + TN/K'_{TN})}{NAD}\right] \qquad (11)$$

In this case noncompetitive inhibition is predicted and the experimental results conformed, as shown in Figures 18 and 20.

Similarly equations 12 and 13 describe the inhibition patterns obtained for chloral hydrate.

When aldehyde is the variable substrate:

$$\frac{1}{v} = \frac{1}{V}\left[\frac{K_{NAD}K'_{ald}(1 + CH/K_{CH})}{NAD} + K'_{ald}(1 + CH/K'_{CH})\right]\frac{1}{Ald} + \frac{1}{V_1} \tag{12}$$

Competitive inhibition is predicted for this inhibitor and was observed experimentally (Figure 26).

When NAD^+ is the variable substrate:

$$\frac{1}{v} = \frac{1}{V_1}\left[\frac{K_{NAD}K'_{ald}(1 + CH/K_{CH})}{Ald}\right]\frac{1}{NAD} + \frac{1}{V}\left[1 + \frac{K'_{ald}(1 + CH/K'_{CH})}{Ald}\right] \tag{13}$$

In this case noncompetitive inhibition is predicted and the experimental results conformed, as shown in Figure 28.

Dead-end inhibition patterns for adenine and adenosine were competitive with respect to NAD^+ and uncompetitive with respect to glyceraldehyde, a pattern which might be interpreted to indicate that aldehyde is the obligatory first substrate. However, these inhibition patterns can also be

expected in the case of rapid equilibrium random mechanism if it is assumed that adenine and adenosine form dead-end complex only with the E.ald complex. Such an interaction is represented in the following diagram

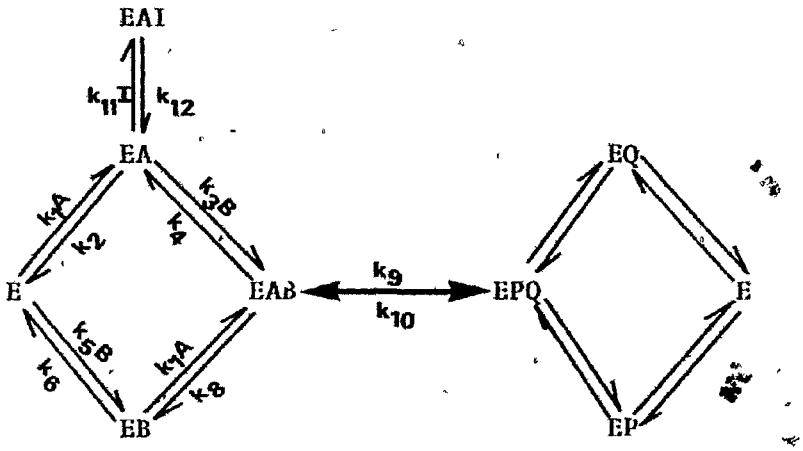

where A = aldehyde

B = NAD^+

I = inhibitor (adenine or adenosine)

The rate equation 14 derived for this mechanism by using Cha's procedure is as follows:

$$v = \frac{E_t k_9 \, AB/K_{A(EA)}K_{B(EAB)}}{1 + \frac{A}{K_{A(EA)}} + \frac{B}{K_{B(EB)}} + \frac{AB}{K_{A(EA)} \cdot K_{B(EAB)}} + \frac{AI}{K_{A(EA)} \cdot K_{I(EAI)}}} \quad (14)$$

In reciprocal form:

$$\frac{1}{v} = \frac{K_{A(EA)} \cdot K_{B(EAB)}}{V_1 AB} + \frac{K_{A(EAB)}}{V_1 A} + \frac{1}{V_1} + \frac{K_{B(EAB)}}{V_1 B} + \frac{K_{B(EAB)} I}{K_{I(EAI)} VB} \quad (15)$$

By rearrangement to equation 15 it can be shown that inhibition versus aldehyde (A) would be uncompetitive.

$$\frac{1}{v} = \frac{1}{V_1}\left[\frac{K_{A(EA)}K_{B(EAB)}}{B} + K_{A(EAB)}\right]\frac{1}{A} + \frac{1}{V_1}\left[1 + \frac{K_{B(EAB)}}{B}\left(1 + \frac{I}{K_I}\right)\right] \quad (16)$$

Similarly, by rearrangement to equation 15, inhibition versus NAD^+ (B) is seen to be competitive.

$$\frac{1}{v} = \frac{K_{B(EAB)}}{V}\left[\frac{K_{A(EA)}}{A} + 1 + \frac{I}{K_{I(EAI)}}\right]\frac{1}{B} + \frac{1}{V_1}\left(\frac{K_{A(EAB)}}{A} + 1\right) \quad (17)$$

Equation 16 and 17 indicate that the experimental inhibition data obtained with adenine and adenosine are consistent with a rapid equilibrium random Bi Bi mechanism. It

is to be noted that adenine and adenosine are very weak inhibitors ($K_{i\ slope}$ = 1.92 ± 0.16 mM and 0.58 ± 0.06 mM respectively) compared to the NAD^+-analogue, thionicotinamide-AD^+.

NADH, a product of the dehydrogenase reaction, inhibits dehydrogenase activity but this can not be treated as a typical product inhibitor because the reaction catalyzed by the aldehyde dehydrogenase is irreversible. Inhibition by NADH was competitive with respect to NAD^+ and noncompetitive with respect to glyceraldehyde. These results are consistent with a rapid equilibrium random mechanism and they fit equation 8. However, a similar inhibition pattern is also expected in case of an ordered mechanism in which NAD^+ is the first substrate. Such a pattern of NADH inhibition was also observed with pig brain aldehyde dehydrogenase (115). In contrast, NADH gave competitive inhibition with respect to NAD^+ and uncompetitive inhibition with respect to aldehyde for yeast aldehyde dehydrogenase (117). This finding was consistent with an ordered mechanism in which aldehyde is the first substrate. In studies on the horse enzyme NADH was reported to be a competitive inhibitor with respect to NAD^+ but data were not reported for the pattern with aldehyde as the variable substrate (116).

The results of dead-end and substrate inhibition studies with the human enzyme fit a rapid equilibrium random Bi Bi mechanism. With respect to random addition, it has traditionally been thought that linear initial velocity

reciprocal plots are indicative of a quasi-equilibrium random mechanism, since the rate equation derived on the basis of this formulation is first degree in both substrates. The equation derived on the basis of a steady state fully random mechanism contains terms in S^2, leading to the expectation of experimentally non-linear reciprocal plots. However, Cleland and Wratten, as well as others, have pointed out that linearity of initial velocity reciprocal plots does not necessarily mean that the mechanism is not a fully random one. Such plots become linear when there are special relationships between the rate constants (137,138) or at low substrate concentration (139). Studies of esterase activity now become pertinent to further defining the dehydrogenase mechanism.

First, the conclusion that NAD^+ as modifier does not bind solely to free enzyme in the esterase reaction and, second, the observation that glyceraldehyde can bind to free enzyme in the absence of NAD^+ (see Discussion, Section D for details), are consistent with random addition of NAD^+ and aldehyde to the enzyme during the dehydrogenase reaction. Inspection of certain kinetic parameters of the esterase and dehydrogenase reactions suggest that the mechanism for the dehydrogenase reaction may, in fact, be fully random rather than rapid equilibrium random. If the rapid equilibrium assumption is valid for the dehydrogenase reaction, K_{ia} for glyceraldehyde at pH 7.3 estimated from Figure 5 should agree with the inhibition constant (slope) obtained for

glyceraldehyde inhibition of ester hydrolysis in the absence of NAD^+ (Figure 70). These constants would be dissociation constants for glyceraldehyde from free enzyme in both cases. The fact that they do not agree (K_{ia} ≈0.1 mM; $K_{i\ slope}$ = 7 mM) suggests that the dehydrogenase mechanism is fully random in spite of the experimentally linear double reciprocal plots. The very high value of 7 mM for $K_{i\ slope}$ may be taken to imply that the dehydrogenase reaction flux is mainly via the enzyme-NAD^+ pathway but substantiation of this inference would require determination of individual rate constants rather than a thermodynamic equilibrium constant ($K_{i\ slope}$). A parallel comparison of K_{ia} for NAD^+ and the kinetic activation constant for NAD^+ with respect to ester hydrolysis cannot be made. This is because the dissociation constant for NAD^+ from free enzyme cannot be unequivocally calculated from this kinetic constant (see Discussion of Esterase Mechanism). However, the vast difference between the activation constant for NAD^+ (75 μM) and the inhibition constant for glyceraldehyde (7 mM) also implies that the pathway in which NAD^+ binds first predominates under certain conditions in the dehydrogenase reaction. Thus, one might expect chloral hydrate to give uncompetitive inhibition with respect to NAD^+ as variable substrate at a sufficiently low fixed concentration of glyceraldehyde. Nevertheless, the experiment (Figure 30) performed for chloral hydrate using a concentration of glyceraldehyde slightly higher than its K_m and NAD^+ as the variable substrate still resulted in noncompetitive in-

hibition. If one accepts the implications of the esterase data, this would indicate that both steady state pathways are operating at these concentrations of glyceraldehyde. At still lower concentrations of glyceraldehyde the flux should shift to an "aldehyde-first" pathway at aldehyde levels approaching saturation.

Pettersson(140) has recently carried out theoretical analysis of initial rate behavior of ternary complex mechanisms and suggested that the so-called compulsory order mechanism is never fully ordered but rather should be considered random-order in which one of the pathways carries most of the reaction flux. The existence of binary complex, EB, should not be ignored. It should be mentioned here that the behavior of such mechanisms in relation to dead-end and product inhibitions was not discussed by Pettersson. This author's theoretical analysis was limited to initial velocity studies. The rapid equilibrium assumption was applied in this study of aldehyde dehydrogenase to the analysis of dead-end inhibition patterns to simplify the mathematics required. The steady state random mechanism equations for dead-end inhibitors have never been derived. However, Rudolph and Fromm (138) have recently pointed out that the inhibition patterns predicted by computer simulation of steady state random mechanism for dead-end inhibitors are similar to those expected on the basis of the more restrictive rapid equilibrium assumption used for the interpretation of data obtained in this study. Wratten and Cleland (141) have reinvestigated

the kinetic mechanism of alcohol dehydrogenase which had been believed to be compulsory-order (NAD^+-first) for many years. They showed that the pathway in which alcohol (B substrate) binds to free enzyme does exist for this enzyme but that most of the reaction flux goes through the NAD^+ pathway. This conclusion was reached on the basis of the results obtained for methanol inhibition of either ethanol oxidation or acetaldehyde reduction. Methanol inhibited noncompetitively with respect to NAD^+ and gave a non-linear inhibition pattern with respect to ethanol or acetaldehyde. When ethanol was varied in the range of very high concentrations, noncompetitive inhibition with respect to ethanol was observed.

In summary, the only mechanism which readily accomodates all the kinetic data reported here for human liver aldehyde dehydrogenase, is a fully random Bi Bi mechanism. The addition of coenzyme and aldehyde and release of products can be diagrammed in the following simplified form:

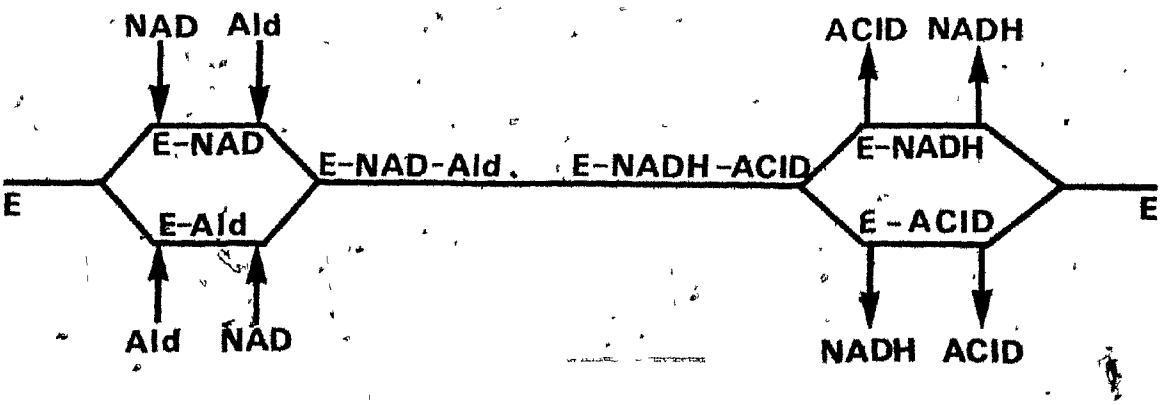

This mechanism is in contrast to that reported for pig brain aldehyde dehydrogenase by Duncan and Tipton (115) yeast aldehyde dehydrogenase by Schwarcz and Stoppani (108), and bovine liver aldehyde dehydrogenase by Freda and Stoppani (107). In all these cases it was concluded that an ordered mechanism in which NAD^+ binds first was operative. In fact, very limited kinetic studies were carried out by these workers. In case of pig brain aldehyde dehydrogenase, NADH inhibition was competitive with respect to NAD^+ and noncompetitive with respect to aldehyde. This and the observation of competitive substrate inhibition by aldehyde were the only criteria used to define the reaction mechanism. Substrate inhibition can not typically differentiate between random and ordered mechanisms unless supported by other inhibition data. Ping pong, ordered and random mechanisms all can show competitive substrate inhibition. Similarly, the same NADH inhibition patterns i.e., competitive with respect to NAD^+ and noncompetitive with respect to glyceraldehyde, are shown by a random mechanism as well as by an ordered mechanism in which NAD^+ binds first.

Competitive and uncompetitive inhibition patterns obtained for hydroxylamine with respect to aldehyde and the NAD^+-analogues, 3-acetylpyridine-AD^+ and deamino-NAD^+, respectively, were used as a basis for proposing an ordered (NAD^+-first) mechanism for yeast aldehyde dehydrogenase (108). It should be mentioned that hydroxylamine did not inhibit this enzyme when NAD^+ was used as a coenzyme.

The effect of structural analogues of coenzyme and aldehyde on the V_{max}, K_m for coenzyme and K_m for aldehyde were interpreted to indicate an ordered mechanism (NAD^+-first) for bovine liver aldehyde dehydrogenase (107).

In the case of horse enzyme (116), esterase data and the competitive inhibition pattern obtained for NADH with respect to NAD^+ were employed to assign an ordered mechanism (NAD^+-first) for this enzyme. The inhibition constant (K_I) for NADH in the dehydrogenase reaction was similar to its activation constant calculated from the esterase activation data. Also, the fact that glyceraldehyde did not inhibit esterase activity under the experimental conditions employed, was interpreted to indicate that a binary enzyme-aldehyde complex was not kinetically significant.

Bradbury and Jakoby (117) have recently reported evidence for an ordered mechanism in which aldehyde binds first to the yeast enzyme. This interpretation was based on the observation that NAD^+ did not bind to free enzyme in the equilibrium binding experiments and that inhibition obtained with NADH was competitive with respect to NAD^+ and uncompetitive with respect to aldehyde.

Since the human enzyme can now be prepared in almost homogeneous form, it would be interesting to perform equilibrium binding experiments on the formation of binary complexes. This approach should provide further information on the kinetic data presented in this thesis.

D. ESTEROLYTIC PROPERTIES

Human liver aldehyde dehydrogenase possesses the ability to catalyze the hydrolysis of a number of p-nitrophenyl esters, e.g., p-nitrophenyl acetate, p-nitrophenyl propionate and p-nitrophenyl butyrate. It appears that an increase in the length of the carbon chain of the acyl moiety of the ester decreases its affinity for the enzyme (Table VIII). Dehydrogenase activity and esterase activity measured in the presence and absence of NAD^+ gave identical elution profiles on DEAE-sephadex column chromatography (Figure 59), demonstrating that the same protein is responsible for both activities. NAD^+ and NADH, obligatory participants for dehydrogenase activity, stimulated ester hydrolysis. This behavior is similar to that reported for horse liver aldehyde dehydrogenase (116). Conversely, glyceraldehyde, a substrate for the dehydrogenase reaction, was a competitive inhibitor of esterase activity (Figure 70). This observation is consistent with ester hydrolysis taking place at the aldehyde binding site for dehydrogenase activity. Further substantiation was provided by the fact that chloral hydrate, a competitive inhibitor of dehydrogenase activity with respect to aldehyde, also competitively inhibited ester hydrolysis (Figure 71). Competitive inhibition of esterase activity by glyceraldehyde was not observed by Feldman and Weiner in the case of horse enzyme (116). The esterase reaction kinetics, i.e., glyceraldehyde and chloral hydrate inhibition and activation by NAD^+ and NADH, provide addition-

al evidence that both activities are associated with the same protein and closely interrelated.

NAD^+ also effects the binding of an aldehyde analogue. The presence of NAD^+ during the esterase reaction lowered the slope inhibition constant for chloral hydrate from 0.8 mM to 5.0 μM. Furthermore, this K_i (slope) value for esterase inhibition by chloral hydrate in the presence of NAD^+ was similar in magnitude to K_i (slope) found for its inhibition of the dehydrogenase reaction (glyceraldehyde varied at pH 9.5). The greatly reduced inhibition constant for chloral hydrate in the presence of NAD^+ with the esterase reaction suggests that NAD^+ not only acts as an electron acceptor in the dehydrogenase reaction but also induces a conformational change in the protein molecule. This hypothesis is consistent with the "induced fit model" of Koshland (142). Support for such a role has been provided by Nirenberg and Jakoby (143) with the observation that $NADP^+$-linked succinic semialdehyde dehydrogenase was more susceptible to trypsin digestion in the presence of NAD^+ or $NADP^+$ than in their absence.

It has been proposed for a number of carbonyl group-specific dehydrogenases that the reaction proceeds via thiohemiacetal formation followed by oxidation to the corresponding thioester. This enzyme intermediate in turn hydrolyses to release an acid product (144). Recent results of Feldman and Weiner have supported this mechanism for horse liver aldehyde dehydrogenase (116). Acylation of a sufhydryl or other group of the enzyme is a reasonable intermediate step

in the esterase reaction (119). Based on the observation of a competitive interaction between glyceraldehyde and p-nitrophenyl acetate with respect to the aldehyde binding site, it is feasible to consider the formation of a common acyl-enzyme intermediate in both the dehydrogenase and esterase reactions. Such a relationship may be depicted as follows:

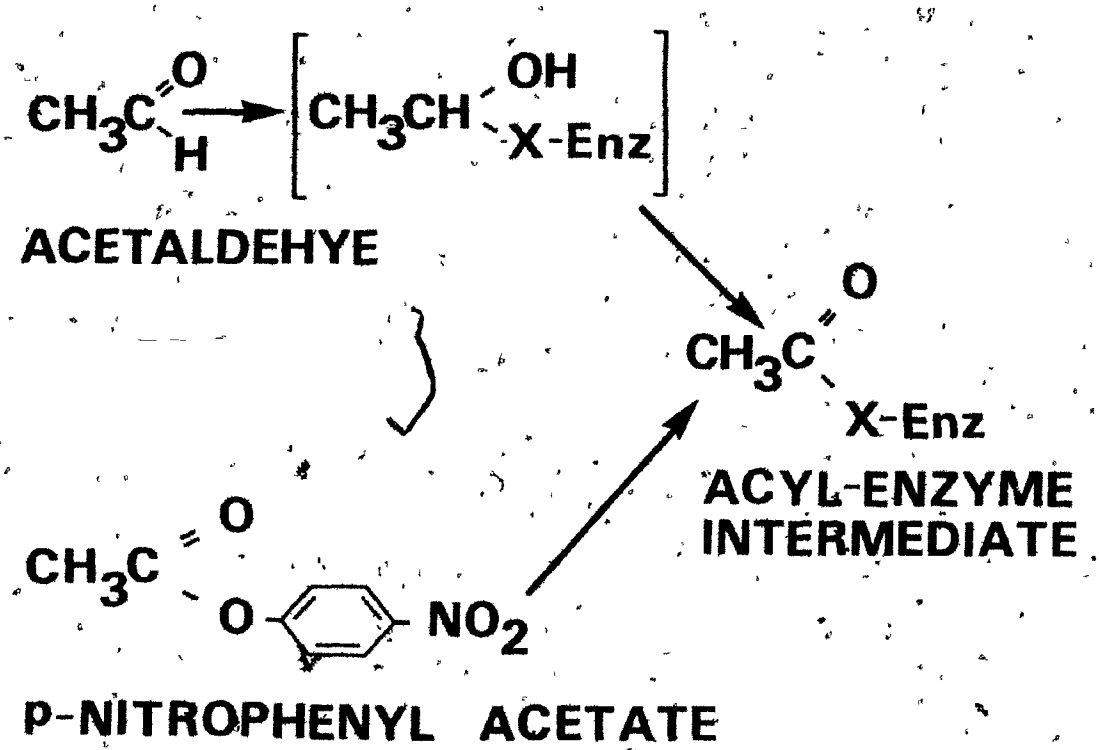

The existence of such an intermediate has been demonstrated in the case of p-nitrophenyl acetate hydrolysis by glyceraldehyde-3-phosphate dehydrogenase (119) and postulated for aldehyde dehydrogenases in general (39). On this basis,

the activation of esterase by NADH also provides information on the rate limiting step in the dehydrogenase reaction. Assuming a common acyl-enzyme intermediate, the esterase reaction in the presence of saturating levels of NADH would proceed via the ternary complex illustrated below:

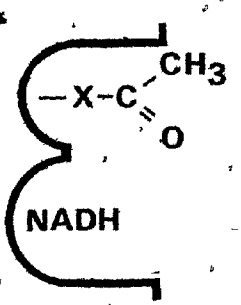

It can be seen from the data in Table IX that V_{max} for the esterase reaction in the presence of NADH is twice the V_{max} for the esterase reaction in the absence of NADH but less than V_{max} for the dehydrogenase reaction (pH 7.3). The fact that V_{max} for the esterase reaction in the presence of NADH is less than V_{max} for dehydrogenase reaction leads to the speculation that the rate limiting step in the esterase action occurs prior to the deacylation step. That is, deacylation could not be the rate limiting step in the esterase reaction since this would require the same step in dehydro-

genase action to be faster -- an impossibility if an identical complex is involved. A similar conclusion was reached for horse liver aldehyde dehydrogenase (116).

Data obtained for the effect of nicotinamide nucleotides on the Michaelis constant for ester also provides information on the order of binding of coenzyme and ester to this enzyme. Modifier (NAD^+ or NADH) could either bind to free enzyme or to binary enzyme-ester complex or both. The ways in which modifier (NAD^+) ester and enzyme can combine to give various enzyme species potentially present in the esterase reaction are shown below:

$$E + S \underset{k_2}{\overset{k_1}{\rightleftharpoons}} ES \xrightarrow{k_9} E + P \qquad K_{is} = \frac{k_2}{k_1}$$

$$E + M \underset{k_4}{\overset{k_3}{\rightleftharpoons}} EM \qquad K_{iM} = \frac{k_4}{k_3}$$

$$ME + S \underset{k_6}{\overset{k_5}{\rightleftharpoons}} MES \qquad K_{s(MES)} = \frac{k_6}{k_5}$$

$$ES + M \underset{k_8}{\overset{k_7}{\rightleftharpoons}} MES \qquad K_{M(MES)} = \frac{k_8}{k_7}$$

$$MES \xrightarrow{k_{10}} ME + P$$

where S = substrate

P = product

M = modifier (NAD^+)

K_{is}, K_{iM}, $K_{s(MES)}$, $K_{M(MES)}$ are dissociation constants

On the assumption of rapid equilibration among various enzyme species, the initial velocity equation derived by using Cha's procedure for the above mechanism is*:

$$v = \frac{V_S S + \frac{V_{S+M} MS}{K_{M(MES)}}}{K_{is} + S + \frac{K_{isM}}{K_{iM}} + \frac{SM}{K_{M(MES)}}} \qquad (18)$$

Under rapid equilibrium condition, steps governed by k_9 and k_{10} are considered slow compared to the other steps. Thus, k_9 and k_{10} in fact define the rate limiting steps in this mechanism. Possible estimates of certain dissociation constants can be obtained from the experimental data in Figures 63 and 68. In the absence of NAD^+, the K_m value for ester of 3.7 μM (Figure 68) will represent K_{is}, the dissociation constant for the enzyme-ester (ES) complex. Since a high concentration of p-nitrophenyl acetate (approaching saturation) was used to determine the activation constant for NAD^+ of 75 μM (Figure 67) this value will be a reasonable approximation of $K_{M(MES)}$, the dissociation constant for M from the ternary complex (MES). It is apparent from the data shown in Table IX that both NAD^+ and NADH increase the observed K_m for ester. A value for K_{iM}, the dissociation con-

---

* This derivation does not take into account substrate activation and applies only to velocities at low ester concentrations.

stant for the enzyme-modifier (EM) complex, may now be obtained by using this apparent Michaelis constant for p-nitrophenyl acetate (8.3 μM), determined in the presence of a constant level of modifier, NAD^+ (Table IX). If equation 18 is written in the form:

$$v = \frac{\left(V_s + \frac{V_{s+M}M}{K_{M(MES)}}\right)S}{\left(K_{is} + \frac{K_{is}M}{K_{iM}}\right) + \left(1 + \frac{M}{K_{M(MES)}}\right)S}$$

it can easily be seen that the apparent Michaelis constant for ester is given by the following expression:

$$\text{Measured } K_m = K_{is}\left[\frac{1 + \frac{M}{K_{iM}}}{1 + \frac{M}{K_{M(MES)}}}\right]$$

The value obtained for K_{iM} by appropriate substitution in this expression was 32 μM. Here it can be said that K_{is} for ester only goes up when $K_{M(MES)} > K_{iM}$. It is important to stress that these calculations are based on the assumption of rapid-equilibrium conditions holding for this reaction. Such an assumption has usually been based on the observation of linear double reciprocal rate plots as in this study. However, it is becoming increasingly evident that fully random mechanisms can give plots which are approximately linear

within experimental error or, in fact, truly linear for certain combinations of rate constants (see also Discussion of the Dehydrogenase Reaction). If modifier and ester add to the enzyme in a fully random mechanism the above calculations of dissociation constants would be invalid — $K_{M(MES)}$ could be either larger or smaller than K_{iM}. The present data do not permit a distinction to be made at this stage between a fully random or rapid equilibrium random mechanism. However, the data rule out a mechanism in which NAD^+ or NADH can only bind to a binary-ester complex.

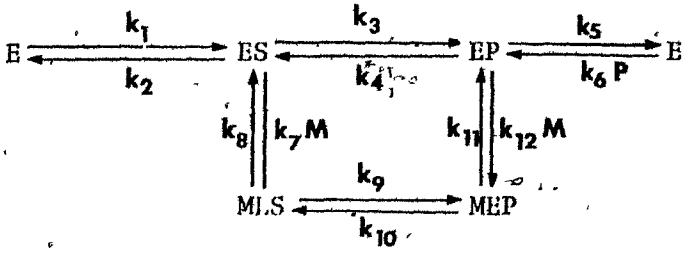

where S = substrate (ester)
M = modifier (NAD^+)
P = product

The rapid equilirbium initial velocity equation which specifies this mechanism is:

$$v = \frac{V_S S + \frac{V_{S+M} MS}{K_{M(MES)}}}{S + \frac{SM}{K_{M(MES)}} + K_{is}}$$

3 3

OF/DE

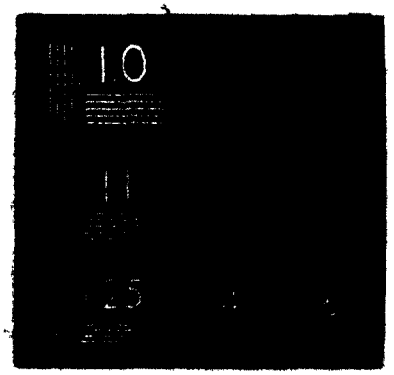

which requires a reduction in apparent K_m for the ester substrate in the presence of modifier. This conclusion was the same when the corresponding steady state formulation was used as a basis for obtaining the rate equation by the computer procedure of Hurst (145):

$$v = \frac{\left[K_1 + K_2M\right] S}{\left[K_3 + K_4M + K_5M^2\right] S + K_6 + K_7M}$$

K's refer to complex expressions made up of groupings of individual rate constants specifying steps in the mechanism

The apparent Michaelis constant is equal to:

$$\frac{K_6 + K_7M}{K_3 + K_4M + K_5M^2}$$

The value of this expression must decrease at high values of M. Conversely, the fact that esterase activity was observed in the absence of any nicotinamide nucleotide disposes of a formulation in which NAD^+ is the obligatory first ligand binding to free enzyme. Hence, the observation that nicotinamide nucleotides increase the K_m for the ester substrate is consistent with random order of addition of ester and activator to the human enzyme. Such a mechanism may be diagrammed in a simple way:

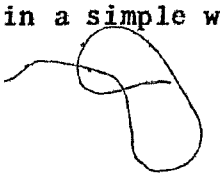

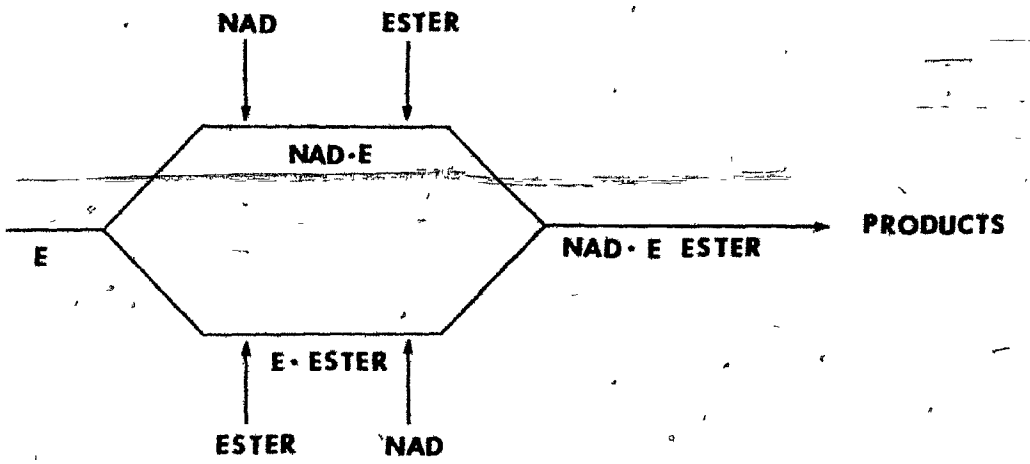

This hypothesis for the esterase reaction is consistent with that proposed for the dehydrogenase reaction (see Discussion under Kinetic Reaction Mechanism).

E. ESTERASE REACTION — SUBSTRATE ACTIVATION HYPOTHESIS

According to the Michealis-Menten formulation, the plot of v as a function of S is a hyperbola, with horizontal asymptote k_2E. The Michaelis-Menten equation may be represented as follows:

$$v = \frac{VS}{K_m + S}$$

In reciprocal form:

$$\frac{1}{V} = \frac{K_m}{V} \times \frac{1}{S} + \frac{1}{V}$$

The downward curvature of the double reciprocal plot in Figure 58 indicates a deviation from normal Michaelis-Menten kinetics. It has been proposed that such downward curvature is due to the activating effect of a second molecule of substrate binding at a site other than the catalytic site but this concept has not been well established experimentally (146,147). The observed downward curvature seen in these double reciprocal plots can be explained by postulating two binding sites for p-nitrophenyl acetate on the same enzyme. Binding of a second molecule of ester at a non-hydrolytic site other than the catalytic site would then alter the properties of the catalytic site. Such a substrate activation mechanism can be represented as follows:

$$E + S \rightleftharpoons ES$$

$$S + E \rightleftharpoons SE$$

$$ES + S \rightleftharpoons SES$$

$$SE + S \rightleftharpoons SES$$

$$SES \longrightarrow SE + P$$

$$ES \longrightarrow E + P$$

It can also be represented in a more simplified form:

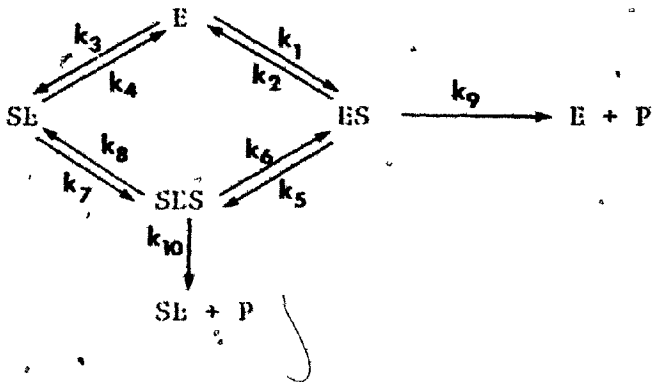

ES represents the enzyme-substrate complex in which S is bound at the catalytic site, SE is enzyme-substrate complex in which substrate is bound at the second site (non-catalytic site), and SLS is activated enzyme-substrate-substrate complex. Both ES and SES are assumed to break down to products + E and E + SE, respectively.

The following quasi-equilibrium rate equation has been derived on the basis of above mechanism (148):

$$v = \frac{V_2 + V_1K_2/(1 - V_1/V_2)S}{1 + K_2/(1 - V_1/V_2)S + K_1K_2/(1 - V_1/V_2)S^2}$$

This rate equation has an S^2 value in the denominator which will lead to non-linear reciprocal plots. The intercept term is affected due to the stimulatory effect of substrate at high concentrations. If $k_{10} > k_9$, the double reciprocal plot will show downward curvature at high substrate

concentrations. Results were fitted to this rate equation and found to be in good agreement as shown in Figures 57 and 58.

Additional insight into the mode of interaction of p-nitrophenyl acetate is provided by the following observations. The plot of initial rate of hydrolysis as a function of ester concentration in the presence of NAD^+ gave a normal hyperbolic curve (Figure 66). In fact, the double reciprocal plot of the data obtained in the presence of NAD^+ over the otherwise stimulatory concentration range of ester is a horizontal line (Figure 69). This result can be interpreted to indicate that NAD^+ blocks the binding of substrate at high concentrations at the second site which is responsible for the activation. There is then no site other than the catalytic site left for the binding of substrate. These results also constitute good evidence that the second binding site for ester is the coenzyme binding site for dehydrogenase activity. In general, an agent which blocks substrate activation could in itself be either an activator or inhibitor of hydrolysis. NAD^+ which blocks the binding of the ester substrate at the second site is an activator of the esterolytic activity of human aldehyde dehydrogenase. The binding of p-nitrophenyl acetate or NAD^+ at the second site may induce a similar conformational change in the polypeptide chain which in turn enhances the catalytic power of the active site with respect to hydrolysis.

Although, these results are consistent with activation of the catalytic site mediated by the second ester binding site, they do not rule out the occurance of hydrolysis also

at this second site. Currently available kinetic techniques are unable to unequivocally distinguish between the two alternatives since the rate equations derived for both mechanisms are of the same form*.

The evidence presented here tends to favour the first mechanism without eliminating the contribution, if any, by the second mechanism. Substrate activation was observed in the case of chymotrypsin but ester hydrolysis at the second site was thought to contribute not more than 10% (149). The only method which can clearly distinguish both mechanisms is the chemical blockage of one site, leaving the other site untouched. However, such chemical modification might well expose other functional groups which could also hydrolyze p-nitrophenyl acetate.

F. ACTIVATION OF THE DEHYDROGENASE REACTION BY BOVINE SERUM ALBUMIN

All aldehyde dehydrogenases which have been purified to homogeneity are composed of subunits (36,75). The nature of interactions between subunits responsible for the molecular integrity and their influence on the catalytic process are not yet known. In the present study, a number of different unrelated proteins of diverse physical and chemical properties

---

* A mixture of two enzymes utilizing the same substrate would also give this type of rate equation. However, chromatographic and kinetic studies have ruled out the possibility of any contamination being responsible for substrate activation and/or esterase activity (see Discussion, Section D).

have been examined for effects on native human liver aldehyde dehydrogenase activity. Among these proteins, only bovine serum albumin produced substantial changes in catalytic behavior. Comparisons among other proteins indicated that molecular size, overall charge character, or sulfhydryl and disulfide content individually, are not major factors responsible for the activation. Failure to observe effects of similar magnitude with albumins from other species suggested that activation of the dehydrogenase reaction is due to a specific interaction between bovine serum albumin and the human enzyme. The effect of bovine serum albumin on other aldehyde dehydrogenases has not been reported. The reduced activation obtained with fatty acid free bovine serum albumin might be due to a change in conformation of bovine serum albumin by the treatment used to remove fatty acids from it.

Activation by bovine serum albumin was strongly pH dependent. The most dramatic relative increase in dehydrogenase activity in the presence of BSA occurred at pH values close to neutrality, both with low and high concentrations of NAD^+ as illustrated by the data in Figures 73 and 74. This behavior raises the possibility that the interaction of BSA with the human enzyme induces a conformational change which is favourable for enzyme catalysis. Such a change might be similar to that caused by a change in the ionization state of some functional group(s) in the protein since enzyme activity reaches a maximum at high pH (above pH 9.0).

The greater effect of BSA on the pH-activity relationship at low NAD^+ levels compared to high NAD^+ levels suggests that interaction of bovine serum albumin with the human enzyme increases its affinity for NAD^+. This is further supported by the following observations. First, the double reciprocal plot of initial velocity versus NAD^+ concentrations in the presence and absence of BSA shows a "competitive" activation pattern. In other words, aldehyde dehydrogenase activity was the same both in the presence and absence of BSA when NAD^+ was saturating (infinite concentration). Only the Michaelis constant for NAD^+ is affected, not the V_{max} (Figures 77 and 78). It should be mentioned that the acetaldehyde concentration in this experiment was 2000 times its K_m. Second, when a similar experiment was performed with glyceraldehyde as variable substrate the Michaelis constant was not affected but V_{max} was increased, as shown in Figures 75 and 76. In this case the effect on V_{max} was expected since the NAD^+ concentration used was not saturating (5 times K_m). Accordingly, true saturation with NAD^+ would eliminate any effect of albumin under these conditions. Thus, albumin appears to activate aldehyde dehydrogenase by reducing the Michaelis constant for NAD^+, i.e., increasing its affinity for the enzyme.

According to Frieden, activation of two substrate reactions can be treated in the same way as activation of single substrate reactions if the modifier affects only one substrate and not the other. Activation by albumin may then

be represented by the following simplified scheme:

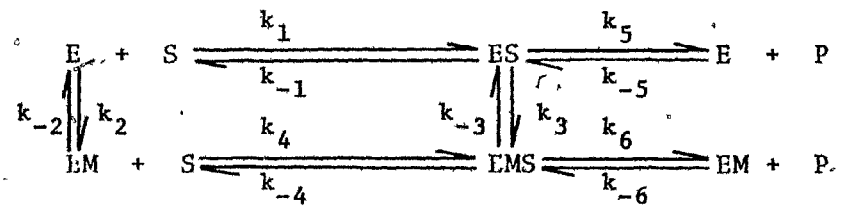

where S = $[NAD^+]$

M = [albumin]

If $k_5 = k_6$ and $k_{-4} = k_{-1}$, i.e., if bovine serum albumin does not affect the rate of breakdown of ES or EMS, the following equation, adapted from Frieden (see equation 11 in reference 150) holds:

$$v = \frac{V_S}{S + \frac{K_1(1 + M/K_2)}{(1 + M/K_3)}}$$

Activation occurs if K_2, the dissociation constant for the enzyme-modifier complex, is greater than K_3, the dissociation constant for the enzyme-modifier-substrate complex with respect to M. Since K_1K_3 must equal K_2K_4 on thermodynamic grounds, this implies that $K_1 > K_4$, which corresponds to increased affinity for NAD^+ in the presence of albumin. This formulation must remain tentative since data are insufficient for determination of all the various constants involved. From these observations the hypothesis is advanced that

activation of human aldehyde dehydrogenase by bovine serum albumin occurs through a change in the conformation of the protein and that the altered conformation has a higher affinity for NAD^+.

Physiological Implications of Activation by Bovine Serum Albumin

The role of protein-protein interactions between functional subunits of allosteric enzymes in the regulation of their activity is well recognized. The present study with bovine serum albumin draws special attention to the potential importance of protein-protein interactions between different proteins in the physiological systems. The activating effect of bovine serum albumin has been observed with many other enzymes *in vitro*, but in no case reported so far, has it been studied in detail in order to delineate the mechanism of activation. It has generally been considered to stabilize enzymes non-specifically at the high dilutions encountered under assay conditions.

Bovine serum albumin activates this enzyme maximally in the physiological pH range where activity in the absence of bovine serum albumin is relatively low. It is tempting to speculate that human liver aldehyde dehydrogenase may be activated *in vivo* by some specific protein or proteins, with a concomitant effect on aldehyde metabolism under physiological conditions. It may well be the case that the human enzyme occurs in a complex with some protein in the cell and this associated protein is lost during enzyme isolation and frac-

tionation. It is generally thought that enzymes, in vivo, operate most efficiently at a substrate concentration in the region of their apparent Michaelis constants. The present observation that activation of human liver aldehyde dehydrogenase by BSA is higher with NAD^+ concentrations close to K_m than at concentrations above K_m both at low and high pH, is also in keeping with this speculation on the contribution of protein-protein interactions between different proteins to the catalytic efficiency of the human enzyme in vivo. This suggestion raises the further possibility that many other enzymes which are not maximally active at physiological pH range in vitro may be activated or regulated in vivo by such protein-protein interactions.

G. MODE OF ACTION OF CHELATING AGENTS

Zinc is a structural and functional component of many dehydrogenases, e.g., alcohol dehydrogenase from yeast (151-153), horse (153-157) and human liver (158-161), D-glyceraldehyde-3-phosphate dehydrogenase from hog muscle (167), glutamic dehydrogenase from bovine liver (153,162-166), bovine muscle (168) and yeast (168,169), lactic dehydrogenase from rabbit muscle (170) and malic dehydrogenase from bovine heart (171). Inhibition of an enzyme by a chelating agent has generally been considered due to the co-ordination of metal atoms present in the enzyme. Thus, zinc-metallo enzymes are inhibited by zinc-complexing agents. In the present study, various chelating agents such as 1,10-phenanthroline, 2,9-dimethyl-1,

10-phenanthroline and α,α´-dipyridyl, were found to inhibit the dehydrogenase reaction instantaneously. Inhibition was competitive with respect to NAD^+. It is interesting to note that the inhibition constants for 1,10-phenanthroline and its analogue, 2,9-dimethyl-1,10-phenanthroline, are quite similar whereas the stability constants for zinc complexes of these chelators are quite different (Table VII). Since there is a steric hinderance in 2,9-dimethyl-1,10-phenanthroline, the zinc complex with this chelator is less stable than that formed with 1,10-phenanthroline. The low stability constant for 2,9-dimethyl-1,10-phenanthroline would suggest that a high inhibition constant should be observed for the enzyme compared to that obtained with 1,10-phenanthroline. However, this was not the case. Similar behavior was observed with α,α´-dipyridyl and its analogue γ,γ´-dipyridyl. These two dipyridyls differ greatly in their ability to form zinc complexes. Two heterocyclic ring nitrogens are present in both compounds, but these donor nitrogens are too far apart to form a bidentate complex in the case of γ,γ´-dipyridyl. Therefore, it is expected that the inhibition constant for γ,γ´-dipyridyl should be greater than that for α,α´-dipyridyl if chelation of zinc (or some other transition metal) were involved in the inhibition of the dehydrogenase reaction. In fact, the inhibition constants were similar in magnitude for both dipyridyl compounds. Quinoline, a bicyclic compound with a single heterocyclic nitrogen, cannot form a bidendate chelate complex. In spite of this, it inhibited the dehydro-

genase reaction. Benzoic acid is another example of an inhibitor which does not form a stable complex with zinc since there is only one donor group (—COOH).

The similar inhibition constants obtained for these various agents, differing widely in their ability to form zinc complexes, strongly suggests that the basis of inhibition of the enzyme is not due to the chelation of any metal atom present in the human enzyme, but rather, is the result of a competition between NAD^+ and inhibitor for the NAD^+-binding site. The competitive nature of the inhibition by these compounds suggests that the NAD^+-binding site has an affinity for aromatic ring structures. Since these are non-polar, it suggests that a hydrophobic area is present in the region of the NAD^+-binding site and the inhibition of the dehydrogenase reaction occurs through hydrophobic interactions between this area and the chelating agent described here.

Comparison of inhibition constants also showed that compounds in which aromatic rings are attached to a common C—C bond and can freely rotate, were less inhibitory than those which have fused ring aromatic structures. Dipyridyls (biphenyls) belong to the first group of compounds and phenanthrolines to the latter group. The inhibition constants for dipyridyls were ten times higher than those for phenanthrolines. Data also indicated that biphenyls and compounds with single aromatic rings act in a similar manner. For

instance, the inhibition constant for benzoic acid, a single aromatic ring compound, was not considerably greater than that for the dipyridyls. The genreal conclusion drawn from the present data is in contrast to that reached by Stoppani et al. for yeast and bovine liver aldehyde dehydrogenases (79). These authors concluded that the competitive inhibition of both enzymes by 8-hydroxyquinoline, 1,10-phenantholine, α,α'-dipyridyl and thiourea was due to the co-ordinaiton of zinc with these chelators. In fact, Jakoby et al. (38,47) have not reported zinc to be present in homogeneous preparations of yeast aldehyde dehydrogenase.

BIBLIOGRAPHY

1. Lieber, C.S. (1967) Annu. Rev. Med. 18, e35
2. Batteli, F. and Stern, L. (1910) Biochem. Z. 28, 145
3. Leloir, L.F. and Munoz, J.M. (1938) Biochem. J. 32, 299
4. Moser, K., Papenberg, J. and von Wartburg, J.-P. (1968) Enzym. Biol. Clin. 9, 447
5. Orme-Johnsen, W.H. and Ziegler, D.H. (1965) Biochem. Biophys. Res. Commun. 21, 78
6. Lieber, C.S. and DeCarli, L.M. (1968) Scinnce 162, 917
7. Roach, M.K., Reese, W.N. and Creaven, P.J. (1969) Biochem. Biophys. Res. Commun. 36, 596
8. Lieber, C.S. and DeCarli, L.M. (1970) J. Biol. Chem. 245, 2505
9. Juni, E., and Heym, G.A. (1956) J. Biol. Chem. 218, 365
10. McManus, I.R., Contag, A.D. and Olson, R.E. (1966) J. Biol. Chem. 241, 349
11. Himwich, H.E. (1956) in Alcoholism (Thompson, G.N., ed) pp. 291, Thomas, C.C., Springfield, Illinois.
12. Perman, E.S. (1958) Acta Physiol. Scand. 43, 71
13. Eade, N.R. (1959) J. Pharmacol. Exp. Ther. 127, 29
14. Duritz, G. and Truitt, E.B., Jr. (1963) Fed. Proc. 22, 272
15. Truitt, E. B., Jr., Bell, F.K. and Krantz, J.C., Jr. (1956) Quart. J. Stud. Alc. 17, 594

16. Beer, C.T. and Quartel, J.H. (1958) Can. J. Biochem. Physiol. 36, 531

17. Kiessling, K.-H. (1963) Exp. Cell. Res. 30, 569

18. Racker, E. (1949) J. Biol. Chem. 177, 883

19. von Wartburg, J-P. (1971) in The Biology of Alcoholism (Kissin, B. and Begleiter, H., eds) Vol. 1, pp. 63, Plenum Press, New York - London

20. Burton, R.M. and Stadtman, E.R. (1953) J. Biol. Chem. 202, 873

21. Rudolph, F.B., Purich, D.L. and Fromm, H.J. (1968) J. Biol. Chem. 243, 5539

22. Palmer, G. (1962) Biochim. Biophys. Acta 56, 444

23. Bray, R.C. (1963) in The Enzymes (Boyer, P.D., Lardy, H. and Myrbäck, M., eds) 2nd Ed Vol. 7, pp. 533

24. Mahler, H.R., Mackler, B., Green, D.M. and Bock, R.M. (1954) J. Biol. Chem. 210, 465

25. Richert, D.A. and Westerfeld, W.W. (1954) J. Biol. Chem. 209, 179

26. Mahler, H.R. (1955) Methods Enzymol. 1, 523

27. Rajagopalan, K.V., Fridovich, I. and Handler, P. (1962) J. Biol. Chem. 237, 922.

28. Racker, E. (1952) J. Biol. Chem. 196, 347

29. Karasek, M.A. and Greenberg, D.M. (1957) J. Biol. Chem. 227, 191

30. Gorr, G. (1932) Biochem. Z. 254, 12

31. Tanko, B., Munk, L. and Abonyi, I. (1940) Z. Physiol. Chem. 264, 91

32. Knox. W.E. (1942) J. Biol. Chem. 145, 69

33. Stoz, E., Westerfeld, W.W. and Berg, R.L. (1944) J. Biol. Chem. 152, 41

34. Juni, E. (1952) J. Biol. Chem. 195, 727

35. Westerfeld, W.W. and Bloom, R.J. (1970) in Alcohol and Alcoholism (Popham, R.E., ed) pp. 1, University of Toronto Press, Toronto

36. Feldman, R.I. and Weiner, H. (1972) J. Biol. Chem. 247, 260

37. von Tingerstrom, R.G. and Razzell, W.E. (1968) J. Biol. Chem. 243, 2691

38. Steinman, C.R. and Jakoby, W.B. (1967) J. Biol. Chem. 242, 5019

39. Jakoby, W.B. (1959) in The Enzymes (Boyer, P.D., Lardy, H. and Myrbäck, M., eds) 2nd Ed, Vol. 7, pp. 203, Academic Press, Inc., New York

40. Maxwell, E.S. and Topper, Y.J. (1961) J. Biol. Chem. 236, 1032

41. Raison, J.K., Henson, G. and Rienits, K.G. (1966) Biochim. Biophys. Acta 118, 285

42. Shepperd, J.R., Albersheim, P. and McClearn, G. (1970) J.Biol. Chem. 245, 2876

43. Gillette, J.R. (1959) J. Biol. Chem. 234, 139

44. Blair, A.H. and Bodley, F.H. (1969) Can. J. Biochem. 47, 265

45. Erwin, V.G. and Deitrich, R.A. (1966) J. Biol. Chem. 241, 3533

46. Duncan, R.J.S. and Tipton, K.F. (1971) Eup. J. Biochem. 22, 257

47. Steinman, C.R. and Jakoby, W.B. (1968) J. Biol. Chem. 243, 730

48. Seegmiller, J.E. (1953) J. Biol. Chem. 201, 629

49. King, T.E. and Cheldelin, V.H. (1956) J. Biol. Chem. 220, 177

50. Jakoby, W.B. (1958) J. Biol. Chem. 232, 75

51. Oppenheim, A. and Castelfranco, P.A. (1967) Plant Physiol. 42, 125

52. Jakoby, W.B. and Scott, E.M. (1959) J. Biol. Chem. 234, 937

53. Albers, R.W. and Koval, G.K. (1961) Biochim. Biophys. Acta 47, 2005

54. Kammeraat, C. and Veldstra, H. (1968) Biochim Biophys. Acta 151, 1

55. Jakoby, W.B. and Fredericks, J. (1959) J. Biol. Chem. 234, 2141

56. Stachow, C.S. Stevenson, I.L, and Day, D.J. (1967) J. Biol. Chem. 242, 5294

57. Strecker, H.J. (1960) J. Biol. Chem. 235, 3218

58. Monder, C. (1967) 242, 4603

59. Strittmatter, P. and Ball, E.G. (1955) J. Biol. Chem. 213, 445

60. Rose, Z.B. and Racker, E. (1962) J. Biol. Chem. 237, 3279

61. Black, S. and Wright, N.G. (1955) J. Biol. Chem. 213, 39

62. Kraemar, R. and Deitrich, R.A. (1968) J. Biol. Chem. 243, 6402

63. Elder, T.D. and Topper, Y.J. (1962) Biochim. Biophys. Acta 64, 430

64. Erwin, E.G. and Deitrich, R.A. (1966) J. Biol. Chem. 241, 3533

65. Shum, G.T. and Blair, A.H. (1972) Can. J. Biochem. 50,741

66. Fridovich, I. (1966) J. Biol. Chem. 241, 3126

67. Naylor, J.F. and Fridovich, I. (1968) J. Biol. Chem. 243, 341

68. Bodley, F.H. and Blair, A.H. (1971) Can. J. Biochem. 49, 1

69. Walkenstein, S.S. and Weinhouse, S. (1953) J. Biol. Chem. 200, 515

70. Deitrich, R.A. (1966) Biochem. Pharmacol. 15, 1911

71. Marjanen, L. (1972) Biochem. J. 127, 633

72. Smith, L. and Packer, L. (1972) Arch. Biochem. Biophys. 148, 270

73. Maxwell, E.S. (1962) J. Biol. Chem. 237, 1699

74. Deitrich, R.A. (1972) J. Biol. Chem. 247, 7232

75. Clark, J.F. and Jakoby, W.B. (1970) J. Biol. Chem. 245, 6072

76. Kaplan, N.O. (1951) in the Enzymes (Boyer, P.D., Lardy, H. and Myrbäck, M., eds) 1st Ed, Vol. 2, Part I, pp. 55, Academic Press, Inc., New York

77. Burton, K. and Wilson, T.H. (1953) Biochem. J. 54, 86

78. Burton, K. and Stadtman, E.R. (1953) J. Biol. Chem. 202, 873

79. Stoppani, A.O.M., Schwarcz, M.N. and Freda, C.E. (1966) Arch. Biochem. Biophys. 113, 464

80. Jakoby, W.B. (1957) Arch. Biochem. Biophys. 76, 625

81. Black, S. (1951) Arch. Biochem. Biophys. 34, 86

82. Stoppani, A.O.M. and Milstein, C. (1957) Biochim. Biophys. Acta 24, 655

83. Theorell, H. and Bonnichsen, R. (1951) Acta Chem. Scand. 5, 1105

84. Racker, E. and Krimsky, I. (1952) J. Biol. Chem. 198, 731

85. Velick, S.F. (1953) J. Biol. Chem. 203, 563

86. Kaplan, N.O. and Ciotti, M.M. (1954) J. Biol. Chem. 211, 431.

87. Stoppani, A.O.M. and Milstein, C. (1957) Biochem. J. 67, 406

88. Deitrich, R.A. (1967) Arch. Biochem. Biophys. 119, 253

89. Jakoby, W.B. (1957) Arch. Biochem. Biophys. 70, 625

90. Jakoby, W.B. (1958) J. Biol. Chem. 232, 89

91. Hald, J., Jacobsen, E. and Larsen, V. (1948) Acta Pharmacol. Toxicol. 4, 285

92. Hald, J. and Jacobsen, E. (1948) Acta Pharmacol. Toxicol. 4, 305

93. Asmussen, E., Hald, J. and Larsen, V. (1948) Acta Pharmacol. Toxicol. 4, 311.

94. Perman, E.S. (1962) Acta Physiol. Scand. 55, 190 (Supp), pp. 1

95. Racker, E. (1949) Ann. Rept. Long Island Biol. Assoc. 38

96. Graham, W.D. (1951) J. Pharm. Pharmacol. 3, 160

97. Deitrich, R.A. and Hellerman, L. (1963) J. Biol. Chem. 238, 1683

98. Detrich, R.A. and Erwin, V.G. (1971) Mol. Pharmacol. 7, 301

99. Vennesland, B. and Westheimer, F.H. (1954) in The Mechanism of Enzyme Action (McElroy, W.D. and Glass, B., eds) pp. 357, John's Hopkins Press, Baltimore

100. Kaplan, N.O. and Sarma, R.H. (1970) in Pyridine Nucleotide Dependent Dehydrogenases (Sund, H., ed) pp. 39, Springer-Verlag, Berlin and Heidelberg

101. Kaplan, N.O. and Ciotti, M.M. (1954) J. Amer. Chem. Soc. 76, 1713

102. Kaplan, N.O. and Ciotti, M.M. (1956) J. Biol. Chem. 221, 823

103. Kaplan, N.O., Ciotti, M.M. and Stolzenbach, F.E. (1956) J. Biol. Chem. 221, 833

104. Anderson, B.M. and Kaplan, N.O. (1959) J. Biol. Chem. 234, 1226

105. Kaplan, N.O., Ciotti, M.M., Hamolsky, M. and Bieber, R.E. (1960) Science 131, 392

106. Kaplan, N.O. (1963) Proceedings of the Fifth International Congress of Biochemistry, Vol. IV, pp. 295, Pergamon Press, Oxford-New York-London-Paris

107. Freda, C.E. and Stoppani, A.O.M. (1970) Enzymologia 38, 225

108. Schwarcz, M.N. and Stoppani, A.O.M. (1970) Enzymologia 38, 269

109. Shore, J.D. and Theorell, H. (1967) Eup. J. Biochem. 2, 32

110. Sarma, R.H., Ross, V. and Kaplan, N.O. (1968) Biochemistry 7, 3052

111. Sarma, R.H. and Kaplan, N.O. (1970) Biochemistry 9, 539

112. Sarma, R.H., Moore, M. and Kaplan, N.O. (1970) Biochemistry 9, 549

113. Sarma, R.H. and Kaplan, N.O. (1970) Biochemistry 9, 557

114. Cleland, W.W. (1963) Biochim. Biophys. Acta 67, 104

115. Duncan, R.J.S. and Tipton, K.F. (1971) Eup. J. Biochem. 22, 538

116. Feldman, R.I. and Weiner, H. (1972) J. Biol. Chem. 247, 267

117. Bradbury, S.L. and Jakoby, W.B. (1971) J. Biol. Chem. 246, 1834

118. Park, J.H., Meriwether, B.P., Clodfelder, P. and Cunningham, L.W. (1961) J. Biol. Chem. 236, 136

119. Mathew, E., Meriwether, B.P. and Park, J.H. (1967) J. Biol. Chem. 242, 5024

120. Pocker, Y. and Stone, J.T. (1967) Biochemistry 6, 668

121. Alfanzo, M. and Apitz-Castro, R. (1971) Fed. Eur. Biochem. Soc. Lett. 19, 235

122. Suarez, Z. and Apitz-Castro, R. (1972) Biochim. Biophys. Acta 258, 339

123. Dirks, B.M. and Boyer, P.D. (1951) Cereal Chem. 28, 483

124. Tildon, J.T. and Ogilve, J.W. (1972) J. Biol. Chem. 247, 1265

125. Horton, A.A. (1971) Biochim. Biophys. Acta 253, 514

126. Sheppard, J.R., Albersheim, P. and McClearn, G. (1970) J. Biol. Chem. 245, 2876

127. Redmond, G. and Cohen, G. (1970) Science 171, 387

128. Deitrich, R.A. (1971) Science 173, 334

129. Lowry, O.H., Rosebrough, N.J., Farr, A.L. and Randall, R.J. (1951) J. Biol. Chem. 193, 265

130. Cleland, W.W. (1963) Nature 198, 463

131. Lineweaver, H. and Burke, D. (1934) J. Amer. Chem. Soc. 58, 658

132. Mahler, H.R. and Cordes, E.H. (1966) Biologecal Chemistry, pp. 54, Harper & Row, New York

133. Cecil, R. (1963) in The Proteins (Neurath, H., ed) 2nd Ed, pp. 379, Academic Press, Inc., New York

134. Bodley, F.H. (1969) M.Sc. Thesis, Dalhousie University

135. Cleland, W.W. (1963) Biochim. Biophys. Acta 67, 173

136. Cha, S. (1968) J. Biol. Chem. 243, 820

137. Cleland, W.W. and Wratten, C.C. (1969) in The Mechanism of Action of Dehydrogenases (Schwert, G.W. and Winer, A.D., eds) pp. 103, University Press of Kentucky, Lexington.

138. Rudolph, F.B. and Fromm, H. (1967) J. Biol. Chem. 246, 6611

139. Pettersson, G. (1969) Acta Chem. Scand. 23, 2717

140. Pettersson, G. (1972) Biochim. Biophys. Acta 276, 1

141. Wratten, C.C. and Cleland, W.W. (1965) Biochemistry 4, 2442

142 Koshland, D.E., Jr. (1958) Proc. Nat. Acad. Sci. U.S.A. 44, 98

143. Nirenberg, M.W. and Jakoby, W.B. (1960) Proc. Nat. Acad. Sci. U.S.A. 46, 206

144. Racker, E. (1955) Physiol. Rev. 35, 1

145. Hurst, R.O. (1969) Can. J. Biochem. 47, 941

146. Alberty, R.A., Massey, V., Frieden, C. and Fuhlbrigge, A.R. (1954) J. Amer. Chem. Soc. 76, 2485

147. Dixon, M. and Webb, E.C. (1964) Enzymes, 2nd Ed, pp. 81 Academic Press, Inc., New York

148. Alberty, R.A. (1956) Advan. Enzymol. 17, 1

149. Kezdy, F.J. and Bender, M.L. (1962) Biochemistry 1, 1097

150. Frieden, C. (1964) J. Biol. Chem. 239, 3522

151. Vallee, B.L. (1955) Advan. Protein Chem. 10, 317

152. Vallee, B.L. and Hoch, F.L. (1955) Proc. Nat. Acad. Sci. 41, 327

153. Vallee, B.L. (1960) in The Enzymes (Boyer, P.D., Lardy, H. and Myrbäck, eds) 2nd Ed, Vol. 3, pp. 11, Academic Press, Inc., New York

154. Theorell, H., Nygaard, A.P. and Bonnichsen, R. (1955) Acta Chem. Scand. 9, 1148

155. Vallee, B.L. and Hoch, F.L. (1957) J. Biol. Chem. 225, 185

156. Åkeson, Å. (1964) Biochem. Biophys. Res. Commun. 17, 211

157. Drum, D.E., Harrison, J.H., Li, T.K., Bethune, J.L. and Vallee, B.L. (1967) Proc. Nat. Acad. Sci. 57, 1434

158. Bethune, J.L., von Wartburg, J.-P. and Vallee, B.L. (1963) Abstr. 143rd Meeting American Chemical Society pp. 100 C, Sept., 1963

159. von Wartburg, J.-P. and Vallee, B.L. (1963) Abstr. 143 rd Meeting American Chemical Spciety, pp. 100 C, Sept., 1963

160. von Wartburg, J.-P., Bethune, J.L. and Vallee, B.L. (1964) Biochemistry 3, 1775

161. Blair, A.H. and Vallee, B.L. (1966) Biochemistry 5, 2026

162. Adelstein, S.J. and Vallee, B.L. (1958) J. Biol. Chem. 233, 589

163. Ito, K., Kisanuki, A. and Koyama, Y. (1958) Chem. Abstr 52, 15621C

164. Ito, K. (1958) Chem. Abstr. 52, 4726B

165. Kubo, p.H., Yamano, T., Iwatsubo, M., Watari, H., Soyama, T., Shiraishi, J., Sawads, S., Kawashima, N., Mitani, S. and Ito, K. (1958) Bull. Soc. Chim. Biol. 40, 431

166. Vallee, B.L. Adelstein, S.J. and Olson, J.A. (1955) J. Amer. Chem. Soc. 77, 5196

167. Keleti, T. (1964) Biochim. Biophys. Acta 89, 422

168. Keleti, T., Gyorgyi, S., Telegdi, M. and Zaluska, H. (1962) Acta Physiol. Acad. Sci. Hung. 22, 11

169. Keleti, T. (1966) Biochem. Biophys. Res. Commun. 22, 640

170. Vallee, B.L. and Wacker, W.E.C. (1956) J. Amer. Chem. Soc. 78, 1771

171. Harrison, J.H. (1963) Fed. Proc. 22, 493

END

28 • 11 • 74

FIN